Optical trapping takes shape: the use of structured light fields

K. Dholakia and W.M. Lee

3rd March 2008

SUPA, School of Physics and Astronomy, University of St Andrews, North Haugh, Fife, Scotland KY16 9SS

CONTENTS **PAGE**

Abstract

Optical micromanipulation is a powerful and versatile technique across all of the physical and biological sciences. Whilst the forces exerted by optical traps are naturally very small, they are sufficient to realize non-invasive mechanical control over mesoscopic particles within atomic, biological and colloidal systems. The inherent compatibility with modern microscopy enhances the reconfigurability of the trap while the accuracy achieved in a calibrated optical trap presents itself as a quantitative force probe. Thus forces can be applied in a controlled manner to biological systems including cells and molecular motors and processes measured with high precision. The impact is not limited to biology. Optical traps have provided seminal studies in colloidal and optical physics including the phase dynamics of thermodynamic systems, Brownian diffusion, aspects of microfluidics, and fundamental issues related to optical angular momentum. This article aims to focus upon the emergent theme of optical trapping with structured light fields. By structured light fields we refer to areas such as the generation of multiple arrays of traps and the use of specialist light fields such as Bessel beams and Laguerre-Gaussian beams. All of these are making a major impact in optical trapping and in subsequent applications including those in biomedicine.

1. Introduction

Laser microscopy has unravelled a wealth of complex processes in cell and molecular biology. The prominent imaging methods of laser scanning confocal fluorescence imaging and two-photon fluorescence excitation are established techniques for visualizing cells and molecules. The light-matter interaction has had a profound impact upon fundamental science and enabled a deeper understanding not only in biology but in the domain of atomic and molecular theory. Notable advances in the last few decades have included the concept of light exerting mechanical forces upon atomic ensembles paving the way for the very powerful methods of laser cooling (Chu, 1998) and the achievement of ultra cold quantum gases and onset of Bose-Einstein condensation (Davis *et al.*, 1995; O'Hara *et al.*, 2000). The forces of light have made an impact at these size scales that are much larger than that of an atom (angstrom) or molecule: importantly light forces can readily manifest themselves upon objects of up the size of a single biological cell (micrometer).

How do such forces arise? – light may be considered as quanta of energy that possesses momentum. Overall, the exchange of momentum with matter may result in physical motion: in this manner, light may move, hold and exert a very controllable force upon material objects and importantly for our purposes to objects the size of a single cell or smaller. This form of optical momentum transfer and subsequent force is at the heart of the area of optical trapping or optical micromanipulation.

The use of laser sources is crucial to the field though one must acknowledge that we are limited to exerting forces of the order of piconewtons. The interaction between light and the particle (microscopic or smaller) produces a change of photon momentum upon the particle at a rate that would lead to small forces that are sufficient enough to move or hold a microparticle. At such a size level, this concept can be utilized particular by the biological sciences in pursuit of studying several macromolecular and cellular processes in a quantifiable manner. The field of fundamental physics too has benefited in numerous ways using optical traps: seminal studies in the last fifteen years include a deeper

understanding of the optical angular momentum of light, exploration of colloidal hydrodynamics, microfluidics and the study of thermodynamics at small scales, this latter topic related to the exciting topic of non-equilibrium physics. Such experimental studies of light-matter interaction have, in turn, advanced physicists towards a more complete appreciation of the theoretical basis for optical forces.

It is now over thirty five years since the first optical trapping experiments and over twenty years since the inception of the popular "optical tweezers" (Ashkin *et al.*, 1986). Beginning in 1970, Ashkin (Ashkin, 1970) performed experiments with a visible argon ion laser. In a single horizontally propagating beam, microspheres were seen to align along the propagation axis and propelled along the propagation direction of the beam: this is now commonly known as optical guiding. He then added a second beam (of equivalent optical power) at counter-propagating geometry halted the motion of a sphere along the beam axis whilst retaining its position within the bright region of the two beams: the first optical trap was formed. This counter-propagating (or dual) beam optical trapping geometry (Ashkin, 1970) has been realized with fibers (Constable *et al.*, 1993) and is making a comeback as we shall discuss later in the form of the optical stretcher (Guck *et al.*, 2001) and for longitudinal optical binding (Tatarkova *et al.*, 2002; Singer *et al.*, 2003). In subsequent studies Ashkin (Ashkin and Dziedzic, 1974) also investigated the stability of trapping of hollow and glass spheres with optical beams by balancing optical forces against gravity. Indeed the levitation of hollow spheres constituted the first use of "structured light fields" in optical traps. An output TEM^*_{01} mode from a laser was needed as for such a hollow particle is repelled from regions of high light intensity (its refractive index is lower than its surroundings) and thus needs to be "caged" by light (Ashkin and Dziedzic, 1974). Sixteen years after the dual beam trap, Ashkin and colleagues realized the single beam gradient trap (popularly known as ***optical tweezers***) (Ashkin *et al.*, 1986) that is the simplest incarnation of optical forces for moving microscopic particles and indeed forms the basis for most of the discussion within this article. This trap has now been well-recognized as having the largest impact within the field of optical micromanipulation.

This article aims to give the reader an insight into some of the most exciting areas of this research field with the spotlight firmly upon the topics of multiple trapping or use of specific light modes within optical micromanipulation. We broadly group these topics under the heading of ***structured light fields or beams***: that is moving away from a standard single Gaussian light field. The types of structured light beams include multiple, reconfigurable Gaussian arrays of traps, as well as non-zero order light modes such as Laguerre-Gaussian modes and Bessel modes. We refer the reader elsewhere for more concise reviews (Molloy and Padgett, 2002; Grier, 2003; Neuman and Block, 2004; Dholakia and Reece, 2006; McGloin *et al.*, 2008; Dholakia. K, 2008) of this topical area. As a precursor to the discussion of these structured light patterns in this article, we shall begin with an introduction to optical tweezers, its operation and a brief consideration of some of the experimental issues for its implementation. This is followed by a review particularly how this powerful optical concept is applied to biology namely the study of molecular motors and other biological macromolecules as well as studies of cells as well as some aspects of colloidal science. Optical tweezers have produced some seminal studies within single molecule biophysics and allowed an insight into this field in a manner hitherto unforeseen (Block *et al.*, 2007). We then move specifically to the topic of structured light fields and give examples of how such fields may be generated and implemented as well as their applications. The field is dynamic and though in some senses established it is still very contemporary and if anything expanding its remit across the natural sciences. Many of the applications within biology and chemistry are very active current areas of research which are continually evolving, so the aim will be to give the reader a proficient grounding in the various techniques to facilitate the reasoning behind the future use of such structured light beams.

2. Single beam optical tweezers

2.1 Optical tweezers : theoretical treatment of trapping forces

The light – matter interaction is at the heart of optical trapping and the subsequent forces may be understood in a number of ways. Perhaps the most straightforward case is to consider an object in the Mie regime: where the particle radius, $\boldsymbol{r}$, is much larger than the trapping wavelength, $\boldsymbol{\lambda}$). When trapping in the Mie regime, one can invoke the use of

geometrical ray optics to picture the forces involved. Ashkin shows a clear calculation of how to derive the forces present in this instance by ray tracing and use of the Fresnel equations at the sphere- medium boundary (Ashkin, 1992), by consider the scattering and gradient forces as arising from the reflection and refraction of light. A trapped microsphere (if of higher refractive index than its surroundings and transparent to the incident light) acts as a microscopic lens that focuses the light field. This focusing effect in turn causes the particle to move to the position of highest light intensity as may be seen in figure 1. Figure 1 shows how we may visualize optical trapping forces in the Mie regime with a high numerical aperture (N.A) microscope objective (Ashkin, 1992). Both lateral trapping (figure 1(a) and axial trapping (figure 1(b) are considered. In this diagram, we can see that gradients of light intensity both in the lateral and axial direction are key to the operation of this technique. Here, the microsphere has a higher refractive index than its surrounding medium. A Gaussian beam, tweezing beam, is being focused through a high numerical aperture (typical NA > 1) microscope objective and in front of the microsphere. In the transverse plane **(x-y)** and axial direction **(z),** the refracted light rays **(a)**, produce net forces **($\mathbf{F_a}$)** on the microsphere that draws the microsphere towards the center of the focus while the reflected light rays (**b**) creates a net forces **($\mathbf{F_b}$)** that pushes microsphere away. The resultant net forces, $\mathbf{F_a}$ and $\mathbf{F_b}$, contribute to the overall gradient forces **($\mathbf{F_{gradient}}$)** and the scattering forces **($\mathbf{F_{scattering}}$)** (figure 1(a)). When the microsphere is located away from the center of the beam focus (maximum intensity), the resultant gradient forces **($\mathbf{F_{gradient}}$)** in both the transverse plane **(x-y)** and axial direction **(z)** act to pull the microsphere into the center of the focus. At the same time, the resultant scattering forces **($\mathbf{F_{scattering}}$)** act to push the microspheres away from the center of the beam focus. (figure 1(a)) Thus by balancing the gradient **($\mathbf{F_{gradient}}$)** and scattering **($\mathbf{F_{scattering}}$)** forces with a highly focused beam, the microsphere is stably held in three dimensions by optical forces (figure 1(b)).

Any light scattering should result in a force opposing the direction of light propagation and any refraction of the light results in a force attracting the particle to the region of highest light intensity. This physical picture cannot be used to explain optical forces exerted upon objects that are a far smaller than the wavelength: in this Rayleigh regime

($r \leq \frac{\lambda}{20}$), it is more appropriate to consider the particle as a dipole that minimizes its energy in the field gradient created by the light (Malagnino *et al.*, 2002; Harada and Asakura, 1996). A full theoretical treatment of how an optical tweezers performs for a given object in a light field is a non-trivial question. In the Rayleigh regime, the object may be considered as a point dipole and the contributions of the time-averaged gradient force $F_{gradient}$ and scattering forces $F_{scattering}$ may be readily separated as follows:

$$F_{gradient} = \frac{2\pi\alpha}{cn_m^{\ 2}}\nabla I \qquad (1)$$

$$F_{scattering} = \frac{I\sigma n_m}{c} \qquad (2)$$

where α denotes the polarisability of the sphere which for a standard non-absorbing dielectric object is proportional to the volume of the particle is equal to $n_m^2 r^3 \left(\frac{m^2-1}{m^2+2}\right)$, σ is the scattering cross section of the sphere equal to $\frac{128\pi^5 r^6}{3\lambda^4}\left(\frac{m^2-1}{m^2+2}\right)^2$, r is the particle radius, I is the intensity, n_m is the refractive index of the surrounding medium, c denotes the speed of light, m refers to the ratio of the refractive indices of particle (n) to that of the surrounding medium (n_m) and λ is the wavelength of the trapping laser used . We can see from this that the scattering force is directly proportional to the trapping laser intensity and the gradient (or dipole) force upon the object is due to the inhomogeneous field gradient created by the tightly focusing the light beam (Svoboda and Block, 1994b; Neuman and Block, 2004). Chaumet and Nieto-Vesperinas derived the expressions for the time averaged forces for the Rayleigh regime. (Chaumet and Nieto-Vesperinas, 2000). In general, we see the gradient force as proportional to the polarizability, which when considering the dielectric particle scales with the volume of the particle. This means it is quite difficult in practice to trap very small dielectric objects (e.g. diameter of 50 nanometers) but one can readily hold dielectric objects from diameter of ~ 0.5 -5 micrometer in diameter a tweezers. These considerations also explain why gold nanoparticles (with their very large polarizability) may be readily trapped at sizes of

100nm and below (Hansen *et al.*, 2005) though absorption is a key consideration to take note (Seol *et al.*, 2006).

Other work looked at different aspects of the problem. Barton and co-workers (Barton and Alexander, 1989; Barton *et al.*, 1989) derived a fifth order corrections to the focused Gaussian beam such as to compute the forces using a Maxwell stress tensor approach. Rohrbach and Stelzer (Rohrbach and Stelzer, 2002) extended the Rayleigh theory to make it valid for large particles by inclusion of second-order scattering terms. The incident field is expanded in terms of constituent plane waves allowing apodization and aberration transformations (due to the high numerical aperture microscope objective) to be incorporated in the theoretical model to yield the resultant optical forces upon the dipole, in this instance without resorting to use of the Maxwell stress tensor method. The vast majority of optical tweezers and trapping experiments are performed where the particle size is comparable to the wavelength of the trapping laser beam. In this region key studies by Rohrbach reported good quantitative agreement between the theory calculations and experimental measurements pertaining to the strength of the optical tweezers (Rohrbach, 2005). His theoretical approach for trapping forces computed the Lorentz force density. He found that the optimal trapping performance is reached when the wavelength of light (within the viscous medium) is comparable to the diameter of the particle, $d \approx \frac{\lambda}{n}$ (Rohrbach, 2005), where λ denotes the wavelength and n the refractive index of the medium. Overall, it is important to note that the numerical and theoretical modeling of optical forces at these scales still presents many challenges.

2.2 Design considerations of an optical tweezers system

The single beam optical tweezers has been widely implemented. The fact it is a calibrated optical force transducer has been the core of many of its applications (Neuman and Block, 2004). Constructing an optical tweezers involves some important physical optics principles and due consideration of certain mechanical components. A more comprehensive technical discussion of this may be found elsewhere (Lee *et al.*, 2007).

The basic optical tweezers requires only a single laser beam for its operation and may be based around standard microscope which already comes equipped with a high numerical aperture (N.A) objective lens (Lee *et al.*, 2007). Alternatively one may build the optical tweezers from standard cage plate or other opto-mechanical components (Rohrbach *et al.*, 2004; Appleyard *et al.*, 2007). Many of the deliberations are upon the types of lasers, choice of microscope objective and the beam delivery by the optical setup which are all crucial for three dimensional (x, y and z) trapping.

The vast majority of optical trapping experiments use monochromatic continuous wave (CW) sources that have the key properties of low absorption of the light by the subject being trapped, especially when using biological materials: the laser wavelength is chosen in the near-infra red region to avoid damage to biological specimens. Wavelengths of 830nm and 970nm have been shown to be particularly favorable to these studies (Neuman *et al.*, 1999). In the near infra red there are ample laser sources with good beam shape (denoted by M^2 ~1 (Kogelnik and Li, 1966; Siegman, 1998) and beam pointing stability) notably the new generation of near infra-red fibre lasers. In the domain of colloidal science, there has been a widespread use of visible lasers notably at 532nm due to the low absorption of water that reduces heating effects (McGloin *et al.*, 2008). Ultra-short pulsed lasers have also been used when one wishes to combine optical trapping with nonlinear phenomena (e.g. two photon excitation). For the case of pulses of ~100 femtosecond duration if the repetition rate of the laser is high enough (eg 80MHz), any anomalies due to particle diffusion in between pulses are not significant and the forces exerted equal to their continuous wave counterparts (Agate *et al.*, 2004). Temporal coherence of the light field is not such an issue (except of course where the laser bandwidth encroaches upon an absorption band within the trapped sample). Some recent experiments have even used a "white light" laser sources based on a supercontinuum generation (Li *et al.*, 2005) to combine optical trapping with spectroscopy.

To achieve a diffraction-limited beam spot (radius = 0.61 λ/ N.A) at the focal plane, a high numerical aperture ($\min. N.A. \approx 1$) microscope objective lens is a natural choice. Today, microscope objectives can produce an image at infinity. With such "infinity

corrected" objectives, researchers may use an additional telescope and optical conjugates to relay the collimated laser source to the microscope objective (within the "infinity space") without affecting the bright-field or fluorescence imaging aspect of the system. The optical telescope is desirable for achieving a diffractive limited spot for true three dimensional tweezing. One needs to slightly overfill the back aperture of the microscope objective (Lee *et al.*, 2007). The use of optical conjugates for the trapping beam enables the optimum steering of beam before entering the microscope objective. The input beam needs to be translated across the sample stage whilst ensuring the beam does not "walk off" or is deviated in a way that might cause it to miss or clip any apertures in the beam path, notably the back aperture of the microscope objective. Ensuring that input beam is centered upon the back aperture during steering would mean a good quality trapping beam at the focal plane at all times. In figure 2 we illustrate the idea of optical conjugates for the steering of the trapping beam. The back aperture of the microscope objective is imaged onto a mirror: thus positioning the light onto that mirror is equivalent to positioning the beam onto the objective: tilting the mirror in the lateral plane now moves the beam at the sample plane but does not move it across the back aperture of the microscope objective. We now look in some detail at figure 2. The beam steering system is made of up two lenses as seen in the figure, denoted as L1 and L2, and a rotating mirror M1. Each lens is placed at one focal length away from the other and the rotating mirror M1 is positioned at one focal length away from one of the lens L1. By placing the back aperture of a microscope objective at one focal length away from lens L2, a beam steering system is formed. Here, the rotating mirror M1 and the back aperture of the microscope objective form conjugate planes. Both the green thin line (deflected beam) and the red thick line (deflected at 45 degree angle illustrates the rays from rotating the mirror M1 maintains its position with central rays at the back aperture of the microscope objective. The central purpose of the conjugate planes is to ensure that a collimated beam (light blue line) before the mirror M1 maintains overfilling of the back aperture of microscope objective without any "walk off".

Preparing a sample for tweezing also requires some careful thought. Colloidal particles are usually dispersed in deionized water and approximately 10 microliters is placed on

the sample, while biological cells are often suspended in suitable buffer solution. When using cells, these are suspended in suitable buffer medium. In both cases, when employing an oil-immersion microscope objective for tweezing, the beam would propagate through a layer of oil, a thin piece of glass (coverslip) and then into the sample solution which is of a lower refractive index than the glass and oil. Thus the beam will, unsurprisingly, experience a large change in refractive index that generates spherical aberrations along the axial plane, broadening the beam spot along the axial plane. Thus, a well aligned optical tweezers may still suffer inherent aberrations due to refractive index mismatches. As the results, the trap performance degrades when operating in deeper region of the sample (Rohrbach and Stelzer, 2002). With the use of immersion oils with varying refractive indices, Reihani and Oddershede succeeded in minimizing spherical aberrations to allow trapping at depth using oil immersion objectives (Reihani. S. N. S. and Oddershede, 2007). On the other hand, water immersion objectives are corrected for the refractive index of water (removing the requirement of using immersion oil and a coverslip) which reduces the spherical aberration (Rohrbach and Stelzer, 2002; Vermeulen *et al.*, 2005). Alternative adaptive optical techniques to obviate these aberrations are available in the form of dynamic holographic (Wulff *et al.*, 2006) elements or the use of deformable mirror (Theofanidou *et al.*, 2004) technology by imposing correction terms of the appropriate Zernike polynomials upon the input wavefront of the tweezing beam.

Trapping a particle is of course a key step but how do we then use this trapped object to make force measurements? Converting an optical tweezers into a highly accurate force measurement system requires an understanding of the underlying physical principles of its operation with relationship to particle dynamics and Brownian motion. The crucial tenet is that an optical tweezers may be modelled as a near ideal highly overdamped simple harmonic oscillator. In particular, the particle resides in a parabolic potential well created by the optical trapping beam. When the particle is at equilibrium, it tends to rest at centre of the potential well (trap) where it has the minimum energy. Once the particle is perturbed, it will experience a restoring force that is proportional to the distance away from centre of the well (the resting position) akin to a miniscule spring that obeys

Hooke's law: this perhaps innocuous statement embodies some of the most powerful principles of optical trapping as illustrated in figure 3. This idealized case may be represented by a one dimensional equation of motion in direction *x* for a Brownian particle in a harmonic potential:

$$m\frac{\partial^2 x}{\partial t^2}+\gamma\frac{\partial x}{\partial t}+\kappa\, x = F_f(t) \tag{3}$$

If we examine the left-hand side of the equation 3, the first term represents the inertial force component for a particle mass m; the second term is the velocity dependent viscous damping force, where γ is the drag coefficient; and the final term is the optical restoring force for the trap stiffness, κ. The right hand side of the equation represents the fluctuating force, $F_f(t)$, due to the Brownian motion. By monitoring either the distribution of the particle position within the trap or the frequency response of the particle motion we may obtain two independent methods of determining the trap stiffness, κ. Under typical trapping conditions (which is the low Reynolds number regime (Squires and Quake, 2005)) , the viscous damping forces dominate and inertial effects ($m\frac{\partial^2 x}{\partial t^2}$) may be neglected. As illustrated in figure.3, the particle in this potential well essentially behaves like a spring obeying Hooke's law where the force on the object is proportional to the displacement (Δx and Δz as seen in figure 3) of its position from the center of the trap (see figure 3) with the constant of proportionality denoted as the trap stiffness. The particle position may be recorded as a histogram that may be described by a Boltzmann distribution that in turn will be directly related to the shape of the trapping potential, which is harmonic over the size range of a fraction of the trapping wavelength (Berg-Sorensen and Flyvbjerg, 2004; Svoboda and Block, 1994a).

To use optical tweezers for measuring small forces, we require the addition of an optoelectronic sensor capable of measuring the mean position of the trapped object in all three dimensions to extract the corresponding trap stiffness, κ. The sensor and detection circuitry is calibrated by moving the trapped objects over a known distance. With the

relationship of signal (voltage) and the distance (nanometer), the sensor can be calibrated for specific distances. Once this position calibration factor and the stiffness κ of the optical tweezers, which is calculated from analysis of the thermal motion of the trapped object or by application of known viscous drag forces, are quantitivity collected, the optical tweezers can then be implemented as a force transducer. A popular method of detection is the imaging of the back focal plane interference pattern of the trapped object (Allersma *et al.*, 1998) onto an optoelectronic detector (quadrant photodiode or position sensitive detector) (Berg-Sorensen and Flyvbjerg, 2004). Such a detector has a high bandwidth and fast response and the signal can be collected from either back scattered light or forward scattered light with the aid of a probe laser beam (Volpe *et al.*, 2007a; Huisstede *et al.*, 2005). The detector measures the geometrical center of the trapped bead, in three dimensions, over a given time scale. In the absence of any biological forces, the motion of a trapped microsphere is determined by the balance between the thermal Brownian motion and the tweezers trapping force. We refer the reader to the paper by Lee *et al* (Lee *et al.*, 2007) that explains in detail the assembly and calibration of an optical tweezers and the choices regarding the detection system. Neuman and Block also make pertinent comments regarding the choice of a quadrant photodiode and position sensitive detector detection system (Neuman and Block, 2004). A recent direct comparison of video and quadrant photodiode detector techniques has been presented by Keen *et al* (Keen *et al.*, 2007) shows the viability of using a high-speed video camera to measure trap stiffness with relevance to multi-particle trapping. Recent techniques in optical tweezers have started to make use of evanescent light scattering to capture weaker long range forces between a single colloidal particle and a flat surface as a function of separation (Clapp *et al.*, 1999). This type of geometry has been successfully applied for the direct determination of weak critical Casmir forces (Hertlein *et al.*, 2008). We remark in concluding this section that most excitingly the particle position may be determined to dimensions that are at least one to two orders of magnitude smaller than that of the trapping wavelength: this is the crux of the reason why such small displacements (and thus forces) may be discerned with this method.

2.3 Other incarnations of optical trapping

Significant attention in the field has been invested into the designing of alternative trapping geometries to that of single beam optical tweezers. Many of the technical developments aim to accommodate specific trapping geometry and add flexibility for forces analysis, simultaneous spectroscopy or the trapping of larger objects. Here we describe a few of these developments.

An elegant and inexpensive approach to create two adjacent but independent optical tweezers has been desired by the biophysics community for stretching and holding macromolecules: the dual beam optical tweezers (Fallman and Axner, 1997) achieves this goal and is seen in figure 4. Figure 4a shows a simple illustration of the dual beam optical trapping setup using a single near infra-red fiber laser and an inverted fluorescence microscope system. Using a set of polarization optics, a single beam can be split into two beams of equal power but each orthogonally polarized (to minimize optical interference effects) with the aid of a Mach Zender interferometer setup, with each beam creating an independently steerable optical tweezers. Here the two tweezers are formed in the same transverse plane, as seen with the tweezing of polystyrene microspheres and gold nanoparticles in figure 4b. In some instances, this form of dual beam tweezers may used together with the high speed steering provided by an acousto-optical modulator (Greenleaf *et al.*, 2005; Shaevitz *et al.*, 2003; Vossen *et al.*, 2004). We shall describe the acousto-optic modulator later in this article.

Other forms of trapping arrangements exist, amongst which the dual beam optical fiber trap (Constable *et al.*, 1993; Guck *et al.*, 2000; Singer *et al.*, 2003; Metzger *et al.*, 2006a; Jess *et al.*, 2006) has taken prominence. As mentioned earlier Ashkin's first trap (Ashkin, 1970) was made with two counter-propagating Gaussian beams. A powerful and now common variant of that experiment is the dual beam fiber trap where the (divergent) output of the two single mode optical fibres are meticulously aligned to be co-axial with respect to each other at a separation of around 100 micrometers. Here the two emergent beams from the fibre create a counter propagating geometry for a single trap. In this trapping geometry, the scattering force dominates due to the divergence of the output beam. The total gradient force from the two beams acts to draw a high refractive index particle into the overlap region between the two beams, whilst the scattering force from each of the beams balances to hold the object in between the two beams. Here, the risk of

optically induced thermal effects i.e photodamage from two photon absorption (Konig *et al.*, 1996), especially when manipulating biological cells, is much lower due to the absence of tightly focused light fields. One is able to immobilize a single particle and collect scattered signal i.e. fluorescence or Raman scattering through an auxiliary microscope objective (Jess *et al.*, 2006). The system has led to the development of the optical stretcher that controllably deforms cells held in the trap. The deformation has a dependency upon the cytoskeleton of the trapped cell and ultimately gives a signature of cancerous versus non cancerous cells (Guck *et al.*, 2001; Lincoln *et al.*, 2004; Guck *et al.*, 2005) The dual fibre optical trapping system may not be readily integrated into a commercial microscope system when compared to the single beam/dual beam optical tweezers system, but is notably compatible with microfluidic flow chambers (Lincoln *et al.*, 2007).

3. Applications within biophysics and the colloidal sciences

Optical tweezers are not usually used to move macromolecules directly. However they offer a powerful method that can indirectly manoeuvre such macromolecules with the trapped microparticles acting as “anchors”. By labeling DNA (deoxyribonucleic acid) strands with biotin and mixing them with polystyrene microspheres (coated with streptavidin - this binds to biotin with high affinity), one can obtain for example DNA strands tethered to microspheres, which the form the “handles” required to indirectly manipulate the DNA strands. From the preceding sections we know that for a single beam tweezers to work well, we must use optically transparent dielectric particles (usually of size 0.5-5 microns in diameter). The determination of the position of the microsphere when trapped is the crucial step to ultimately make quantitative measurements. The behavior of an optical tweezers transducer is very different from a macroscopic force transducer; this is because it works in the very low force regime, where thermal forces are significant. It is also rather different from the atomic force microscopes (AFM) because the motion of an AFM probe is dominated by its relatively high mass and high stiffness so the probe tip shows resonant behavior.

3.1 Molecular and cell biology

Prior to the use of optical tweezers much of the knowledge of mechanical processes in biological systems was gleamed from bulk samples. In many senses this was unsatisfying and gave insufficient insight into the exact mechanisms of processes at the single molecule level. The emergence of optical traps made available non-invasive biological tools with sensitivity and range that is beyond other forms of transducer in this field. In terms of force, optical traps exert forces in the piconewton range so are ideally suited to unravelling DNA, exploring the world of protein-protein interactions and importantly the work cycles of motor proteins. However such forces fall well short of those required to break covalent bonds (1nN) (Grandbois *et al.*, 1999).

The initial studies with optical tweezers were on biological samples that were relatively large in size. Ashkin and colleagues first employed optical tweezers to trap and move bacteria and small numbers of tobacco mosaic virus (Ashkin and Dziedzic, 1987) and then to manipulate single cells (Ashkin and Dziedzic, 1989b), cell organelles (Ashkin and Dziedzic, 1989a) and finally to measure the force of cell organelle movement inside living cells (Ashkin *et al.*, 1990). However such studies did not involve truly quantitative measurements which later followed, opening up the realm of quantifiable single molecule dynamic. We now progress to describing some of these studies.

3.1.1 Single molecule studies

Understanding the living cell is a fascinating aspect of modern biology: the cell has a range of *molecular motors* that operate by converting chemical energy to mechanical work. Exploring the work cycles of such motors and their behaviour has become a major application of optical tweezers in the last two decades. We may broadly group such motors into the two categories of rotary motors and linear motors. Membranes possess what are termed “rotary motors” which derive energy from ionic flow across transmembrane electrochemical gradients. Linear motors use chemical reactions as their power source, for example the hydrolysis of the chemical, adenosine triphosphate (ATP) to adenosine diphosphate (ADP) and phosphate. Optical tweezers can not only give

insights into the forces exerted by both of these types of motor but also into the manner of their motion (Block, 1996)

A major step forward in the use of optical tweezers for single molecule studies occurred when researchers (Block *et al.*, 1990) measured the individual steps taken by kinesin, a molecular *porter* (a subclass of a linear motor described above) during its motion along a fixed microtubule track created upon a microscope slide. The single kinesin molecule was bound with appropriate surface chemistry as described earlier to a microsphere and this was then held close to its microtubule track (Visscher *et al.*, 1999). A buffered salt solution containing the chemical fuel ATP constituted the sample medium. The use of the optical trap and a quadrant diode for imaging permitted detailed observations of the kinesin motor and microtubule track interaction. The trapped sphere was pulled along by the kinesin and the experiment was able to observe approx eight nanometer sized, steps taken by the kinesin molecule as seen in the figure.5. The behaviour of the kinesin molecule is attributed to it pausing for a random interval after taking each step as it waited for a fresh ATP molecule to arrive. In essence a single chemical reaction and its consequences were thus seen in real time!

The optical tweezing geometry needed to be adapted to enable them to be applied to the study of the actin-myosin system, which is the molecular motor associated with muscle action. This interaction occurred in an intermittent fashion and to understand this system a dual trapping arrangement was required. Finer *et al.* (Finer *et al.*, 1995) adapted the dual trap system (Fallman and Axner, 1997) described earlier to hold the two proteins, actin and myosin, in close proximity so several interactions could be recorded from a single molecule. The dual trap system enabled them to hold a single actin filament suspended between two trapped microspheres. This allowed them to manoeuvre the actin filament into close proximity of a third (fixed) myosin coated microsphere. When the proteins made contact with a single molecule of fuel (the sample solution contained the chemical fuel, ATP), the protein breaks down resulting in a single kick, or displacement of actin. This movement was measured by monitoring the position of one of the trapped beads. Subsequent studies by Molloy and colleagues (Molloy *et al.*, 1995) shed more

information upon this process and indeed this system is one of the most widely studied to date using optical tweezers. The studies on motor proteins are likely to be paradigms for future single molecule mechanical studies. Readers who would like further information on optical tweezers based studies of rotary and linear motor proteins are directed to the excellent recent reviews (Greenleaf *et al.*, 2007; Mehta *et al.*, 1999) and the references therein.

Watson and Crick's determination of the double-helix structure of DNA (Deoxyribonucleic acid) is an undoubted landmark for Structural Biology (Watson and Crick, 1953). DNA has been studied extensively woth optical traps. For example, a length of DNA was attached to a microsphere and then extended by dragging through a viscous medium in order to measure its mechanical properties (Perkins *et al.*, 1994). This gave useful information about its polymer mechanics. Knowledge of its mechanical bend-persistence length (about 50 nanometers) informs the biologist about the probability of adjacent regions of DNA forming some contact with one another. For instance, we know that if two pieces of the sequence are 20 nanometers apart then the intervening length of DNA is relatively stiff, if they are 500 nanometers apart then the linking region will be flexible enough to allow the two regions to come together. Later, researchers (Smith *et al.*, 2003; Bustamante *et al.*, 2003) applied very large forces ($> 60\,pN$) to DNA and found that it suddenly overstretches and breaks the double-helical B-form to give a parallel ladder. Figure 6a illustrates force versus extension for dsDNA and ssDNA molecules, obtained with a micropipette and an optical trap. Figure 6b shows the changes in extension observed at a constant extension during polymerization (Poly) or force-induced exonuclease activity (Exo) (Wuite *et al.*, 2000).

A major advance in displacement and force studies with optical tweezers was recently achieved by Abbondanzieri and colleagues (Abbondanzieri *et al.*, 2005) where they achieved resolution of angstrom level motion, as seen in figure.7. In this figure we see a single, transcriptionally active molecule of RNA poymerase (green) is attached to a bead (blue) held in trap T_{weak} (the right hand tweezers) and tethered via the upstream DNA (dark blue) to a larger bead held in trap T_{strong} (the left hand tweezers). The right hand

bead is maintained at a position near the peak of the force-extension curve of T_{weak}, where trap stiffness vanishes (white arrow), creating a force clamp (trap stiffness *k*). During elongation, the DNA tether lengthens and the beads move apart. Owing to the force clamp arrangement, only the right bead moves: displacement is measured for this bead. With the configuration shown in figure.7, they measured the force produced by RNA polymerase as it transcribed a DNA gene. They attached a glass bead to one end of a DNA strand and then allowed the other end to bind to an immobilised molecule of RNA polymerase. When a "transcription buffer" was added (containing all the necessary nucleotides for transcription) RNA polymerase moved along the DNA proceeding with its task of transcribing the gene and producing a new RNA chain. The authors grabbed the bead that was attached to the free end of the DNA and then measured the pulling force produced by the RNA polymerase. The force was about 25 piconewton, perhaps surprisingly this is five times greater than that produced by either of the studied motor proteins myosin or kinesin. The authors measured a mean distance of 3.4 angstrom in discrete steps taken in the transcription process. The advancement reported in this paper included the development of an ultra-stable trapping system. The authors encased the optical path in helium gas so as to stabilize the trapping position removing any instability in laser pointing arising from the surrounding environment. The fact that the refractive index of helium was closer to unity than the use of air reduced variations in the laser positioning. Furthermore, the team developed a constant force clamp by placing one of the two trapped beads slightly off-axis on the non-linear part of the force versus extension curve (Abbondanzieri *et al.*, 2005).

One may explore very exciting aspects of statistical mechanics using optical traps and macromolecules. Intriguingly, developments in statistical mechanical theory can be used to solve fundamental problems in experimental thermodynamics. In 1997, Jarzynski (Jarzynski, 1997) proved an equality relating the irreversible work to the equilibrium free energy difference. This work put forward the notion that it is possible to obtain equilibrium thermodynamic parameters from processes occurring well away from equilibrium. Liphardt *et al.* (Liphardt *et al.*, 2002) explored the Jarzynski's equality by using optical tweezers to mechanically stretch a single molecule of RNA reversibly and

irreversibly between two conformations. Application of this equality to the irreversible work trajectories recovered the equilibrium free energy difference profile of the stretching process. Excitingly this experiment and interpretation forms a link between the statistical mechanics of equilibrium and non-equilibrium systems (Liphardt *et al.*, 2002). A very good account of further experiments and studies of the physics of non-equilibrium systems is given elsewhere (Bustamante *et al.*, 2005).

3.1.2 Cell biology

As mentioned before, Ashkin's early work dealt with the possibility of using optical tweezers to move and manipulation biological cells and its internal organelles (Ashkin, 1997). The trapped microsphere can also be used to tether onto cell membranes such as blood cells (Dao *et al.*, 2005) which had led to the measurements of its mechanical structures. Liang *et al* (Liang *et al.*, 1993) used optical tweezers in combination with pulsed laser cutting (laser scissors), to manipulate and explore the behaviour of chromosomes during cell division in view of studying the complexities of mitosis. Seeger *et al* (Seeger *et al.*, 1991) used the same type of technique for isolation of a microdissected gene. An excellent and thorough review of optical microbeams (laser scissors) may be found in the articles by Berns (Berns *et al.*, 1998) We have already mentioned the optical stretcher that uses the dual beam counter-propagating geometry trap. Guck (Guck *et al.*, 2002; Guck *et al.*, 2001) showed that the forces from two diverging beam (output from optical fiber ends) can steadily measure the mechanical deformation on red blood cells without any tethering. In this way the elastic and viscoelastic properties of red blood cells (RBCs) alter in manner that is often correlated with the manner in which the cells respond to structural and molecular alternation induced by the onset and progression of a disease within the cell. Hence the cell deformation in the presence of the calibrated force can be used to calculate the mechanical properties (shear modulus). Optical traps have been applied to study infected RBCs with optical tweezers by Mohanty *et al* (Mohanty *et al.*, 2005). In hypertonic buffer, a normal RBC rotated by itself when trapped by optical tweezers and the rotational speed increases linearly at lower trap-beam powers and more rapidly at higher powers. In contrast, a malarial parasite-infected RBC did not rotate under the same

experimental conditions. The rotational speeds of other RBCs from malaria-infected sample were found to be an order of magnitude less than for normal RBCs. Biological processes i.e. cell division, vesicle trafficking, endocytosis and phagocyotsis within the cells are crucial to its proper functionality and may be probed with optical tweezers. Using a calibrated optically trapped latex bead, Kress *et al* (Kress *et al.*, 2005; Kress *et al.*, 2007) were able to measure direct cell binding of beads to membranes of living cells during the process of phagocytosis. Kress and co workers were able to measure with a trapped microsphere that the F-actin-dependent stepwise retraction of filopodia, which is responsible to act as cellular tentacles that pulls particles into the cells during cell ingestion, with a mean step size of 36 nm and at counteracting forces of up to 19 pN.

Optical tweezers operating at 980nm were explored for the movement of mature isolated retinal cells. Such studies may lead to the creation of synaptic circuits in vitro. Rod and cone photoreceptors as well as other retinal nerve cell types were manipulated and approximately 60% of the tweezed cells survived for at least 48 hours. The tweezing was observed not to affect the organelle, nuclear and cytoplasmic structure of the manipulated cells. Additionally, in photoreceptors, synaptic vesicles and ribbons were also unaffected. Optical micromanipulation seems to offer provide a strong technique to manoeuvre whole neurons (Townes Anderson *et al.*, 1997). Ehrlicher and colleagues (Ehrlicher *et al.*, 2002) performed intriguing work showing that neuronal growth could be influenced by laser light and attributed the behaviour to the optical gradient force enhancing the neuronal growth. The exact mechanism for such behaviour is still elusive (Ehrlicher *et al.*, 2002; Stevenson *et al.*, 2006)

Optical tweezers are also finding their niche in the immobilization of cell over a probe beam (Xie *et al.*, 2002; Jess *et al.*, 2006; Creely *et al.*, 2005). The probe acts to scatters enough light off the cell (the vibrational energies level) which is then recorded by a detector. This form of optical trapping and detector techniques opens up a new range of spectroscopy technique where the optical traps are used to fix cell in three dimensions. This allows research to choose the specific site for detection i.e. Raman scattering. Combining optical tweezers, Raman spectroscopy and microfluidics allow interesting

prospects for cell studies. Ramser *et al* (Ramser *et al.*, 2005) had control over the media surrounding the cell in their microfluidic chamber that is defined by electron beam lithography that is then moulded into rubber silicon. Different buffers flowed through the channels, while the resonance Raman response of an optically trapped red blood cell (RBC) was recorded. The authors were able to monitor the oxygenation cycle of the cell in real time and understand the effects of photo-induced chemistry. This system has prospects for *in vivo* monitoring of cellular drug response (Ramser *et al.*, 2005). Jess and colleagues were able to combine the dual beam counter-propagating trap with simultaneous Raman spectroscopy creating a form of Raman flow cytometer (Jess *et al.*, 2006). They also were able to take definitive Raman spectra from local parts of the trapped cell and perform multivariate analysis on the spectra ascribing the spectra to specific cell regions.

3.2 Examples of studies of colloidal systems with single beam optical tweezers

A calibrated optical trapping system has application in areas of colloidal sciences, especially in the measurements of weak interaction forces between small particles suspended in a viscous medium (~micrometer). Furthermore, in the microfluidic environment (of low Reynolds number), these small interaction becomes more pronounced. Meiners and Quake (Meiners and Quake, 1999) made use of a dual beam trapping system (Fallman and Axner, 1997) and measured the hydrodynamic interaction between two trapped spheres. They recorded the position fluctuations of each bead and from this determined both the correlation and anti-correlation functions. They showed that these trapped spheres exhibit a pronounced, time-delayed dip in the cross-correlation. This time delay is linked to the relaxation time of the harmonic well created by the tweezers. Further detailed study by the authors showed that the anti-correlations seen were well understood by using the Langevin equation and invoking a standard Oseen tensor hydrodynamic coupling (Meiners and Quake, 1999).

Microrheology refers to the study of the deformation of viscoelastic materials or fluid flow in response to applied force. Crocker *et al* (Crocker *et al.*, 2000) introduce a new form of two-point microrheology that is centered on the measurement of the cross

correlation of the thermal motion of pairs of tracer particles. Thus it is not surprising to infer the possibility of using optical traps for such local viscosity measurements (Nemet *et al.*, 2002; Bishop *et al.*, 2004; Pesce *et al.*, 2005). A more recent paper by Brau *et al* (Brau *et al.*, 2007) summarizes the range of microrheology applications that optical tweezers can be employed in. The non-invasive nature of optical tweezers lends itself very well to exploring the local viscoelastic properties of solutions. The optical trap may both act in an active or passive mode for microrheology applications. In the passive mode one simply monitors the position of the particle and relates these observations with the predictions of the Stokes-Einstein equations. A more active role is also possible: the trapped particle may be dragged through the sample, thus mechanically deforming the medium under study.

4. Optical trapping with structured light field and their applications

4.1 Structured light fields

The previous sections have shown how a single focused light beam in the form of optical tweezers can be a remarkable tool for a diverse range of biological and colloidal science. We firstly consider and indeed question why we might wish to deviate from the use of a single Gaussian beam for a single optical trap and use structured light fields (or beams), either as traps on their own or replicated in arrays. Though the optical tweezers have proven themselves as a general interdisciplinary tool, serious drawbacks and limitations remain. The basic tweezing geometry uses a microscope objective lens and a standard Gaussian laser beam. This arrangement can only provide a single trap with an approximately ellipsoidal focal volume, thus constraining the ratio of trap stiffness in lateral and axial directions. These conventional techniques offer little flexibility for tailoring the trap (and its stiffness) in a three dimensional space. A Gaussian beam expands and diffracts as one knows upon high focusing and potentially limits the types of applications, e.g. optical guiding or the even transportation of particles separated over large distances (millimeter). Rotation would be beneficial to add to the optical toolkit: If one can gain precise rotational control within optical tweezers, a new capability is attained and a calibrated rotational torque (La Porta and Wang, 2004; Volpe *et al.*, 2007b) can be applied upon bio-molecules. In the field of microrheology, a rotating

particle may be used to measure a range of viscoelastic behavior in different media. In a microfluidic environment, rotating single particles or groups of particles can induce pumping action within a laminar flow (Friese *et al.*, 2001; Galajda and Ormos, 2001; Terray *et al.*, 2002) which has potential for controlling flow rates and pumping and mixing small volumes of analyte. By increasing the number of the optical tweezers – creating multiple trap arrays - researchers may start to explore different trapping experiments in parallel or work with larger array of cells or colloids. One can also view a large array of optical tweezers as an ***optical potential energy landscape*** (a topographic array of potential energy wells) which can thus impose a distribution of optical forces over a large area. These landscapes can in turn optically organize colloidal particles into two and three dimensional quasi-crystals structures and can be used to tune the interparticle interaction over an extended physical space. Such an ensemble of self assembled colloidal particles provide a strong platform for potential rich scientific studies in areas such as materials science and thermodynamics (Bechinger *et al.*, 2001; Korda *et al.*, 2002a). The full impact of this technology is yet to be realized. In the following section we aim to address these issues and broadly group our discussion under the heading of ***structured light fields***. There is a consensus in the community that this area is burgeoning and potentially one of the most powerful for future studies within the field of optical trapping. From the materials science viewpoint for example, a system by a given set of microparticles that can be organized and assembled into any form of geometry would be of great importance to material sciences. There is a wealth of novel science that may be performed with not just creating large arrays of trap but also controlling each trap site independently. Additionally one opens up the prospect of collective or co-operative effects between objects held at individual trap sites within a potential landscape. Self assembling of colloidal particles (Dillen *et al.*, 2004) play a vital role in the understanding of phase (liquid-solid) transitions and depending on the optical properties of the particles, one can form composite materials with these colloids. We start by detailing the different ways of multiplexing a single beam optical tweezers into many traps. We then progress to mention some emerging applications, in colloidal and biological science, that have employed such arrays of optical traps and where appropriate compare and contrast different approaches. After this we discuss two popular forms of

non zero order light beams: Firstly Laguerre-Gaussian beams which are light fields with inclined wavefronts and accompanying orbital angular momentum. Then we look at light fields of a "non-diffracting" or propagation invariant nature. These Bessel beams that offer interesting dynamics for guiding and sorting in particular. Both Laguerre-Gaussian and Bessel modes may provide an added ability within different geometries of optical micromanipulation.

4.2 Large arrays of optical traps

In this section we give a brief introduction to four major techniques that allow crafting arrays of optical traps and look at each of these methods involved and comment upon some of the experiments that have been performed using each technique. A direct and straight forward way of obtaining multiple trapping sites is with the use of interference. A second method capitalizes on the fact that optically trapped particles are typically suspended within a viscous medium (i.e. water, glycerol, buffer solution) and operate in a highly overdamped regime. The outcome of such damping is that it brings about relatively slow rate of diffusion of particles over a given space. Thus if a single optical trap is scanned to discrete locations at a rate and returns to its original position quickly enough the diffusion rate of the particle within a given area is not so significant. It would be possible to simultaneously tweeze multiple particles at each of the discrete sites by time sharing the beam between each trapping location. Another technique uses the principles of holography and, for example, imprints the phase of several beam splitters onto a single holographic (photo-sensitive) element: one beam can then be split into multiple beams at the same time but at different spatial points. The beams can then be relayed directly onto the trapping plane forming individual traps. Finally, it is possible to convert phase structure of any form into its corresponding intensity with high optical efficiency by using the generalized phase contrast technique, which increases the optical efficiency of the output power. We remark before continuing that trap multiplexing may be achieved by other means than the four we describe, for example the use of vertical cavity emitting lasers (Birkbeck *et al.*, 2003; Flynn *et al.*, 2002; Shao *et al.*, 2006) . Near-field micromanipulation is also another power method to obtain large area self assembly of particles (Garces-Chavez *et al.*, 2005; Garces-Chavez *et al.*, 2006; Reece *et al.*, 2006;

Righini *et al.*, 2007) is the emergent area of light induced dielectrophoresis (Chiou *et al.*, 2005). Here though we concentrate on the four areas mentioned as they are the most prominent. Let us now look at these in some more detail.

4.2.1 Interferometric trapping

Optical interference is inherently linked to the temporal and spatial properties of the generating light field. Laser sources typically offer very high spatial and temporal coherence that may be used in a number of ways. In the area of optical trapping, interferometric patterns can instantaneously provide an optical potential energy landscape over a large area. If we overlap two light fields taken from a single laser source with an appropriate coherence length, two dimensional interference patterns can be formed which is possibly the most straightforward way to generate multiple beams (traps). To achieve this, one can directly modify the dual beam optical trap, described earlier in figure 4 (Fallman and Axner, 1997) with non-polarizing optics. This creates a Mach Zender interferometer and it is possible to create a periodic linear intensity fringes from the two trapping beams from this system to form an extended optical potential landscape (Chiou *et al.*, 1997; MacDonald *et al.*, 2001). In this manner, Chiou *et al* (Chiou *et al.*, 1997) made use of the translating intensity line traps formed with the help of a microscope objective and the interference fringes from two coherent laser beam, where high refractive index microspheres are trapped and transported. Macdonald *et al* (MacDonald *et al.*, 2001) manipulated low index particles of appropriate size relative to the fringe spacing in between the bright fringes of such an interference pattern. Such two beam interference was also employed by Chowdhury and colleagues (Chowdhury *et al.*, 1985) in studies of laser induced freezing.

With three or more beams, it would be possible to form three dimensional optical lattices for tweezing large arrays of particles (Rubinov *et al.*, 2003; Casaburi *et al.*, 2005; MacDonald *et al.*, 2001). Indeed past studies in optical binding which we will discuss later (Burns *et al.*, 1990, 1989) have shown how multi-beam interference may be used for studies in optical binding, where particle-particle interaction arising from multiple scattering are taken into consideration. As shown in figure.8, a basic three dimensional

optical interference pattern or lattice can be made up from three interfering beams each having a complex amplitude denoted by ψ_1, ψ_2, ψ_3. The complex amplitude of the final interference light field, $\psi_{\text{int}}(\mathrm{r})$, which can be described by

$$\begin{aligned}\psi_{\text{int}}(\mathrm{r}) &= \psi_1 + \psi_2 + \psi_3 \\ &= \mathrm{A}_0\, \mathrm{e}^{\,\mathrm{i}\mathbf{k}_0\cdot\mathrm{r}} + \mathrm{A}_1\, \mathrm{e}^{\mathrm{i}\mathbf{k}_1\cdot\mathrm{r}} + \mathrm{A}_2 \mathrm{e}^{\mathrm{i}\mathbf{k}_2\cdot\mathrm{r}}\end{aligned} \qquad (4)$$

where r is a position vector, $\mathrm{A}_0, \mathrm{A}_1, \mathrm{A}_2$ are arbitrary complex amplitude constants, and $\mathrm{k}_0, \mathrm{k}_1, \mathrm{k}_2$ are the wave vectors in the plane and that $l\mathrm{k}_0 + m\mathrm{k}_1 + n\mathrm{k}_2 = 0$ where *l, m, n* are the optical lattice indices. In figure.8, we show a three beam interference that can generate an array of discrete high intensity spots (inset) spread out with an overall Gaussian distribution. In fact one finds that with only four non co-planar light beams can actually form fourteen different types of three dimensional optical lattices (Bravais lattices), as indicated by L. Z. Cai *et al (Cai et al., 2002)* .

4.2.2 Time shared optical trapping

As mentioned in the introduction of the section 4.2, a particle trapped in an optical tweezers in liquid (medium of high viscosity) is equivalent to an overdamped oscillator. The concept of time shared optical traps is that one may remove the tweezing beam for a very short period of time to tweeze another object and return to this original tweezed particle some time later. Of course, once the optical field is moved away from particle's current position, the particle is left free to diffuse due to Brownian motion. If the tweezing beam returns to its original position within a relatively short time scale (less than a 0.1 millisecond or so) before a micron-sized particle diffuses away due to Brownian motion, the mean position of the particle essentially remains unchanged (it would only have diffused the order of a few nanometres). The distance *d* which the particle would diffuse away from its original trapping position is given by

$$d = \sqrt{2\frac{k_B T}{6\pi\eta r}t} \qquad (5)$$

where k_B is the Boltzmann constant, T is the temperature, η is the viscosity, r is the radius of the particle and t is the time of absence of the optical tweezing beam. Hence, the smaller the particle the further the diffusion distance will be whilst the trap is absent. This characteristic of the time-shared multiple optical traps is also its Achilles' heel and needs careful consideration in design of all such systems.

Using a pair of fast scanning mirror driven by galvanometers, Sasaki and colleagues (Sasaki *et al.*, 1991, 1992) demonstrated that by scanning a single trap in a designed path repetitively one may obtain a specific two dimensional light pattern, where microspheres would find themselves aligned onto the designated light patterns. By rotating the trap in a circular path over a few hundred Hertz, they were also able to cage and transport reflective metallic particles or low refractive index microdroplets. Visscher and colleagues (Visscher *et al.*, 1993) integrated a two-axis galvanometer mirror onto a confocal fluorescence microscope system to achieve rotational control of *E. coli bacterium*. K. Visscher et al. (Visscher *et al.*, 1996) improved the scanning laser trapping system with acoustic optical deflectors (AOD, where the optical trap can be steered at a rate of a few KHz (> natural frequency response of a micrometer sphere)). This form of automated tweezing technique has greatly improve the precision and repeatability of single molecule experiments (Lang *et al.*, 2004). In essence, these beam steering systems provide a reasonably accurate and reproducible two dimensional (x-y) intensity pattern by deflecting the input beam.

The modes of scanning can be achieved by the galvanometer controlled mirror (Sasaki *et al.*, 1991, 1992), piezo-driven deflecting mirrors (Mio *et al.*, 2000) or acousto-optic deflector (AOD) (Visscher *et al.*, 1996; Terray *et al.*, 2002). The scanning mirror techniques operate by scanning a pair of oscillating mirrors made use of two highly reflective mirrors aligned such that each provides scanning in each of the axis (x, y). While the AOD technique makes use of deflection by a diffractive grating formed with acoustic wave. The relatively slow scan rates (few hundred hertz) offered by the galvanometer mirrors (due to inertia) impedes the possibility of being able to form multiple traps. The fastest rate at which a mechanically deflecting mirror can be put into

oscillation is around ~ 12kHz (GSI-Lumonics Inc) as we need to consider the mechanical inertia of the system. However, an AOD can easily accomplish a repetitive scan rate of the order of a MHz due to the fast travelling speed of the acoustic waves. At such high speed scanning, a single beam can be "shared" between different positions. A two axis acousto-optic deflector (AOD) is typically made up of two crystals (tellurium dioxide, $TE0_2$ or Lithium Niobate, $LiNbO_3$) lined up orthogonally along the propagation axis for steering of infrared laser beam. Within one AOD, a standing acoustic wave modulates the refraction index of the crystals which in turn diffracts the light propagating through it much like a phase grating. Tuning the depth of the phase change can also modulate the intensity of the laser beam and by moving the grating you can steer the first diffracted order in one direction. Two AODs scanning in orthogonal directions can be combined in series to provide both *x* and *y* deflections of the optical trap as shown in figure 9. Each deflector consists of a crystal e.g. Tellurium oxide with piezoelectric transducers with an applied RF voltage to creating a standing wave across the crystal. The input laser beam is incident at the Bragg angle (θ) is efficiently diffracted by the sound wave grating and deflected by an angle φ (see figure 9).

The AOD system does however suffer from some optical efficiency tradeoff due to its diffractive nature, whereas the galvanometer scanning mirrors have a high optical efficiency owing to the high reflectivity in the mirrors, though of course, as noted inertia is a limitation for this latter system. The first diffracted order which typically contains around 60% of the total input optical power is used. Furthermore, the AOD optical efficiency gradual decrease with respect to the deflection angle of the grating and thus create a less than ideal spread of intensity distribution. This can be compensated by imposing an amplitude modulation to even out the intensity which would mean that each AOD needs to be characterized for the change of intensity versus deflection angle. This change of intensity would have a marked effect on the stiffness of the trap generated. This would also mean that the number and quality (trap stiffness) of each of the "time-shared" optical traps is very much dependent on the response time of the all optoelectronic components: the quality of the electronics and the programming aspects (Wallin *et al.,* 2007) . In figure 9, we illustrate the operation of the two-axis AOD system.

A linear polarized laser beam passes through a half waveplate (controls the direction of the polarization of the light beam) before entering the pair of AODs. A simple demonstration of the two dimensional scanning from an AOD can be seen in figure 9. A slow linear scan is applied on each individual AOD and each sound wave grating from each AOD diffracts the input beam into its individual diffracted orders. In figure 9 we illustrate the first four diffracted orders (x, y) arranged over a two dimensional grid where the intensity at each of the diffracted orders (0, 0) is the undiffracted Gaussian spot, (0,1) and (1,0) vertical and horizontal scanned line intensity (each of the AODs) and (1,1) is a diagonal scanned line intensity which is the combination of the two scanning axis of AODs, as seen in the figure 9.

4.2.3 Holographic optical trapping

Dennis Gabor won the Nobel Prize in 1971 for "his invention and development of the holographic method", where he was able to reconstruct three dimensional images by way of interferometry. Gabor has also looked in the reconstruction of images for the purpose of microscopic imaging (Gabor, 1951). Holography is a technique where the intensity and phase (complex amplitude) of an object is captured by the interference patterns between the light scattered of the object and a reference light field and recorded upon a light sensitive medium (hologram). Illuminating the hologram with the reference beam can therefore reveal a virtual image of the object. One of the first implementations of the tweezing of an ensemble of colloids was by Fournier *et al* (Fournier *et al.*, 1995.) who illuminated a binary hologram and generated self-images of the grating (Talbot images) in planes that are periodically positioned along the direction of propagation. Holographically generated Laguerre-Gaussian beams were used for trapping and rotation in 1995 by He *et al*. (He *et al.*, 1995b; He *et al.*, 1995a). This study will be discussed in more detail later.

One can numerically superimpose the complex amplitude of a "desired" (output) light pattern and a reference (input) beam to form a computer generated hologram from which the desired light pattern can be reconstructed. As such, one can effectively transform an input Gaussian light field into a more elaborate form at will. This means that the

technique of computer generated holography can be utilized to shape the optical potential of the trap by altering the complex amplitude of the input light field, $\left|\mathrm{I}_{\mathrm{int}}(x,y)\right| \mathrm{e}^{\,\mathrm{i}\alpha(x,y)}$, where $\mathrm{I}_{\mathrm{int}}$ is the amplitude, α is the phase of the light field, (x ,y) are the Cartesian coordinates and (u,v) are the corresponding spatial frequency co-ordinates. In modern optics, Fourier methods play a major role in many of the adaptive optical system where a lens can be considered as performing a fourier transform, see figure 10. A complex amplitude of $\left|\mathrm{I}_{\mathrm{int}}(x,y)\right| \mathrm{e}^{\,\mathrm{i}\alpha(x,y)}$ at the back focal plane of the lens is the fourier transformed onto the front focal plane as

$$I_{front}(u,v) = \iint \left|\mathrm{I}_{\mathrm{int}}(x,y)\right| \mathrm{e}^{\,\mathrm{i}\alpha(x,y)} \mathrm{e}^{-\mathrm{i}\frac{2\pi}{\lambda f}(ux+vy)} dxdy \qquad (6)$$

where *f* is given as the focal length of the lens and λ is the wavelength of the light. By manipulating the input complex amplitude function $\left|\mathrm{I}_{\mathrm{int}}(x,y)\right| \mathrm{e}^{\,\mathrm{i}\alpha(x,y)}$ with a numerical algorithm, the output complex amplitude $I_{front}(u,v)$ can be manipulated. For trapping, one would need to place a microscope objective with its back focal plane coinciding with the fourier planes of the lens in figure 10 (a) such as to image the intensity patterns onto the sample plane.

A number of numerical algorithms such as superposition algorithms, Gerchberg-Saxton algorithms, random mask encoding, direct-binary search algorithms and simulated annealing can be use to optimized the holograms (Tricoles, 1987). However, in this section, we choose to give attention to the Gerchberg-Saxton algorithm due to its high conversion efficiency and popularity in the field. In figure.10 (b), a simple flow chart is drawn to illustrate the initial loop on the iterative Gerchberg-Saxton (GS) algorithm with a fast Fourier transform (FFT). In figure 10 (b) we show that the algorithm starts by first obtaining the initial complex field in the hologram plane $U_n(x,y)$ with the input beam $I_{int}(x,y)$ and the estimated phase at the target plane $\Phi_{n-1.}$ By using a FFT, one can then obtain the initial calculated phase at the target plane ψ_n. After which combined this phase distribution in the target plane with the target intensity, $I_{final}(x,y)$, giving the complex field $U_n(x,y)$. Lastly, one calculates the corresponding phase distribution in the hologram plane, Φ_n, by inverse Fourier transforms (IFFT). Over a number of iterations, the actual

intensity in the target plane matches to the desired intensity there, $I_{final}(x,y)$. Φn is the corresponding phase-hologram pattern needed to produce this intended field at the target plane. In figure 10 (a), we see the reconstructed image $I'_{final}(x,y)$ after 50 iterations. The reconstructed pattern does fit the intended intensity up to > 90% with the GS algorithm. Such a holographic technique can generate a two dimensional intensity pattern (image) which will only allow tweezing in a single transverse plane. Whyte and Courtial (Whyte and Courtial, 2005) showed that this technique can be extended to allow three dimensional shaping of the beam which forms a three dimensional holographic optical traps. For the sake of completeness, it is also worthwhile to note that binary direct binary search, time sharing and encoding multiple holograms of a Fresnel lens have also been demonstrated to be able to generate three dimensional arrays holographic traps (Melville *et al.*, 2003; Jesacher *et al.*, 2004; Leach *et al.*, 2004).

The holographic element can be made with the use of computer generated holograms and result in a static diffractive optical elements, or implemented with a liquid crystal display, spatial light modulators, to generate arrays of beams at will. The calculated hologram (binary or phase) pattern can be etched into glass or plastic which can only be used to generate one type of complex trap pattern. Due to the recent progress in display technology, programming spatial light modulators can now dynamically change the phase holograms. With current high resolution programmable spatial light modulators and reasonable refresh rates has opened up the prospect of dynamically changing the hologram in real time and thus actuating multi-particle motion. Many of the current spatial light modulators (SLM) used for holographic optical tweezers make use of the reflective nematic liquid-crystal (LC) display which usually operate by electrically or optically addressing the individual liquid crystals within the display. In the electrical case, the electrical potential difference causes the liquid crystal molecules to align themselves along a direction thereby changing its refractive index which in turn modulates the phase of the input light field. Most nematic SLMs typically have 256 phase levels but these have slow refresh rates (typically up to~60 Hz). Ferroelectric SLMs, in contrast, have been employed in optical trapping and have demonstrated their higher

refresh rates of ~10 kHz, but they are limited to only two level of phase changes (Hossack *et al.*, 2003).

Holographic optical trapping (HOT) remains possibly the most enticing of the upcoming prospects for multiple trapping and generation of structured light fields (Liesener *et al.*, 2000; Dufresne *et al.*, 2001; Curtis *et al.*, 2002; Hossack *et al.*, 2003; Melville *et al.*, 2003; Leach *et al.*, 2004; Sinclair *et al.*, 2004a; Sinclair *et al.*, 2004b; Polin *et al.*, 2005; Lee and Grier, 2005; Schmitz *et al.*, 2005; Grier and Roichman, 2006; Martin-Badosa *et al.*, 2007). This is due to three overriding issues: firstly, they do not involve time sharing of the light field as observed with acousto-optical devices and all of traps operate simultaneously; the diffractive optic element (DOE) can also be implemented in a manner that allows the beam to overcome any inherent aberration present, i.e. seidel aberrations present in the optical path can be compensated for (Wulff *et al.*, 2006). Finally the use of appropriate algorithms can generate structures in three dimensions. We refer the reader to recent papers that discuss the technicalities of setting up and optimizing a HOT system in detail (Martin-Badosa *et al.*, 2007; Polin *et al.*, 2005). Despite the dynamic potential of the holographic optical trap, a spatial light modulator does suffer from relatively poor diffraction efficiency at the first order (~30-40%) and inability to withstand a input beam of high optical power (>2 Watt).

The Generalised Phase Contrast (GPC) technique is an alternative that does not use the SLM as a hologram device but rather more directly as a phase element. Since the GPC is not a holographic method and therefore does not suffer from the potential complexities associated with calculating and updating new holograms for trapping and motion of many particles (Eriksen *et al.*, 2002; Rodrigo *et al.*, 2002). We describe this briefly in the next section.

4.2.4 Generalized phase contrast technique for multiple traps

In 1676, Antonie van Leeuwenhoek became one of the first man to have ever set his eyes on the bacteria with a home-made microscope, which he later reported to the Royal society and ignited the field of microbiology (Pontecorvo, 1963). As we now know, many

biological microparticles are often difficult to see due to their refractive index being very close to that of their surrounding medium. It took another two hundred years before Frits Zernike invented an imaging technique that circumvented these issues with an elegant physics solution: converting faint phase gradients into intensity variations by the method of phase contrast with phase contrast technique (Zernike, 1955). In a related fashion, Eriksen *et al* (Eriksen *et al.*, 2002) and co-workers reformulated Zernike's phase conversion such as to convert phase structures into intensity pattern. This technique makes use of a phase modulated SLM that is placed at the conjugate (fourier plane) to the trapping plane with a small phase shift, positioned at focal plane between the two fourier lenses. This generalized phase contrast technique (GPC) is a very straightforward and efficient method as no numerical algorithms are used since it is a direct phase to intensity conversion. It is possible to extend the GPC method to three dimensional trapping with counter propagating dual beam geometry (Perch-Nielsen *et al.*, 2005) and to develop systems with automatic alignment.

4.2.5 Studies with structured light fields

Now that we have explored the various major methods of multiple trap generation we progress to describing some of the major experiments using these trap arrays.

4.2.5.1 Brownian diffusion

A microsphere suspended within a viscous medium may be considered a Brownian particle. Optical tweezers generates a parabolic potential well that acts to suppress the Brownian motion of a microsphere. One can imagine that a trapped microsphere is situated at the lowest point of the potential well. By switching the potential off, the microsphere will exhibit diffusive motion due to the Brownian thermal noise. In order for the sphere to escape from the potential well, it would need to generate a potential energy larger than the energy potential of the well. By creating a modulated potential (high and low intensity gradient) over time and large region (potential landscape), a particle would seek to diffuse towards the region of higher optical gradient. Faucheux (Faucheux *et al.*, 1995b) and colleagues devised an experiment using a pair of galvanometer scanning mirrors to introduce a toroidal trap with an intensity modulation to observe biased forms

of Brownian diffusion with optically trapped objects. Such optically induced thermal ratchets may have some analogy to the biological Brownian motors (Derenyi and Vicsek, 1995). Lutz *et al* (Crocker *et al.*, 1999; Lutz *et al.*, 2004a; Lutz *et al.*, 2004b) studied the diffusive behavior of colloidal particles while they are optically confined within a scanning optical tweezers and have observed that single-file colloidal diffusion occurs. Such Brownian ratchet effects can be studied with other structured light fields, namely Laguerre-Gaussian light beams (ref Roichmann 2007).

4.2.5.2 Large scale colloidal dynamics

Colloidal science has undergone a major renaissance in recent times and remains an area where optical trapping continues to make an important impact. On the most basic level, individual colloidal interactions are complex because they are *solvent-mediated*. The Nobel prize winner Jean Perrin pioneered the use of monodisperse colloidal particles as model thermodynamic systems. Perrin's works involved the detailed observation of the different ways in which colloidal particles aggregate and interact. His early experimental studies showed concrete evidence that colloidal systems offer an excellent level of controllability and tunability of inter-particle interaction that can give important insights into the working of atomic systems and that are readily amenable to measurements. Furthermore, the strong and weak interacting forces between chemically treated surfaces or other solvent may illuminate our understanding in surface bonds i.e Van der Waals forces. With the use of multiple optical traps and patterned optical potential energy landscapes, one has unprecedented access to *colloidal interactions*. The pair potential between two particles controls thermodynamic behavior (such as the crystallization vital to photonic applications), is also inherently many-bodied: in principle the potential depends on the positions of *all* particles. While the two-body part of the potential has been studied using optical tweezers for some time, studies of the many-body counterpart with trapping is still in its infancy in many respects. We now progress to looking at some of the key experiments in this area.

Chowdhury *et al* (Chowdhury *et al.*, 1985) imposed a simple periodic two beam interferometric light pattern upon a two dimensional system of colloidal particles

confined between two glass plates. By modulating the periodic of the interferometric pattern, they were able to examine phase transition (liquid to solid) in such a colloidal structure much like a freezing process which is now termed as "laser induced freezing" based on observation with light scattering detection. The effects of optical forces over a large amount of colloidal are subsequently studied in detail by Golovchenko and Fournier (Burns *et al.*, 1990, 1989) where they arranged particles using a large Gaussian beam and again by interfering multiple beams from a single Argon-ion laser source. Their observations led to the creation of matter (fixed colloidal structures) with just the optical forces. More recently, Brunner and Bechinger (Brunner and Bechinger, 2002) studied an optically induced "melting process" with optical lattices formed from three interfering beams to obtain trimers (three colloids) at each trap site as seen figure 11. In this figure we see the contour plots of the lateral density distribution p and the averaged local particle density $ploc(x, y)$ for different light potentials $V0$: (a),(b) $0k_BT$, (c),(d) $40k_BT$, (e),(f) $60k_BT$, and (g),(h) $110k_BT$. The horizontal axes are x and y, respectively. All units are in μm. The optical potential energy landscape was formed by three beams of a linearly polarized Nd:YVO_4 laser (wavelength 532nm with maximum optical power of 5 Watts) which intersected at an angle of 60 degree in the sample plane, where they formed a triangular interference pattern.

Studying the Brownian dynamics between two colloids (Meiners and Quake, 1999; Crocker, 1997) researchers have detected the weak hydrodynamic coupling between two spheres, each held in close proximity by independent optical tweezers, while suspended an incompressible fluid. With large potential energy landscapes and high resolution video microscopy, it is possible to extend that study onto long range entropic forces between colloids in a confined in an extended potential (Crocker and Grier, 1996; Crocker *et al.*, 1999). Lutz (Lutz *et al.*, 2006) investigated interesting behavior with three colloidal spheres travelling along a circular scanning tweezers with a periodic peak potential barrier. Hydrodynamic interactions between the colloids assist the three-body system to surmount the optical potential barrier. With holographic optical tweezers, Korda (Korda *et al.*, 2002a) looked at dynamics of hydrodynamic forces from an ensemble of colloids

distributed in a single monolayer. With the use of video tracking programs, they were able to determine the evolution of the "phase transition" of the monolayer of colloidal.

4.2.5.3 Optical sorting

Biomedical scientists are interested in selecting or sorting cells at will. For example when considering a blood sample, one may wish to perform a cell count to exactly determine the number of red cells present. A cell biologist or clinician would be very interested in selecting rare cells e.g. stem cells from a large cell population. This has provided the impetus for bone marrow transplantation and a more detailed understanding of diseases of the haematopoietic system. In regenerative medicine sources of stem cells can be exploited to provide new disease free tissue and in cancer where the key target cells for disease development and thus for successful therapy are the tumour stem cell populations. Recent advances in optically based methods for sorting at the micrometer size scale have shown promising results in the sorting of different types of biological cells. For optical sorting, we can start to look at the microfluidic flow and the optical forces at work. Figure.12 shows a straightforward method to implement optical sorting which is simply to have an optical force "switch" that drags pre-selected cells into a desired chamber or flow cell (Wang *et al.,* 2005). This is akin to a microscopic fluorescent activated cell sorter (FACS). Cells are aligned to the center of the channel by hydrodynamic focusing. Cells are analyzed and then switched based on their detected fluorescence. Target cells are directed by the laser to the collection output while all other cells flow to the waste output. However, for higher throughput, we need to start looking at higher flow rates or dealing with a more highly dense population. It would also be desirable to sort based upon intrinsic properties (passive sorting) such as size or shape rather than make use of markers (active sorting). If we were to flow the liquid that is bearing individual particles (colloidal or cells) across such an optical potential energy landscape, we would open up a competition between Stokes forces within the liquid and optical forces imposed on the particle (Korda *et al.*, 2002b). Each particle may have a range of physical response based on their size, overall refractive index and geometrical shape. With controllability over the landscape, it would be possible to sort particles into the sizes and shapes (MacDonald *et al.,* 2003; Lacasta *et al.*, 2005; Ladavac *et al.*, 2004;

Cizmar *et al.*, 2006b). Optical potential energy landscapes formed by multiple optical traps could take the form of an array of line traps or two or three dimensional array of trap spots (see figure 8). Such landscapes have intriguing properties when they interact with cells and colloidal particles placed upon them. In the presence of flow over such an optical potential energy landscape particles can follow paths across the landscape that are inclined with respect to the flow direction: indeed different particles experience different potential energy landscapes thus ultimately following different trajectories. This can form the basis for some interesting competitive effects and more generally optical separation in two dimensions in a wholly passive or marker-free manner.

Sorting of colloids is also fascinating and provides monodisperse samples that would be otherwise difficult to achieve otherwise. Ladavac *et al* (Ladavac *et al.*, 2004) made use of a holographic generated array of optical traps to selectively deflect large silica spheres (diameter 0.79microns) from small ones (diameter 0.5 microns) within a single flow channel by virtue of their size relying upon a differing response to the landscape. As mentioned before, interferometric traps can form large three dimensional optical lattices that may be used for this same purpose of passive sorting. MacDonald *et al* (MacDonald *et al.*, 2003) created a three dimensional optical lattice using five light beams independently controlled and focused through an aspheric lens. By flowing particles through this lattice they observed the phenomena of optical sorting (or separation): particles flowing through the lattice were seen to follow trajectories that were dependent upon the particles intrinsic properties: deflection of particles was observed based both upon size and refractive index. Low index particles in the form of protein microcapsules (ultrasound contrast agent) were also separated by size. Subsequent studies by the authors showed some preliminary evidence for the passive sorting of red and white blood cells in such a system (MacDonald *et al.*, 2004). In more recent work, a time modulated optical sieve created by interference was also used for sorting of poly-disperse colloids without any flow present (Ricardez-Vargas *et al.*, 2006). Moving interferometric pattern imposed onto surface can also be applied to the sorting of nanometric particles (Cizmar *et al.*, 2006b). The simultaneous sorting of four different types of colloidal sizes into four parallel laminar flow streams purely using a time-generated optical potential energy

landscape with AODs (Milne *et al.*, 2007b), was seen. This optical fractionation is shown in figure 13 where once can see the plotted trajectories of four different types of silica spheres (D) 2.3 μm,(C) 3.0 μm, (B) 5.17 μm, and (A) 6.84 μm against the direction of the flow. AODs offer certain advantages to the use of SLMs due to their ability to handle higher power and create potentially larger area optical potential energy landscapes. We refer the interested reader to other more concise reviews in particle separation using optical fields (Dholakia *et al.*, 2007b; Dholakia *et al.*, 2007a).

4.2.5.4 Optical organization of particles and cells

The assembly function of optical tweezers can readily be achieved through computer controlled spatial light modulators or counter propagating AOD traps With multiple optical traps, one can also start to look at creating colloidal crystals or cells fixed in a specific geometry. In the material sciences, the engineering of crystalline structures requires the control of orderly arrangement of the atomic lattices to modify the properties of a material. There are many forms of crystalline structures defined by its crystallographic axes and the angles between the axes i.e. isometric, tetragonal, orthorhombic, monoclinic, triclinic. It is also possible to engineer quasi-crystals which have long-ranged orientational order that can be made up of dielectric materials with specific optical properties, thus provides a route to the development of photonic band gaps materials. Macdonald and co-workers (MacDonald *et al.*, 2002) first used interferometric patterns from two co-propagating Laguerre Gaussian (LG) beam to trap and rotate cubic structures. With holographic optical traps, many researchers (Melville *et al.*, 2003; Leach *et al.*, 2004; Grier and Roichman, 2006; Roichman and Grier, 2005) have looked extensively into this area of generating three dimensional quasi crystal structures and unit cells. In figure 14, we see a large ensemble of particles trapped and arranged in a quasi-crystalline structure work by Grier and colleagues. In figure 14, a laser beam is reflected by two mirrors M1, M2 and M3 is expanded and directed onto a liquid crystal spatial light modulation (SLM), which imprints a computer generated hologram (CGH) onto its wavefronts. The 200 × 200 pixel region of a CGH shown encodes a pattern, $I(\mathrm{r})$ of 119 optical tweezers that are arranged in a quasiperiodic

arrangement. The phase hologram is relayed onto the input pupil of an objective lens that focuses it into holographic optical traps. Each optical tweezers traps an individual 1.5 micrometer (in diameter) colloidal sphere in water.

With a time-shared optical tweezing system, Vossen *et al* (Vossen *et al.*, 2004) have shown interesting results where three dimensional colloidal structures are trapped and organized with two layers of optical traps steered with a single dual axis AOD. To create the two layers of time-shared multiple traps at different planes, a single laser beam is split into two beam paths that are recombined at back of microscope objective with different divergence, thus resulting in a different axial trapping position. By synchronizing the Pockels cell after the polarizing beam splitter cube with the AOD they were able to create two independent arrays of optical tweezers that trapped fluorescence particles in three dimensions as shown in figure 15(a). Figure 15(b) shows the confocal images of fluorescent particles trapped in a three dimensional array of tweezers created by synchronizing the Pockels cell and the AODs where (i) Six particles were trapped in the upper plane and (ii) nine in the lower plane (iii) Between the two trapping planes fluorescence from particles in both planes was detected. The height difference between the two trapping planes was 1.7 micrometer. The upright objective was used for trapping while the inverted objective was used for imaging. The 1.4 micrometer diameter FITC–SiO_2 (fluorescein isothiocyanate silica spheres) particles were dispersed in ethanol, and only their fluorescent cores were imaged and (iv) shows an image was computer generated on the basis of the confocal data. The three dimensional fluorescence colloidal structures are optically assembled and imaged with confocal fluorescence microscopy as shown in figure 15.

Recently, studies have organised and permanently fixed both colloid and separately cells using multiple optical traps. For example, Jordan (Jordan *et al.*, 2004) *et al* fixed three dimensional crystals structures in a polymeric host while held in the traps. Jordan (Jordan *et al.*, 2005) also applied the technique to move individual *E. coli* cells in the liquid gelatin at predefined positions. When the cells are fixed in place, the lasers were switched off. The three dimensional configurations of cells within a gelatin sample at predefined

positions remained intact for many days. The cells survived within the gelatin matrix for several days when provided with the approximate nutrients. This technique can be used to help understanding the role of position, proximity and number of neighboring cells, not only in cell culture, but also in cell differentiation. The arrangement of a variety of different cell types in complex architectures promotes tissue differentiation and growth within the field of cell/tissue engineering.

Akselrod and colleagues (Akselrod *et al.*, 2006) used multiple optical traps to generate three dimensional heterotypic networks of living cells in a hydrogel complex (see figure 16). They showed cell viability after assembling Swiss 3T3 fibroblasts cells which are surrounded by a ring of bacteria and also amass hundreds of *Pseudomonas aeruginosa* into two- and three-dimensional arrays. In essence the AOD and its fast dynamical behaviour was used generated the trap array whereas the SLM here was exploited as a device to impose both a diffraction grating (lateral offset of the arrays) and a Fresnel lens (to offset the array along the beam propagation axis) to yield a three dimensional nature to the arrays. The dynamic optical trapping systems combined the strengths of the spatial light modulator with that of the acousto-optic modulator. Apart from the technical novelty, this particular shown that living cell microarrays generated with optical traps may pave the way for exploiting the functionality of cells and processes such as cell differentiation and could prove to be powerful tool within systems biology and tissue engineering.

4.2.5.5 Multi-point force transducers

An issue for any multiple trap array is the ability to measure trap stiffness for all the trap sites simultaneously and in real time: such a measurement is of course crucial if one is for example trying to perform complex cell mechanotransduction studies and needs force measurements at various positions upon a given cell or perform multiple single molecule studies in parallel. Whilst the quadrant photodiode has the high bandwidth and rapid response time desired, it is only realistically able to measure when one or two traps are involved and is not readily suitable for a multiple trap array. Digital video devices (charge couple device (CCD) or complementary metal–oxide–semiconductor (CMOS))

have, in recent years, improved in terms of capture speed and frame rates that has been widely implemented in microscopy imaging systems (Howard, 2007).The image of the trapped particle is relayed onto an imaging plane of the digital camera which captures the particle's fluctuation of its position using an ordinary (~30 frames per second) or even a fast speed camera (~ 400 frames per second) over a length of time (Polin *et al.*, 2005; Polin *et al.*, 2006) . A histogram of positions over a given time period is then plotted so as to measure the variance of the position, $\langle x^2 \rangle$. An object in a harmonic potential would have a potential energy (thermal fluctuation) equal to its trap stiffness, *k* (position fluctuation). By employing the equiparition theory it would then to possible to determine the trap stiffness,

$$\frac{1}{2}k_B T = \frac{1}{2}k\langle x^2 \rangle \qquad (7)$$

where k_B is the Boltzmann's constant, and *T* is the absolute temperature. This measurement technique does not rely on the value of the viscous drag and can be extended to multiple trapping sites with simply imaging the trapping plane onto the camera's imaging plane. The advantage of using this technique is the possibility of calculate the trap stiffness for each trapped particle. Thus one can envisage that with the equipartition theory and a high speed camera (> 10 thousand frames per second), it would possible to calibrate multiple force transducers is a good way to ascertain the several trap stiffnesses in real time. This would likely to emerge as a key area in the instrumentation of advanced optical trapping apparatus in the near future. Already we are seeing the first indications of this possibility: Leonardo and co-workers (Di Leonardo *et al.*, 2007) explored the hydrodynamics of a ring of microparticles held by an array of holographic optical traps. The hydrodynamic coupling between the particles gives a set of eigenmodes. Each such eigenmode relaxes with a characteristic decay rate (eigenvalue) that may be recorded with analysis of the position of each particle. The authors saw good agreement between their experimentally recorded eigenvalues and the numerical predictions of the Oseen theory.

4.3 Non-zero laser modes

Whilst multiple trap arrays created with the various methods above are undoubtedly powerful one may also wish sculpt the phasefront of a given light field or alter the wavevectors of the light field to create more elaborate light fields. Light beams emitted from a laser cavity are electromagnetic fields that, solutions of the wave equations, satisfy appropriate boundary conditions. Some of the solutions form a complete and orthogonal set of functions (Kogelnik and Li, 1966) and are called the "higher modes of propagation". Essentially, any transverse mode optical distribution can be expanded in terms of these modes. These higher order transverse modes are often referred to as non-zero order light fields. These non-zero order light fields have come to the fore in recent years in several fields in atomic, molecular and optical physics: optical micromanipulation is no exception. Light fields may impart linear momentum to trapped objects which has been to core to our discussions so far. With higher order modes, in particular the Laguerre-Gaussian (LG) modes, angular as well as linear momentum transfer can take place to trapped objects due to the helical wavefronts of the field. This helical wavefront leads to an unusual trajectory to the Poynting vector: this vector denoting energy flow possesses an azimuthal component, that in turn leads to the concept of orbital angular momentum (Allen *et al.*, 1992). The tunability of the orbital angular momentum $l\hbar$, where l is the azimuthal index of the beam, in such light beams offers itself as a useful tool in the exertion of torques on particles on a toroidal trap by simply increasing the in contrast to the optical torque arising from spin angular momentum which varies with optical power (Friese *et al.*, 1998) and is limited to $\hbar$ per photon. Another light field that has seen many applications in optical micromanipulation is the Bessel beam. These beams may exhibit propagation invariant or “non-diffractive” characteristics: thus it maintains its beam waist size without considerable broadening. The beam can even reform or reconstruct beyond obstacles when partly obscured. With such abilities, the Bessel beam definitely brings valuable features to the field of optical trapping and even in the broader area of biophysics (Tsampoula *et al.*, 2007). We commence our discussion of these unusual light modes with the Laguerre-Gaussian beam.

4.3.1.1 Laguerre-Gaussian light beams and its applications

In the context of the transverse laser mode theory, the circularly symmetric Laguerre-Gaussian (LG) laser modes form a complete basis set for paraxial light beams and thus one may express any given light mode as a sum of them. A given mode is usually denoted LG_p^l where *l* and *p* are the two integer indices that describe the mode. The azimuthal index *l* refers to the number of 2π phase cycles around the circumference of the mode and (*p*+1) indicates the number of radial nodes in the mode profile (see figure17). For each increment of *p*, an additional concentric ring is added to the mode profile while an increment of *l* results in an increase in the diameter of the dark core, termed optical vortex, located on the beam axis. The azimuthal index *l* is often referred to the topological charge of the optical vortex. LG modes with $l \neq 0$ have garnered much interest owing to their azimuthal phase term $\exp(-il\phi)$ and that gives rise to a well defined orbital angular momentum (OAM), of $l\hbar$ per photon (Mair *et al.*, 2001). This may exceed any angular momentum associated with the spin angular momentum state of the field. The physical interpretation of the orbital angular momentum was given earlier, being couched within the idea of an inclined optical wavefront (Allen *et al.*, 1992; Allen *et al.*, 1999) and azimuthal component of the Poynting vector. Under the paraxial approximation, this form of angular momentum in the LG beam can be decoupled from spin angular momentum arising from its polarisation state(Barnett, 2002). A general description of the electric field of a LG mode $E(LG_p^l)$ of indices *l* and *p* may be written as:

$$E\left(LG^{l}{}_{p}\right) \propto \exp\left[\frac{-ikr^2 z}{2\left(z_r^2 + z^2\right)}\right].\exp\left[\frac{-r^2}{\omega^2}\right].\exp\left[-i\left(2p + l + 1\right)\arctan\left(\frac{z}{z_r}\right)\right].\exp\left[-il\phi\right] \times(-1)^p.\left(\frac{r\sqrt{2}}{\omega}\right)^l.L_p^l\left(\frac{2r^2}{\omega^2}\right) \tag{8}$$

where z denotes the distance from the beam waist, z_r is the Rayleigh range, k is the wave number, ω is the radius at which the Gaussian term $e^{\left(\frac{-r^2}{\omega^2}\right)}$ falls to 1/e of its on-axis

value, r is the radius, ϕ is the azimuthal angle and L_p^l is the generalised Laguerre polynomial. The term $(2p+l+1)\arctan\left(\frac{z}{z_r}\right)$ is the Guoy phase of the LG mode that varies with the mode indices.

Laguerre-Gaussian laser modes may be generated in a number of ways either within or outside a given laser cavity. Generating the LG modes (circular symmetry) from within the laser resonator cavity is possible if the cavity has a certain asymmetry (Okida M, 2007), however most laser cavities do not possess the symmetry required to output such circularly symmetric transverse laser modes. One of the first techniques of LG mode generation made use of output higher order Hermite-Gaussian (HG) transverse modes (rectangular symmetry) by inserting of an intra-cavity cross-wire into a laser cavity. The Hermite-Gaussian (HG) modes may then be converted to a Laguerre-Gaussian (LG) laser mode using a mode converter (Beijersbergen *et al.*, 1993). A mode converter consists of two cylindrical lenses of focal length, *f*, canonically disposed with respect to one another. When placed at a distance of $\sqrt{2}f$ between the two cylindrical lens this system of lenses introduces a Guoy phase shift of $\pi/2$ on an incident HG mode laser beam of indices *m* and *n* and transforms it to a LG mode of indices $l=(m-n)$ and $p=\min(m,n)$. Although the purity of the generated LG mode may be high, this requires the careful selection of the HG laser mode desired and the avoidance of any undesired astigmatism in the optical system. A more practical and versatile method would be the generation of LG modes directly from a fundamental TEM_{00} Gaussian beam, external to the laser cavity. Two main methods that satisfy this requirement, each using diffractive optical elements, have been established. These are a spiral phase element or a computer-generated hologram. When considering a spiral phase elements, a high refractive index substrate is shaped into the spiral phase ramp (Beijersbergen *et al.*, 1994; Oemrawsingh *et al.*, 2004). With recent microfabrication techniques, the spiral phase element has been miniaturized (Cheong *et al.*, 2004; Lee *et al.*, 2004). The exact output mode here is a superposition of LG modes (Beijersbergen *et al.*, 1994) but the system can yield a high conversion efficiency >80% and uses on axis optical components. The computer

generated holographic generation method requires little in the way of "fabrication process" as one can mathematically encode the spiral phase with a given input field at an angle onto a computer generated pattern as seen in the inset of figure 17 . The transmission function of the off-axis hologram *T* required to generate a single ringed (*p*=0) LG beam of azimuthal order $\pm l$ may be represented as

$$T = \frac{1}{2}\left(1-\cos(k_x x \pm l\phi)\right) \tag{9}$$

where k_x define the periodicity of the grating along x axis and *l* is the azimuthal order and ϕ is $\tan^{-1}\left(\frac{y}{x}\right)$. By directing a Gaussian beam, $G(r,\phi,z)$, through the hologram T, we will obtain the resulting mathematical equation will have three functions that contributes to the zeroth order and the two conjugate orders. The Gaussian beam is merely diffracted into different orders of the beam with helical wavefront. It is important to know that the topological orders from the two diffraction order are of equal but opposite in charges (positive and negative).

$$\begin{aligned} G(r,\phi,z).T &= G(r,\phi,z).\left[\frac{1}{2}\left(1-\cos(k_x x \pm l\phi)\right)\right] \\ &= G(r,\phi,z).\left[\frac{1}{2}-\frac{e^{i(k_x x \pm l\phi)}-e^{-i(k_x x_1 \pm l\phi)}}{4}\right] \\ &= \left[\frac{1}{2}G(r,\phi,z)-\frac{1}{4}G(r,\phi,z)e^{i(k_x x \pm l\phi)}-\frac{1}{4}G(r,\phi,z)e^{-i(k_x x \pm l\phi)}\right] \end{aligned} \tag{10}$$

This holographic technique has gained more popularity due to the ease and versatility of LG beam generation. The orbital angular momentum of these light fields can be seen by careful consideration of the helical wavefronts of an LG beam. The inclined helical wavefront leads one to consider the energy flow in such fields: the Poynting vector moves in a corkscrew like manner (Allen *et al.*, 1992). This angular momentum is therefore linked with the azimuthal component of the Poynting vector. A trapped particle placed in such a (e.g. LG_0^1) field would rotate continuously around the inclination of wavefront which is illustrated by the red arrow in figure 18 due to orbital angular momentum transfer by scattering.

However the first experiments to explore this orbital angular momentum looked at transfer by absorption. Two groups (He *et al.*, 1995a; Simpson *et al.*, 1996; Simpson *et al.*, 1997; Friese *et al.*, 1996) from Australia and the United Kingdom, have independently observed this mechanical torque exerted by the LG beam by transfer of its orbital angular momentum to absorptive microparticle. In the first studies in 1995 He and colleagues (He *et al.*, 1995a) set absorptive copper oxide particles into rotation using LG modes: in fact as already mentioned this was one of the first ever implementations of holographic optical trapping. The experiment trapped particles in two dimensions and showed that the rotation rate was not due to any asymmetric scattering. By reversing the winding direction of the of 2π azimuthal phase of the LG beam the particle was seen to rotate in the opposite sense. In another experiment, data from which may be seen in figure 19 , Simpson and co-workers (Simpson *et al.*, 1997) used the mode converter to generate LG modes which were then used to rotate absorptive objects and experimentally decoupled of the spin angular momentum of light from the orbital angular momentum of light by observing the rates of rotation due to each form of angular momentum. Friese *et al* achieved analogous results using holographically generated LG modes of azimuthal index l=3 (Friese *et al.*, 1996). In these first experiments that exploited these LG modes, the particles used were optically absorptive which naturally would not be ideal for biological applications but clearly elucidate the physics of these distinctive light modes. Later studies showed that one could actually transfer orbital angular momentum onto transparent dielectric particles simply by scattering off the inclined wavefronts (O'Neil *et al.*, 2002) as might be infered from figure 18. Particles were placed off axis within the circumference of the LG beams and were seen to show differing forms of motion based upon whether they were responding to the spin or orbital component of the light field. In turn this gives insight into the intrinsic and extrinsic nature of spin and orbital angular momentum.

Laguerre-Gaussian beams have had a significant influence in the advancement of optical trapping. It is important to explore further applications of such modes within the context of biological and colloidal sciences as it is only their phase structure that has gained attention but their annular intensity profile is also of importance for this field. Before we

progress to their applications in optical micromanipulation of colloid and cells we remark that such light fields are making major in-roads into atomic systems with applications that purely exploit the beam profile for blue detuned toroidal traps (Kuga *et al.*, 1997), atom guiding (Schiffer *et al.*, 1998; Rhodes *et al.*, 2002) and studies in Bose-Einstein condensation(Wright *et al.*, 2000; Andersen *et al.*, 2006). More details of the use of such light fields for atomic trapping and guiding may be found elsewhere(Grimm *et al.*, 2000).

Low index particles are finding ever more applications notably in chemical and biological contexts. Ashkin first observed that low refractive index particles are repelled from the high intensity region of light while high refractive index particles are draw into the trap (Ashkin, 1970). He later used a high order mode laser beam (TEM^*_{01}) to levitated and hold a low glass sphere against gravity (Ashkin and Dziedzic, 1974; Ashkin, 1997). Using a pair of fast scanning mirror driven by galvanometers, Sasaki and his colleagues (Sasaki *et al.*, 1991, 1992) demonstrated that by repetitive scanning of a single trap into a specific two dimensional light pattern microspheres would find themselves aligned onto the designated locations. By rotating the trap over a few hundred Hertz, they were also able to cage and transport reflective metallic particles or low index microdroplets. In the general context of optical tweezing applications, one is typically focused upon the trapping of high index refractive index. When focused to a tight spot through a high numerical aperture microscope objective, these vortex beams form a special type of optical tweezers that are distinguished by their ability in the manipulation of low refractive index microparticles: all higher order LG beam ($p = 0$, $l > 1$) possesses a smooth annular intensity profile, resembling a doughnut and as mentioned a low index particle will be repelled from the light region and be confined within the dark core. As witnessed by the studies of Gahagan and Swartzlander (Gahagan and Swartzlander, 1999) If we now refer back to figure 1 and revisit the optical tweezing of a higher index particle with a Gaussian beam we see that light coming straight through the centre of back aperture of the objective leads to axial scattering forces that act against the gradient forces to destabilize the trap. If a radius of the microparticles matches approximately the size of the beam waist of the LG beam, high refractive index particles can also be tweezed with an LG beam but will experience a much lower on-axis light scattering force

compared to the use of a Gaussian beam due to the LG beam profile. This reduces the on-axis scattering force exerted along the axial direction as shown by Simpson *et al* (Simpson *et al.*, 1998).

Optical vortices provide a much needed solution for the manipulation of droplets where the refractive indices of most liquids are essentially lower than their surrounding medium. For selective mixing of droplets without cross contamination, it requires minor positioning of the droplets. In a recent work, Lee *et al* (Lee *et al.*, 2005) explored placing a spiral phase element at gradual step away from the center of an incident Gaussian beam and manipulated the position of the dark vortex core: off-axis optical vortex. In this way a low index microparticle can be manipulated around the beam central axis without moving the entire beam. R. M. Lorenz *et al* (Lorenz *et al.*, 2007) adapted the technique with the use of two such off-axis LG (optical vortex) beams to controllably fuse two aqueous droplets. In figure 20 (a-d), a series of off-axis optical vortex beams are shown with the position of the dark core shifted at different distances away from the centre of the beam. By displacing a spiral phase element (azimuthal charge l=1) to different transverse locations (y) on the beam waist, w, and orthogonally across the propagation direction; figure 20 (a) to (d). This action gradually diminishes the overall annular ring intensity pattern into C-shaped intensity pattern. In figure 20 (e) to (g), a vortex-trap-induced fusion of two aqueous droplets in acetophenone is shown. The images in the inset were obtained by recording the back-scattered laser light from the vortex trap off the interface between the coverslip and water. The scale bar represents 10 μm. In a similar fashion, ultrasound contrast agent may be trapped in the dark core of the vortex and used in combination with exposure to ultrasound for microbubble cavitation and subsequent drug delivery. Such sonoporation was demonstrated by Prentice *et al* (Prentice *et al.*, 2005; Prentice *et al.*, 2004). O'Neil *et al* (O'Neil and Padgett, 2000) also showed the ability to trap and rotate micron-sized metallic particles in three dimensions using an inverted optical vortex trap that demonstrated a decoupling of spin and orbital angular momentum. As such, these vortex tweezing experiments demonstrate that shaping the tweezing beam profile can enhance the ability to trap other types of particle. This

technique potentially requires less effort than continuous scanning (Sasaki *et al.*, 1992) of a Gaussian beam.

At the micrometer size scale, fluid flow can be laminar. Within such a low Reynolds number regime, we need methods to induce rapid direction changes within flow channels to control flow or mixing processes of different species of particles or different fluids. Rotating trapped objects with optical tweezers thus becomes an important consideration for such studies as well as microrheology (Bishop *et al.*, 2004; La Porta and Wang, 2004; Oroszi *et al.*, 2006). As mentioned earlier than rotating optically trapped particles also hold immense promise for microrheology where the rotational stokes drag reaches equilibrium with the rotating birefringent object permitting a local measurement of viscosity (Bishop *et al.*, 2003b) with only picolitres amount of liquid (Parkin *et al.*, 2007). Other examples include the spinning of photopolymerised structures (Kelemen *et al.*, 2007) which may be set into rotation by asymmetric scattering. Micropumps may be created by simultaneously trapping and rotating microspheres held by multiple optical tweezers created by acousto–optic modulators (Terray *et al.*, 2002). Naturally the optical angular momentum of light, be it spin or orbital, can induce rotation in trapped objects. If we first consider the case of spin angular momentum one can set a trapped birefringent particle into rotation due to the exchange of spin angular momentum, where the trapped particle acts like a microscopic waveplate. The experiment is a microscopic analogue to Beth's famous experiment (Beth, 1936). Friese *et al* (Friese *et al.*, 1998; Friese *et al.*, 2001) set a calcite particle into rotation with a circularly polarized trapping beam. Two birefringent microspheres may be set into rotation in opposite senses to one another, creating an optical pump though the flow rates and speed of particle motion are slow (Di Leonardo *et al.*, 2006; Leach *et al.*, 2006b). To obviate the reliance upon intrinsic birefringence Neale *et al* (Neale *et al.*, 2005) engineered birefringence into SU-8 polymer which could be considered as "form birefringence" (Bishop *et al.*, 2003a) and allowed rotation of arbitrary structures with circularly polarized light. Notably optical torques can be imparted onto particles with the orbital angular momentum of the LG beams via scattering or absorption and we have mentioned these above. In terms of applications, LG beams too can be extended to the generation of optically driven pumps: K. Ladavac and

D. Grier (Ladavac and Grier, 2004) used holographically created rows of alternating single ringed LG beams of very high azimuthal index (p=0, l=±21) to trap and rotate large numbers of microspheres to generate fluid flow as seen in figure 21. The figure shows a time-lapse composite of 16 images in half-second intervals of colloidal spheres in the "holographic pump". The circles identify the trajectory of a single sphere as it moves 25 micrometer to the left in 7 seconds. Its peak speed is 5 micrometers per second. In turn this caused other particles to flow through the system. By pushing particles toward the water-air interfaces (away from a hard surface), Jesacher *et al* (Jesacher *et al.*, 2006) observed high rotation rates of particles trapped in holographic optical vortex traps and also demonstrated interactive particle flow steering with arrays of optical vortex pumps.

Applying and controlling a small amount of torque upon biological particles i.e cells or chromosomes, often require that the beams to be tailored to the shape of the biological particles. Orientation of particles with optical traps is also a desirable quantity in this respect. With higher order laser modes, Sato *et al* (Sato *et al.*, 1991) have demonstrated that Hermite-Gaussian modes are capable of rotating elongated biological particles. Can the LG beam offer a possibility to apply optical torques onto different types of microparticles? Interfering LG beams with either plane waves or with other LG beams is an alternative beam shaping technique to create rotating light patterns as pioneered by Paterson and colleagues (Paterson *et al.*, 2001). In this work chromosomes were controllably oriented and spun by controlled adjustment of the relative optical path length in the LG beam interferometer. Interfering two LG beams of equal but opposite azimuthal index can be used to generate an array of spots that again may be rotated with careful adjustment of the relative path length between the two arms of the interferometer. These patterns can create and rotate three-dimensional structures (MacDonald *et al.*, 2002). The interfering spiral pattern of the LG beams can be modified to fit the shape of the object. By applying the angular Doppler technique, the particle of interest can be rotated at high frequency (Arlt *et al.*, 2002).

The inclined wavefront and the annular intensity pattern of a LG beam forms in some ways an ideal toroidal optical trap with a given driving force. A constant driving force along a toroidal trap can demonstrate interesting behaviour as already mentioned (Faucheux *et al.*, 1995a; Faucheux *et al.*, 1995b; Harada and Yoshikawa, 2004). In a more recent experiment, C. Lutz *et al* (Lutz *et al.*, 2006) demonstrate that the particles are able to surmount potential barriers due to hydrodynamic interactions amongst the particles circulating in the toroidal trap. Y. Roichman *et al* made uses of a high order LG beam (l = 50 and 80) and observed similar colloidal interactions (Roichman *et al.*, 2007) as shown in figure 22.

4.3.2 Description and Generation of Bessel light modes

Diffraction is inherently linked with the wave nature of light and one that needs careful consideration in any optical system. Modern laser technology produces highly coherent and monochromatic light fields that have low divergence over a long propagation distance (meters). However, if a Gaussian beam is tightly focused, it would tend to spread rather rapidly over a short propagation distance, beyond what is termed the Rayleigh range Z_R. This range is the typical criteria used to characterize the expansion or spread of a Gaussian light field and denotes the distance over which a Gaussian beam increases its cross-sectional area by a factor of two.

$$Z_R = \frac{\pi \omega_o^2}{\lambda} \tag{11}$$

where λ is the wavelength and w_0 is the beam waist size. As one can see in the context of optical tweezers high focusing objectives (large numerical aperture), the Rayleigh range is merely a few microns or so. As the beam spreads and the intensity gradient of the beam diminishes over a certain axial distance and the optical forces will reduce accordingly. If one could overcome such diffractive spreading then a multitude of applications including several in optical micromanipulation would be possible. For example one would be able to create and elongated optical guide that retained strong transverse confinement over its entire length due to minimal intensity variations. In this

manner transport of biological or colloidal material over very long distances with high accuracy would be possible.

Durnin suggested a potential beam by which diffraction is "suppressed" during free space propagation in theory and experiments (Durnin, 1987; Durnin *et al.*, 1987). The beam was the Bessel light beam. Such beams appear to offer a resistance to the nature diffraction over a specific finite distance and thus this is seems like an attractive alternative to using Gaussian beams in a number of scenarios. The ideal version of this beam however implied the need for an infinite input aperture (and thus infinite power) and could not be experimentally realized. In subsequent experimental work, Durnin and colleagues showed (Durnin *et al.*, 1987) was that one could generate an approximation to a Bessel beam (BB) that retained its key propagation invariant features over a limited range. An important point in that when we compare the propagation properties of a Bessel beam to a Gaussian beam the appropriate comparison is between the central core size of the Bessel beam and the spot size of the Gaussian beam (Durnin *et al.*, 1988).

The Bessel beam has proved to be the most popular and widely used "non-diffracting" light field (McGloin and Dholakia, 2005) but it is not the only light field with these intriguing properties. Higher order Bessel functions can be optically realized with LG beams illuminating an axicon (Arlt and Dholakia, 2000). The higher order Bessel beam, where l $(l>=0)$, possesses an inclined wavefront and therefore orbital angular momentum rather like the LG beam. The centre of the beam then is either a bright spot (index l=0) or possesses an hollow core l $(l>=1)$ or vortex. Other modes exist that include zero and higher order Mathieu beams(Chavez-Cerda *et al.*, 2001) from closed-form expressions for solutions to the Helmholtz equation were found for another set of diffraction- free beams, which may be considered as elliptical generalizations of Bessel beams. Mathieu beams are described by the 'ellipticity' parameter q, and the integer l, which denotes the order of the mode. A recent realization of "non-diffracting" Airy beams by Siviloglou *et al* (Siviloglou and Christodoulides, 2007) that are of interest too when considering the evolution of wavepackets and matter waves (Dholakia, 2008).

For most beams under consideration, each plane wave component would take up a different phase shift over a given propagation distance with the wave vector constantly changing. The resulting beam is considered as the interference pattern of the plane waves that naturally changes in its complex amplitude. However, the Bessel beam falls into the category of a special beam where in this case the phase shift accrued is the same for each and every plane wave component. Such beams do not change shape on propagation, and are termed propagation invariant or "diffraction-free". This also leads us to understand how we may actually create "white light Bessel" beams (Fischer *et al.*, 2005; Leach *et al.*, 2006a) where temporal coherence is not an issue. The ideal Bessel beam has an amplitude distribution that may be expressed as:

$$E(r,f,z) = A_0 \exp(ik_z z) J_l(k_r r) \exp(\pm ilf) \qquad (12)$$

where J_l denotes a l^{th}-order Bessel function, k_z and k_r are the longitudinal and radial wavevectors, with $k = \sqrt{k_z^2 + k_r^2} = 2p/l$ (l being the wavelength of the electromagnetic radiation used to form the Bessel light beam). The parameters r, f and z are the radial, azimuthal and longitudinal components respectively. A zero order Bessel is generated from a conical wave vectors where the plane waves overlap along the center of the propagation axis as seen in figure.23 (a). The intensity for a zeroth order Bessel beam in three dimensions is shown in figure 23 (b). One can consider an annulus (infinitely thin for a perfect ideal Bessel beam) in *k*-space and the optical Fourier transform of a ring will result in a Bessel beam. Using an annulus placed in the back focal plane of a lens was in fact the first way a finite approximation to a Bessel beam was generated in the laboratory (McGloin and Dholakia, 2005; Durnin *et al.*, 1987)

A feature of the Bessel beam that we have mentioned is that it contains a given power that is evenly distributed and equally shared between its constituent rings (Durnin *et al.*, 1988; Lin *et al.*, 1992). Thus though more rings imply a longer "diffraction-free" propagation distance, we trade this against power in the central maximum. An efficient and popular way to generate a Bessel beam is by use of conical optical element known as an axicon (McLeod, 1954; Indebetouw, 1989). The axicon is a conically shaped transparent optical element that readily imposes a phase shift $\phi(r,\theta) = k(n-1)\gamma$ onto an

incident Gaussian light beam, as shown in Figure 23 where *n* is the refractive index of the axicon material, and γ is the internal angle of the element. The value of $k(n-1)\gamma$ will dictate the spatial frequency k_r for a specific Bessel beam. The diagram also clearly shows the notion that a Bessel beam is a set of waves propagating on a cone. Microfabricated axicons, much like microfabricated spiral phase plates, have also proven useful for direct integration into optical trapping systems (Cheong *et al.*, 2005). If the axicon is not illuminated at normal incidence, astigmatism is introduced and non circularly symmetric patterns can result (Thaning *et al.*, 2003; Bin and Zhu, 1998; Tanaka and Yamamoto, 2000). If the axicon is illuminated with a converging or diverging beam, one can also change the baseline of the beam profile and obtain an offset or tilt across the beam profile, resulting in a type of biased optical potential energy landscape: such a washboard potential can be used for optical micromanipulation (Tatarkova *et al.*, 2003). Holographic generation of Bessel beams is also now established as a powerful and efficient manner by which to generate such modes. Such holograms can be in the form static, etched elements (Vasara *et al.*, 1989); or fully reconfigurable when using spatial light modulators (Davis *et al.*, 1996b, a). Interestingly, an obstruction at the center of the Bessel beam would not affect its overall the beam propagation: the beam can actually self-heal! This is due to the conical wavevectors that constitute the beam

We now progress to review the experiments that have used Bessel light modes within optical micromanipulation that benefit from the key attributes of this light beam. We note that conical glass axicons and more generally Bessel light modes have been utilized also in the domain of atomic physics for studies involving cold atoms and we refer the interested reader to some relevant papers elsewhere (Arlt *et al.*, 2001a; Schmid *et al.*, 2006)

Arlt and colleagues (Arlt *et al.*, 2001b) implemented a Bessel light mode within an optical trapping system as shown in figure 24. A telescope was used to expand the output beam of a laser that was subsequently incident upon the axicon. The generated Bessel beam is again telescoped down to the size desired to perform micromanipulation experiments within a sample chamber. It is important to note that the absence of any axial intensity gradient along the beam propagation length meant that this is a two dimensional

trap. The experiments showed trapping of a microsphere and separately a glass rod without the use of a microscope objective.

Subsequently, Garces-Chavez and colleagues (Garces-Chavez *et al.*, 2002a) used the Bessel light mode's self–healing properties in a trapping system. This experiment used three sample chambers made with multiple cover slips to illustrate the key self-healing aspects of the beam: showing the direct evidence of conical wave propagation. As shown in figure.25 (a), this beam was incident upon different particle samples within each of three chambers where the top and bottom chamber were separated by around 1 mm. The cells (I and II) are 3mm apart, and 100 mm deep. a–f, Frames from a video taken of objects captured by the Bessel beam(beam spot of radius 5 micrometer) ((i), a hollow sphere (low refractive index) of 5 micrometer in diameter is trapped in cell I between the central spot and the first ring of the Bessel beam. (ii), The beam is at a short distance above i, Here the beam has been distorted by the particle. (iii), Some small distance above the first sample cell, the beam has reformed and is no longer distorted. (iv), The beam enters the cell II, and is able to stack three 5 micrometer in diameter solid silica spheres. (v), (vi), The beam profile above the stack of particles. The beam has reformed once more.).A trapped particle in the beam centre constituted the "obstacle" and deformed the light field. The reformation of the beam was observed in between each chamber and the beam was able to trap in all three chambers simultaneously, however, one could see the beam exhibit a two dimensional trapping effect in each chamber. In one example a low index particle was confined between the central maximum and first bright ring, a calcite particle set into rotation in the beam centre. By using a higher density of colloid, particles were trapped in not only the central maximum but some of the outer concentric rings. Even then the beam was seen to reform sufficiently well to trap more colloid in concentric ring patterns in a chamber placed further along the propagation direction as illustrated in figure 25 (a). As the central core of the Bessel beam facilitates long range guiding of microparticles, Dholakia *et al* (Dholakia *et al.*, 2004) showed two-photon fluorescence signal from the sample medium (with fluorescein added) of diameter 5 micrometer are optically confined and propelled with a femtosecond Bessel beam. In that experiment, the beam can be seen to reforming approximately 90 micrometer in front of the trapped fluorescent sphere, shown in figure.25 (b). This gives an interesting

manner by which the optical field may be visualized around trapped or guided microparticles.

A Bessel beam can naturally persist over an extended range. Cizmar and colleagues (Cizmar *et al.*, 2005) used two counter-propagating zeroth order Bessel beam modes can create a very long (millimeter) interference pattern along the axis of beam propagation. The interference pattern forms a one dimensional optical potential energy landscape that resembles a "conveyor belt", as shown in figure 26 (a). This allowed for three dimensional trapping at the antinodes and subsequent capture and delivery of several submicron particles over a distance of hundreds of micrometers (figure 26 (b)). Precise delivery was achieved by shifting the phase of one of the beams causing the interference pattern to translate in space which thus moved trapped colloidal particles to specific regions. Both theoretical and experimental investigation showed that certain sizes of polystyrene particles jump between neighboring axial traps with higher probability than others. Another geometry that uses extended interferometric landscape and subsequently sorting of colloidal particles with a surface interference pattern was shown by Cizmar and his co-workers (Cizmar *et al.*, 2006b). Experimental measurements of the trap stiffness using video tracking (Cizmar and Zemanek, 2007) has revealed that the ratios of longitudinal and lateral optical trap stiffnesses along the standing waves were around one order of magnitude higher compared to the classical single beam optical trap (optical tweezers). This would mean that such interferometric optical traps may have possible uses for force measurements within biological systems. Using the Bessel beam standing waves created from two independent counter-propagating Bessel beams, they were able to confine polystyrene particles of radius 100 nanometers, and arranged them into a one-dimensional chain over a length one millimeter (Cizmar *et al.*, 2006c). In related studies, such a moving interferometric pattern created by the same Bessel laser beam modes was used to horizontally transport ultracold atoms over macroscopic distances of up to 20 centimeter while ensuring uniform trapping conditions. The stability of the interference traps allow rapid transport with velocities of up to 6 m/s.(Schmid *et al.*, 2006).

With co- propagating Bessel beams, a periodic oscillations of the on- axial intensity maxima (termed as self-imaging) can be changed by having two Bessel beams of different conical angle (slightly different wave-vector) interfering with one another (Chávez-Cerda *et al.*, 1998; Courtial *et al.*, 2006; Cizmar *et al.*, 2006a). By changing the path difference of one of the Bessel beam, particles can be selectively trapped and manipulated. Through numerical simulation, researchers have showed that by simply increasing the number of interfering beams allows one to select the type of particles that would be confined. Experimentally, they trapped particles with radii from 100 nanometers up to 300 nanometers but required the assistance of fluid flow against the beam propagation. Particle hopping from one trap to the neighboring-occupied traps was seen to generate a domino-like effect propagating with constant velocity over the subsequent occupied traps (Cizmar *et al.*, 2006a).

Tatarkova *et al* (Tatarkova *et al.*, 2003) examined an axially misalignment (diverging) of the Gaussian beam that is used to illuminate the axicon: in turn this created an asymmetry in the potential wells created by any one ring of the Bessel profile. This causes a preferential lateral guide that brings particle hopping towards the beam centre. Subsequent studies explored these issues in more detail where Milne *et al* (Milne *et al.*, 2007a) used both theory and experiment to look at the motion of silica microspheres by video tracking when placed within a Bessel beam as shown in figure 27. Two different computational models, Mie scattering and geometrical ray optics, gave analogous data and predicted the existence of a distinct size-dependence of particle dynamics and equilibria positions within a Bessel beam.

Studies with such Bessel beams of higher order (l>0) may complement those performed with Laguerre-Gaussian modes described earlier. In 2002, Garces-Chavez *et al* (Garces-Chavez *et al.*, 2003) explored angular momentum transfer from a higher order Bessel beam to high index particles: in this study the particle rotation rates were accurately determined and supported with the ray optics theoretical model with both showing good agreement and the expected linear relationship between power and rotation rate. The

same team in 2003 explored the transfer of orbital angular momentum to low index particles (Garces-Chavez *et al.*, 2002b) where a low index particle was trapped between two of the bright concentric rings of the Bessel beam this was the first transfer of orbital angular momentum to low index particles. Here, the authors observed that angular momentum can be transferred via scattering and in the absent on any on-axis scattering light. With further observation of rotation in a birefringent particle around the concenetric rings of the higher order Bessel beam showed a conclusive demonstration of the intrinsic and extrinsic nature of optical angular momentum. The birefringent particles can help map the optical angular momentum density in the light field with the particle acting as probe. Further theoretical studies explored the dynamics and equilibrium positions of particles in a Bessel beam more detail (Volke-Sepulveda *et al.,* 2004; Volke-Sepulveda *et al.,* 2002). Mathieu beams, described earlier, have been recently used in optical micromanipulation to explore their orbital angular momentum properties (Lopez-Mariscal *et al.,* 2006) showing non-uniform velocities of particle motion around the beam profile.

In 2005 Paterson *et al* (Paterson *et al.*, 2005) looked at the motion of red and white blood cells with no markers attached across the optical potential energy landscape created by the Bessel beam. This work showed an important result that red and white blood cells could be separated in this purely passive manner by the Bessel beam. White cells were accumulated within the central core whilst red cells, depending upon the exact power and beam parameters, were trapped in the concentric rings where they oriented themselves (flipped) by ninety degrees. The behavior was attributed to the difference between red and white blood cells: lymphocytes are near spherical and have a nucleus whereas erythrocytes are more like bi-concave disk. This study was recently extended to see if passive sorting could be applied to stem cells and human cancer cells. However the intrinsic differences between given cell types was typically not sufficient to initiate sorting and the authors used dielectric tagging of the cells to enhance the sorting process: this involved using antibody-antigen binding and treated microspheres to preferentially attach them to certain cells. Subsequently these “tagged” cells responded more strongly to the Bessel mode (Paterson *et al.,* 2007) , as shown in figure. 28. In figure. 28, (A) The

white and black arrows point to lymphocytes that have been attached to streptavidin-coated microspheres using a mouse, anti-CD2 monoclonal antibody, and a biotinylated anti-mouse antibody. The surrounding cells are other mononuclear cells isolated from venous blood. The mixed ensemble of cells is at the bottom of a sample chamber and imaged using a 60X microscope objective. (B, C) The sphere-labeled cells travel into the central maximum of the Bessel beam and are guided vertically within the centre until they reach the top of the sample chamber where they form a vertical stack (D). Over the time scale required for isolation of the CD2 T-cells seconds, the untagged cells do not move significantly.

5. Optical binding

Trapping of many particles in desired configurations, be it in interferometric, timed shared, holographic, or Bessel light modes, is an important topic. A rather less well discussed but fundamentally significant issue is that multiple microparticles may self organize themselves into arrays by their interaction with light. Indeed when we consider the creation by any means of multiple, optical trap sites and our optical landscapes, we have to date ignored how the very scattering or redistribution of light by one given trapped particle placed within this light field may influence the position of their nearest trapped particle (neglecting taking into account any hydrodynamic interactions). This leads one to the emergent and key area of ***optical binding***.

Light forces interacting between particles may act to optically bind themselves. Particle organization through interactions of optical scattering in the beam propagation direction have been recently seen and allow interactions between micron sized particles separated by distances and order of magnitude larger than their individual diameters. It may manifest itself in a form either transverse to or in the direction of (longitudinal) the beam propagation. There are various types of ‘‘optical binding’’: Burns and coworkers (Burns *et al.*, 1990, 1989) investigated systems where the interaction of coherently induced dipole moments of the spheres were said to interact to bind matter. It took another decade before new experimental results revived the seminal work of binding matter with light

interacting arising from the particles themselves. Tatarkova *et al* (Tatarkova *et al.*, 2002) and Singer *et al* (Singer *et al.*, 2003) conducted separate studies in exploring particles in a dual counter-propagating trap and found very interesting assembly of particle in this trapping geometry, which is now understood as a longitudinal optical binding effect (Metzger *et al.*, 2006b; Metzger *et al.*, 2006c).

Metzger *et al* have subsequently discovered rich dynamics in such systems, including recent observations of bistability (Metzger *et al.*, 2006a) of the system and interesting interparticle correlations (Metzger *et al.*, 2007b). Substantial theoretical work has been performed on such systems (Ng *et al.*, 2005; Karasek *et al.*, 2006; Metzger *et al.*, 2006a; Metzger *et al.*, 2006c; Metzger *et al.*, 2007a) and other manifestations of binding have seen in near field optical geometries (Reece *et al.*, 2006; Mellor and Bain, 2006; Garces-Chavez *et al.*, 2006). This is a young area and likely to have impact across the biological and colloidal sciences and indeed may present a very powerful future method for creation of large scale extended arrays in up to three dimensions. It is noteworthy to emphasize that such "optical binding" is radically different from individually trapping each micro-object: the very interaction between an object and its nearest neighbours creates a self consistent and homogeneous solution. This could be the very technique that would allow a straightforward optical geometry to in principle create a large scale colloidal array.

6. Conclusions

Optical micromanipulation remains a powerful and versatile tool for the natural sciences. The weak forces it exerts may be calibrated and used to measure the dynamics and forces exerted by motor proteins and other biological macromolecules. The system may be readily calibrated to incredible accuracy and resolve femtonewton forces. An upcoming theme within this field has been the use of structured light fields: these can take the form of simple multiple trap arrays or lines of light or indeed more formal non-zero-order light modes such as Laguerre-Gaussian or Bessel beams. These latter modes have made major headway into fundamental science, biomedical and chemical applications as well as capturing the imagination of the atomic and optical physics communities with their unusual propagation characteristics. We have summarized in this article the experiments

and theory behind such light patterns and given a flavour of some of their impact within the ever growing area of optical micromanipulation.

Acknowledgements

The authors would like to thank the UK Science and Engineering Research Council for funding, Michael Mazilu, Tomas Cizmar, Joerg Baumgartl and David Stevenson for proof reading and useful comments.

References

Abbondanzieri E A, Greenleaf W J, Shaevitz J W, Landick R and Block S M, 2005, Direct observation of base-pair stepping by RNA polymerase, *Nature*, **438**, 460

Agate B, Brown C T A, Sibbett W and Dholakia K, 2004, Femtosecond optical tweezers for in-situ control of two-photon fluorescence, *Optics Express*, **12**, 3011

Akselrod G M, Timp W, Mirsaidov U, Zhao Q, Li C, Timp R, Timp K, Matsudaira P and Timp G, 2006, Laser-guided assembly of heterotypic three-dimensional living cell microarrays, *Biophysical Journal*, **91**, 3465

Allen L, Beijersbergen M W, Spreeuw R J C and Woerdman J P, 1992, Orbital angular-momentum of light and the transformation of Laguerre-Gaussian laser modes, *Physical Review A*, **45**, 8185

Allen L, Padgett M J and Babiker M 1999 *Progress in optics, Vol XXXIX*, pp 291

Allersma M W, Gittes F, deCastro M J, Stewart R J and Schmidt C F, 1998, Two-dimensional tracking of ncd motility by back focal plane interferometry, *Biophysical Journal*, **74**, 1074

Andersen M F, Ryu C, Clade P, Natarajan V, Vaziri A, Helmerson K and Phillips W D, 2006, Quantized rotation of atoms from photons with orbital angular momentum, *Physical Review Letters*, **97**, 170406

Appleyard D C, Vandermeulen K Y, Lee H and Lang M J, 2007, Optical trapping for undergraduates, *American Journal of Physics*, **75**, 5

Arlt J and Dholakia K, 2000, Generation of high-order bessel beams by use of an axicon, *Optics Communications*, **177**, 297

Arlt J, Dholakia K, Soneson J and Wright E M, 2001a, Optical dipole traps and atomic waveguides based on bessel light beams, *Physical Review A*, **63**, 063602

Arlt J, Garces-Chavez V, Sibbett W and Dholakia K, 2001b, Optical micromanipulation using a bessel light beam, *Optics Communications*, **197**, 239

Arlt J, MacDonald M, Paterson L, Sibbett W, Dholakia K and Volke-Sepulveda K, 2002, Moving interference patterns created using the angular doppler-effect, *Optics Express*, **10**, 844

Ashkin A, 1970, Acceleration and trapping of particles by radiation pressure, *Physical Review Letters*, **24**, 156

Ashkin A, 1992, Forces of a single-beam gradient laser trap on a dielectric sphere in the ray optics regime, *Biophysical Journal*, **61**, 569

Ashkin A, 1997, Optical trapping and manipulation of neutral particles using lasers, *Proceedings of the National Academy of Sciences of the United States of America*, **94**, 4853

Ashkin A and Dziedzic J M, 1974, Stability of optical levitation by radiation pressure, *Applied Physics Letters*, **24**, 586

Ashkin A and Dziedzic J M, 1987, Optical trapping and manipulation of viruses and bacteria, *Science*, **235**, 1517

Ashkin A and Dziedzic J M, 1989a, Internal cell manipulation using infrared-laser traps, *Proceedings of the National Academy of Sciences of the United States of America*, **86**, 7914

Ashkin A and Dziedzic J M, 1989b, Optical trapping and manipulation of single living cells using infrared-laser beams, *Berichte Der Bunsen-Gesellschaft-Physical Chemistry Chemical Physics*, **93**, 254

Ashkin A, Dziedzic J M, Bjorkholm J E and Chu S, 1986, Observation of a single-beam gradient force optical trap for dielectric particles, *Optics Letters*, **11**, 288

Ashkin A, Schutze K, Dziedzic J M, Euteneuer U and Schliwa M, 1990, Force generation of organelle transport measured invivo by an infrared-laser trap, *Nature*, **348**, 346

Barnett S M, 2002, Optical angular-momentum flux, *Journal of Optics B-Quantum and Semiclassical Optics*, **4**, S7

Barton J P and Alexander D R, 1989, Fifth-order corrected electromagnetic field components for a fundamental Gaussian beam, *Journal of Applied Physics*, **66**, 2800

Barton J P, Alexander D R and Schaub S A, 1989, Theoretical determination of net-radiation force and torque for a spherical-particle illuminated by a focused laser-beam, *Journal of Applied Physics*, **66**, 4594

Bechinger C, Brunner M and Leiderer P, 2001, Phase behavior of two-dimensional colloidal systems in the presence of periodic light fields, *Physical Review Letters*, **86**, 930

Beijersbergen M W, Allen L, Vanderveen H and Woerdman J P, 1993, Astigmatic laser mode converters and transfer of orbital angular-momentum, *Optics Communications*, **96**, 123

Beijersbergen M W, Coerwinkel R P C, Kristensen M and Woerdman J P, 1994, Helical-wave-front laser-beams produced with a spiral phaseplate, *Optics Communications*, **112**, 321

Berg-Sorensen K and Flyvbjerg H, 2004, Power spectrum analysis for optical tweezers, *Review of Scientific Instruments*, **75**, 594

Berns M W, Tadir Y, Liang H and Tromberg B 1998 *Methods in cell biology, vol 55*, pp 71

Beth R A, 1936, Mechanical detection and measurement of the angular momentum of light, *Physical Review*, **50**, 115

Bin Z and Zhu L, 1998, Diffraction property of an axicon in oblique illumination, *Applied Optics*, **37**, 2563

Birkbeck A L, Flynn R A, Ozkan M, Song D Q, Gross M and Esener S C, 2003, Vcsel arrays as micromanipulators in chip-based biosystems, *Biomedical Microdevices*, **5**, 47

Bishop A I, Nieminen T A, Heckenberg N R and Rubinsztein-Dunlop H, 2003a, Optical application and measurement of torque on microparticles of isotropic nonabsorbing material, *Physical Review A*, **68**, 033802

Bishop A I, Nieminen T A, Heckenberg N R and Rubinsztein-Dunlop H, 2003b, Optical application and measurement of torque on microparticles of isotropic nonabsorbing material, *Physical Review A*, **68**, 033802

Bishop A I, Nieminen T A, Heckenberg N R and Rubinsztein-Dunlop H, 2004, Optical microrheology using rotating laser-trapped particles, *Physical Review Letters*, **92**, 198104

Block S M, 1996, Nanometers and piconewtons: Using optical tweezers to study biological motors, *Progress in Biophysics & Molecular Biology*, **65**, SH301

Block S M, Goldstein L S B and Schnapp B J, 1990, Bead movement by single kinesin molecules studied with optical tweezers, *Nature*, **348**, 348

Block S M, Larson M H, Greenleaf W J, Herbert K M, Guydosh N R and Anthony P C, 2007, Molecule by molecule, the physics and chemistry of life: Smb 2007, *Nat Chem Biol*, **3**, 193

Brau R R, Ferrer J M, Lee H, Castro C E, Tam B K, Tarsa P B, Matsudaira P, Boyce M C, Kamm R D and Lang M J, 2007, Passive and active microrheology with optical tweezers, *Journal of Optics A: Pure and Applied Optics*, **9**, S103

Brunner M and Bechinger C, 2002, Phase behavior of colloidal molecular crystals on triangular light lattices, *Physical Review Letters*, **88**, 248302

Burns M M, Fournier J M and Golovchenko J A, 1989, Optical binding, *Physical Review Letters*, **63**, 1233

Burns M M, Fournier J M and Golovchenko J A, 1990, Optical matter - crystallization and binding in intense optical-fields, *Science*, **249**, 749

Bustamante C, Bryant Z and Smith S B, 2003, Ten years of tension: Single-molecule DNA mechanics, *Nature*, **421**, 423

Bustamante C, Liphardt J and Ritort F, 2005, The nonequilibrium thermodynamics of small systems, *Physics Today*, **58**, 43

Cai L Z, Yang X L and Wang Y R, 2002, All fourteen bravais lattices can be formed by interference of four noncoplanar beams, *Optics Letters*, **27**, 900

Casaburi A, Pesce G, Zemanek P and Sasso A, 2005, Two- and three-beam interferometric optical tweezers, *Optics Communications*, **251**, 393

Chaumet P C and Nieto-Vesperinas M, 2000, Time-averaged total force on a dipolar sphere in an electromagnetic field, *Optics Letters*, **25**, 1065

Chavez-Cerda S, Gutierrez-Vega J C and New G H C, 2001, Elliptic vortices of electromagnetic wave fields, *Optics Letters*, **26**, 1803

Chávez-Cerda S, Meneses-Nava M A and Hickmann J M, 1998, Interference of traveling nondiffracting beams, *Optics Letters*, **23**, 1871

Cheong W C, Ahluwalia B P S, Yuan X C, Zhang L S, Wang H, Niu H B and Peng X, 2005, Fabrication of efficient microaxicon by direct electron-beam lithography for long nondiffracting distance of bessel beams for optical manipulation, *Applied Physics Letters*, **87**,

Cheong W C, Lee W M, Yuan X C, Zhang L S, Dholakia K and Wang H, 2004, Direct electron-beam writing of continuous spiral phase plates in negative resist with high power efficiency for optical manipulation, *Applied Physics Letters*, **85**, 5784

Chiou A E, Wang W, Sonek G J, Hong J and Berns M W, 1997, Interferometric optical tweezers, *Optics Communications*, **133**, 7

Chiou P Y, Ohta A T and Wu M C, 2005, Massively parallel manipulation of single cells and microparticles using optical images, *Nature*, **436**, 370

Chowdhury A, Ackerson B J and Clark N A, 1985, Laser-induced freezing, *Physical Review Letters*, **55**, 833

Chu S, 1998, The manipulation of neutral particles, *Reviews of Modern Physics*, **70**, 685

Cizmar T, 2006, Optical traps generated by non-traditional beams, *Ph.D. Thesis, Masaryk University, Faculty of Science. Brno.*,

Cizmar T, Garces-Chavez V, Dholakia K and Zemanek P, 2005, Optical conveyor belt for delivery of submicron objects, *Applied Physics Letters*, **86**,

Cizmar T, Kollarova E, Bouchal Z and Zemanek P, 2006a, Sub-micron particle organization by self-imaging of non-diffracting beams, *New Journal of Physics*, **8**, 43

Cizmar T, Siler M, Sery M, Zemanek P, Garces-Chavez V and Dholakia K, 2006b, Optical sorting and detection of submicrometer objects in a motional standing wave, *Physical Review B* **74**, 035105

Cizmar T, Siler M and Zemanek P, 2006c, An optical nanotrap array movable over a milimetre range, *Applied Physics B-Lasers and Optics*, **84**, 197

Cizmar T and Zemanek P, 2007, Optical tracking of spherical micro-objects in spatially periodic interference fields, *Optics Express*, **15**, 2262

Clapp A R, Ruta A G and Dickinson R B, 1999, Three-dimensional optical trapping and evanescent wave light scattering for direct measurement of long range forces between a colloidal particle and a surface, *Review of Scientific Instruments*, **70**, 2627

Constable A, Kim J, Mervis J, Zarinetchi F and Prentiss M, 1993, Demonstration of a fiberoptic light-force trap, *Optics Letters*, **18**, 1867

Courtial J, Whyte G, Bouchal Z and Wagner.J, 2006, Iterative algorithms for holographic shaping of non-diffracting and self-imaging light beams, *Opt. Express*, **14**, 2108

Creely C M, Singh G P and Petrov D, 2005, Dual wavelength optical tweezers for confocal Raman spectroscopy, *Optics Communications*, **245**, 465

Crocker J C, 1997, Measurement of the hydrodynamic corrections to the brownian motion of two colloidal spheres, *Journal of Chemical Physics*, **106**, 2837

Crocker J C and Grier D G, 1996, Methods of digital video microscopy for colloidal studies, *Journal of Colloid and Interface Science*, **179**, 298

Crocker J C, Matteo J A, Dinsmore A D and Yodh A G, 1999, Entropic attraction and repulsion in binary colloids probed with a line optical tweezer, *Physical Review Letters*, **82**, 4352

Crocker J C, Valentine M T, Weeks E R, Gisler T, Kaplan P D, Yodh A G and Weitz D A, 2000, Two-point microrheology of inhomogeneous soft materials, *Physical Review Letters*, **85**, 888

Curtis J E, Koss B A and Grier D G, 2002, Dynamic holographic optical tweezers, *Optics Communications*, **207**, 169

Dao M, Lim C T and Suresh S, 2005, Mechanics of the human red blood cell deformed by optical tweezers, *Journal of the Mechanics and Physics of Solids*, **53**, 493

Davis J A, Carcole E and Cottrell D M, 1996a, Intensity and phase measurements of nondiffracting beams generated with a magneto-optic spatial light modulator, *Applied Optics*, **35**, 593

Davis J A, Carcole E and Cottrell D M, 1996b, Nondiffracting interference patterns generated with programmable spatial light modulators, *Applied Optics*, **35**, 599

Davis K B, Mewes M O, Andrews M R, Vandruten N J, Durfee D S, Kurn D M and Ketterle W, 1995, Bose-einstein condensation in a gas of sodium atoms, *Physical Review Letters*, **75**, 3969

Derenyi I and Vicsek T, 1995, Cooperative transport of brownian particles, *Physical Review Letters*, **75**, 374

Dholakia K, 2008, Optics: Against the spread of the light, *Nature*, **451**, 413

Dholakia K, Lee W M, Paterson L, MacDonald M P, McDonald R, Andreev I, Mthunzi P, Brown C T A, Marchington R F and Riches A C, 2007a, Optical separation of cells on potential energy landscapes: Enhancement with dielectric tagging, *IEEE Journal of Selected Topics in Quantum Electronics*, **13**, 1646

Dholakia K, Little H, Brown C T A, Agate B, McGloin D, Paterson L and Sibbett W, 2004, Imaging in optical micromanipulation using two-photon excitation, *New Journal of Physics*, **6**, 136

Dholakia K, MacDonald M P, Zemanek P and Cizmar T 2007b *Laser manipulation of cells and tissues*, pp 467

Dholakia K and Reece P, 2006, Optical micromanipulation takes hold, *Nano Today*, **1**, 18

Dholakia. K, Reece. P, Gu. M, , 2008, Optical micromanipulation, *Chem. Soc. Rev*, **37**, 42

Di Leonardo R, Keen S, Leach J, Saunter C D, Love G D, Ruocco G and Padgett M J, 2007, Eigenmodes of a hydrodynamically coupled micron-size multiple-particle ring, *Physical Review E (Statistical, Nonlinear, and Soft Matter Physics)*, **76**, 061402

Di Leonardo R, Leach J, Mushfique H, Cooper J M, Ruocco G and Padgett M J, 2006, Multipoint holographic optical velocimetry in microfluidic systems, *Physical Review Letters*, **96**,

Dillen T V, Blaaderen A V and Polman A, 2004, Shaping colloidal assemblies, *Materials Today*, **7**, 40

Dufresne E R, Spalding G C, Dearing M T, Sheets S A and Grier D G, 2001, Computer-generated holographic optical tweezer arrays, *Review of Scientific Instruments*, **72**, 1810

Durnin J, 1987, Exact-solutions for nondiffracting beams .1. The scalar theory, *Journal of the Optical Society of America a-Optics Image Science and Vision*, **4**, 651

Durnin J, Miceli J J and Eberly J H, 1987, Diffraction-free beams, *Physical Review Letters*, **58**, 1499

Durnin J, Miceli J J and Eberly J H, 1988, Comparison of bessel and Gaussian beams, *Optics Letters*, **13**, 79

Ehrlicher A, Betz T, Stuhrmann B, Koch D, Milner V, Raizen M G and Kas J, 2002, Guiding neuronal growth with light, *Proceedings of the National Academy of Sciences of the United States of America*, **99**, 16024

Eriksen R L, Mogensen P C and Gluckstad J, 2002, Multiple-beam optical tweezers generated by the generalized phase-contrast method, *Optics Letters*, **27**, 267

Fallman E and Axner O, 1997, Design for fully steerable dual-trap optical tweezers, *Applied Optics*, **36**, 2107

Faucheux L P, Bourdieu L S, Kaplan P D and Libchaber A J, 1995a, Optical thermal ratchet, *Physical Review Letters*, **74**, 1504

Faucheux L P, Stolovitzky G and Libchaber A, 1995b, Periodic forcing of a brownian particle, *Physical Review E*, **51**, 5239

Finer J T, Mehta A D and Spudich J A, 1995, Characterization of single actin-myosin interactions, *Biophysical Journal*, **68**, S291

Fischer P, Brown C T A, Morris J E, Lopez-Mariscal C, Wright E M, Sibbett W and Dholakia K, 2005, White light propagation invariant beams, *Optics Express*, **13**, 6657

Flynn R A, Birkbeck A L, Gross M, Ozkan M, Shao B, Wang M M and Esener S C, 2002, Parallel transport of biological cells using individually addressable vcsel arrays as optical tweezers, *Sensors and Actuators B-Chemical*, **87**, 239

Fournier J M, Burns M M and A. G J, 1995., Writing diffractive structures by optical trapping, *Proc. SPIE, ,* **2406**, 101

Friese M E J, Enger J, RubinszteinDunlop H and Heckenberg N R, 1996, Optical angular-momentum transfer to trapped absorbing particles, *Physical Review A*, **54**, 1593

Friese M E J, Nieminen T A, Heckenberg N R and Rubinsztein-Dunlop H, 1998, Optical alignment and spinning of laser-trapped microscopic particles, *Nature*, **394**, 348

Friese M E J, Rubinsztein-Dunlop H, Gold J, Hagberg P and Hanstorp D, 2001, Optically driven micromachine elements, *Applied Physics Letters*, **78**, 547

Gabor D, 1951, Microscopy by reconstructed wave fronts: Ii, *Proceedings of the Physical Society. Section B*, **64**, 449

Gahagan K T and Swartzlander G A, 1999, Simultaneous trapping of low-index and high-index microparticles observed with an optical-vortex trap, *Journal of the Optical Society of America B-Optical Physics*, **16**, 533

Galajda P and Ormos P, 2001, Complex micromachines produced and driven by light, *Applied Physics Letters*, **78**, 249

Garces-Chavez V, Dholakia K and Spalding G C, 2005, Extended-area optically induced organization of microparticies on a surface, *Applied Physics Letters*, **86**, 031106

Garces-Chavez V, McGloin D, Melville H, Sibbett W and Dholakia K, 2002a, Simultaneous micromanipulation in multiple planes using a self-reconstructing light beam, *Nature*, **419**, 145

Garces-Chavez V, McGloin D, Padgett M J, Dultz W, Schmitzer H and Dholakia K, 2003, Observation of the transfer of the local angular momentum density of a multiringed light beam to an optically trapped particle, *Physical Review Letters*, **91**, 093602

Garces-Chavez V, Quidant R, Reece P J, Badenes G, Torner L and Dholakia K, 2006, Extended organization of colloidal microparticles by surface plasmon polariton excitation, *Physical Review B*, **73**, 085417

Garces-Chavez V, Volke-Sepulveda K, Chavez-Cerda S, Sibbett W and Dholakia K, 2002b, Transfer of orbital angular momentum to an optically trapped low-index particle, *Physical Review A*, **66**, 063402

Grandbois M, Beyer M, Rief M, Clausen-Schaumann H and Gaub H E, 1999, How strong is a covalent bond? , *Science*, **283**, 1727

Greenleaf W J, Woodside M T, Abbondanzieri E A and Block S M, 2005, Passive all-optical force clamp for high-resolution laser trapping, *Physical Review Letters*, **95**, 208102

Greenleaf W J, Woodside M T and Block S M, 2007, High-resolution, single-molecule measurements of biomolecular motion, *Annual Review of Biophysics and Biomolecular Structure*, **36**, 171

Grier D G, 2003, A revolution in optical manipulation, *Nature*, **424**, 810

Grier D G and Roichman Y, 2006, Holographic optical trapping, *Applied Optics*, **45**, 880

Grimm R, Weidemuller M and Ovchinnikov Y B 2000 *Advances in atomic molecular, and optical physics, vol. 42*, pp 95

Guck J, Ananthakrishnan R, Cunningham C C and Kas J, 2002, Stretching biological cells with light, *Journal of Physics-Condensed Matter*, **14**, 4843

Guck J, Ananthakrishnan R, Mahmood H, Moon T J, Cunningham C C and Kas J, 2001, The optical stretcher: A novel laser tool to micromanipulate cells, *Biophysical Journal*, **81**, 767

Guck J, Ananthakrishnan R, Moon T J, Cunningham C C and Kas J, 2000, Optical deformability of soft biological dielectrics, *Physical Review Letters*, **84**, 5451

Guck J, Schinkinger S, Lincoln B, Wottawah F, Ebert S, Romeyke M, Lenz D, Erickson H M, Ananthakrishnan R, Mitchell D, Kas J, Ulvick S and Bilby C, 2005, Optical deformability as an inherent cell marker for testing malignant transformation and metastatic competence, *Biophysical Journal*, **88**, 3689

Hansen P M, Bhatia V K, Harrit N and Oddershede L, 2005, Expanding the optical trapping range of gold nanoparticles, *Nano Letters*, **5**, 1937

Harada T and Yoshikawa K, 2004, Fluctuation-response relation in a rocking ratchet, *Physical Review E*, **69**,

Harada Y and Asakura T, 1996, Radiation forces on a dielectric sphere in the rayleigh scattering regime, *Optics Communications*, **124**, 529

He H, Friese M E J, Heckenberg N R and Rubinszteindunlop H, 1995a, Direct observation of transfer of angular-momentum to absorptive particles from a laser-beam with a phase singularity, *Physical Review Letters*, **75**, 826

He H, Heckenberg N R and Rubinszteindunlop H, 1995b, Optical-particle trapping with higher-order doughnut beams produced using high-efficiency computer-generated holograms, *Journal of Modern Optics*, **42**, 217

Hertlein C, Helden L, Gambassi A, Dietrich S and Bechinger C, 2008, Direct measurement of critical casimir forces, *Nature*, **451**, 172

Hossack W J, Theofanidou E, Crain J, Heggarty K and Birch M, 2003, High-speed holographic optical tweezers using a ferroelectric liquid crystal microdisplay, *Optics Express*, **11**, 2053

Howard R P, 2007, Fluorescence microscopy: Established and emerging methods, experimental strategies, and applications in immunology, *Microscopy Research and Technique*, **70**, 687

Huisstede J H G, van der Werf K O, Bennink M L and Subramaniam V, 2005, Force detection in optical tweezers using backscattered light, *Optics Express*, **13**, 1113

Indebetouw G, 1989, Nondiffracting optical-fields - some remarks on their analysis and synthesis, *Journal of the Optical Society of America a-Optics Image Science and Vision*, **6**, 150

Jarzynski C, 1997, Nonequilibrium equality for free energy differences, *Physical Review Letters*, **78**, 2690

Jesacher A, Furhapter S, Bernet S and Ritsch-Marte M, 2004, Diffractive optical tweezers in the fresnel regime, *Optics Express*, **12**, 2243

Jesacher A, Furhapter S, Maurer C, Bernet S and Ritsch-Marte M, 2006, Holographic optical tweezers for object manipulations at an air-liquid surface, *Optics Express*, **14**, 6342

Jess P R T, Garces-Chavez V, Smith D, Mazilu M, Paterson L, Riches A, Herrington C S, Sibbett W and Dholakia K, 2006, Dual beam fibre trap for Raman microspectroscopy of single cells, *Optics Express*, **14**, 5779

Jordan P, Clare H, Flendrig L, Leach J, Cooper J and Padgett M, 2004, Permanent 3d microstructures in a polymeric host created using holographic optical tweezers, *Journal of Modern Optics*, **51**, 627

Jordan P, Leach J, Padgett M, Blackburn P, Isaacs N, Goksor M, Hanstorp D, Wright A, Girkin J and Cooper J, 2005, Creating permanent 3d arrangements of isolated cells using holographic optical tweezers, *Lab On A Chip*, **5**, 1224

Karasek V, Dholakia K and Zemanek P, 2006, Analysis of optical binding in one dimension, *Applied Physics B-Lasers And Optics*, **84**, 149

Keen S, Leach J, Gibson G and Padgett M J, 2007, Comparison of a high-speed camera and a quadrant detector for measuring displacements in optical tweezers, *Journal of Optics a-Pure and Applied Optics*, **9**, S264

Kelemen L, Valkai S and Ormos P, 2007, Parallel photopolymerisation with complex light patterns generated by diffractive optical elements, *Optics Express*, **15**, 14488

Kogelnik H and Li T, 1966, Laser beams and resonators, *Applied Optics*, **5**, 1550

Konig K, Liang H, Berns M W and Tromberg B J, 1996, Cell damage in near-infrared multimode optical traps as a result of multiphoton absorption, *Optics Letters*, **21**, 1090

Korda P T, Spalding G C and Grier D G, 2002a, Evolution of a colloidal critical state in an optical pinning potential landscape, *Physical Review B*, **66**, 024504

Korda P T, Taylor M B and Grier D G, 2002b, Kinetically locked-in colloidal transport in an array of optical tweezers, *Physical Review Letters*, **89**,

Kress H, Stelzer E H K, Griffiths G and Rohrbach A, 2005, Control of relative radiation pressure in optical traps: Application to phagocytic membrane binding studies, *Physical Review E (Statistical, Nonlinear, and Soft Matter Physics)*, **71**, 061927

Kress H, Stelzer E H K, Holzer D, Buss F, Griffiths G and Rohrbach A, 2007, Filopodia act as phagocytic tentacles and pull with discrete steps and a load-dependent velocity, *Proceedings of the National Academy of Sciences*, **104**, 11633

Kuga T, Torii Y, Shiokawa N, Hirano T, Shimizu Y and Sasada H, 1997, Novel optical trap of atoms with a doughnut beam, *Physical Review Letters*, **78**, 4713

La Porta A and Wang M D, 2004, Optical torque wrench: Angular trapping, rotation, and torque detection of quartz microparticles, *Physical Review Letters*, **92**, 190801

Lacasta A M, Sancho J M, Romero A H and Lindenberg K, 2005, Sorting on periodic surfaces, *Physical Review Letters*, **94**,

Ladavac K and Grier D G, 2004, Microoptomechanical pumps assembled and driven by holographic optical vortex arrays, *Optics Express*, **12**, 1144

Ladavac K, Kasza K and Grier D G, 2004, Sorting mesoscopic objects with periodic potential landscapes: Optical fractionation, *Physical Review E*, **70**, 010901

Lang M J, Fordyce P M, Engh A M, Neuman K C and Block S M, 2004, Simultaneous, coincident optical trapping and single-molecule fluorescence, *Nature Methods*, **1**, 133

Leach J, Gibson G M, Padgett M J, Esposito E, McConnell G, Wright A J and Girkin J M, 2006a, Generation of achromatic bessel beams using a compensated spatial light modulator, *Optics Express*, **14**, 5581

Leach J, Mushfique H, di Leonardo R, Padgett M and Cooper J, 2006b, An optically driven pump for microfluidics, *Lab on a Chip*, **6**, 735

Leach J, Sinclair G, Jordan P, Courtial J, Padgett M J, Cooper J and Laczik Z J, 2004, 3d manipulation of particles into crystal structures using holographic optical tweezers, *Optics Express*, **12**, 220

Lee S H and Grier D G, 2005, Robustness of holographic optical traps against phase scaling errors, *Optics Express*, **13**, 7458

Lee W M, Ahluwalia B P S, Yuan X C, Cheong W C and Dholakia K, 2005, Optical steering of high and low index microparticles by manipulating an off-axis optical vortex, *Journal of Optics a-Pure and Applied Optics*, **7**, 1

Lee W M, Reece P J, Marchington R F, Metzger N K and Dholakia K, 2007, Construction and calibration of an optical trap on a fluorescence optical microscope, *Nat. Protocols*, **2**, 3226

Lee W M, Yuan X C and Cheong W C, 2004, Optical vortex beam shaping by use of highly efficient irregular spiral phase plates for optical micromanipulation, *Optics Letters*, **29**, 1796

Li P, Shi K B and Liu Z W, 2005, Manipulation and spectroscopy of a single particle by use of white-light optical tweezers, *Optics Letters*, **30**, 156

Liang H, Wright W H, Cheng S, He W and Berns M W, 1993, Micromanipulation of chromosomes in ptk2 cells using laser microsurgery (optical scalpel) in combination with laser induced optical forces (optical tweezers) *Experimental Cell Research*, **204**, 110

Liesener J, Reicherter M, Haist T and Tiziani H J, 2000, Multi-functional optical tweezers using computer-generated holograms, *Optics Communications*, **185**, 77

Lin Y, Seka W, Eberly J H, Huang H and Brown D L, 1992, Experimental investigation of bessel beam characteristics, *Applied Optics*, **31**, 2708

Lincoln B, Erickson H M, Schinkinger S, Wottawah F, Mitchell D, Ulvick S, Bilby C and Guck J, 2004, Deformability-based flow cytometry, *Cytometry Part A*, **59A**, 203

Lincoln B, Schinkinger S, Travis K, Wottawah F, Ebert S, Sauer F and Guck J, 2007, Reconfigurable microfluidic integration of a dual-beam laser trap with biomedical applications, *Biomedical Microdevices*, **9**, 703

Liphardt J, Dumont S, Smith S B, Tinoco I, Jr. and Bustamante C, 2002, Equilibrium information from nonequilibrium measurements in an experimental test of jarzynski's equality, *Science*, **296**, 1832

Lopez-Mariscal C, Gutierrez-Vega J C, Milne G and Dholakia K, 2006, Orbital angular momentum transfer in helical mathieu beams, *Optics Express*, **14**, 4182

Lorenz R M, Edgar J S, Jeffries G D M, Zhao Y Q, McGloin D and Chiu D T, 2007, Vortex-trap-induced fusion of femtoliter-volume aqueous droplets, *Analytical Chemistry*, **79**, 224

Lutz C, Kollmann M and Bechinger C, 2004a, Single-file diffusion of colloids in one-dimensional channels, *Physical Review Letters*, **93**, 026001

Lutz C, Kollmann M, Leiderer P and Bechinger C, 2004b, Diffusion of colloids in one-dimensional light channels, *Journal of Physics-Condensed Matter*, **16**, S4075

Lutz C, Reichert M, Stark H and Bechinger C, 2006, Surmounting barriers: The benefit of hydrodynamic interactions, *Europhysics Letters*, **74**, 719

MacDonald M P, Neale S, Paterson L, Richies A, Dholakia K and Spalding G C, 2004, Cell cytometry with a light touch: Sorting microscopic matter with an optical lattice, *Journal of Biological Regulators and Homeostatic Agents*, **18**, 200

MacDonald M P, Paterson L, Sibbett W, Dholakia K and Bryant P E, 2001, Trapping and manipulation of low-index particles in a two-dimensional interferometric optical trap, *Optics Letters*, **26**, 863

MacDonald M P, Paterson L, Volke-Sepulveda K, Arlt J, Sibbett W and Dholakia K, 2002, Creation and manipulation of three-dimensional optically trapped structures, *Science*, **296**, 1101

MacDonald M P, Spalding G C and Dholakia K, 2003, Microfluidic sorting in an optical lattice, *Nature*, **426**, 421

Mair A, Vaziri A, Weihs G and Zeilinger A, 2001, Entanglement of the orbital angular momentum states of photons, *Nature*, **412**, 313

Malagnino N, Pesce G, Sasso A and Arimondo E, 2002, Measurements of trapping efficiency and stiffness in optical tweezers, *Optics Communications*, **214**, 15

Martin-Badosa E, Montes-Usategui M, Carnicer A, Andilla J, Pleguezuelos E and Juvells I, 2007, Design strategies for optimizing holographic optical tweezers set-ups, *Journal of Optics A: Pure and Applied Optics*, **9**, S267

McGloin D, Burnham D R, Summers M D, Rudd D, Dewar N and Anand S, 2008, Optical manipulation of airborne particles: Techniques and applications, *Faraday Discussions*, **137**, 335

McGloin D and Dholakia K, 2005, Bessel beams: Diffraction in a new light, *Contemporary Physics*, **46**, 15

McLeod J H, 1954, The axicon: A new type of optical element, *Journal of the Optical Society of America*, **44**, 592

Mehta A D, Rief M, Spudich J A, Smith D A and Simmons R M, 1999, Single-molecule biomechanics with optical methods, *Science*, **283**, 1689

Meiners J C and Quake S R, 1999, Direct measurement of hydrodynamic cross correlations between two particles in an external potential, *Physical Review Letters*, **82**, 2211

Mellor C D and Bain C D, 2006, Array formation in evanescent waves, *Chemphyschem*, **7**, 329

Melville H, Milne G F, Spalding G C, Sibbett W, Dholakia K and McGloin D, 2003, Optical trapping of three-dimensional structures using dynamic holograms, *Optics Express*, **11**, 3562

Metzger N K, Dholakia K and Wright E M, 2006a, Observation of bistability and hysteresis in optical binding of two dielectric spheres, *Physical Review Letters*, **96**, 068102

Metzger N K, Dholakia K and Wright E M, 2006b, Observation of bistability and hysteresis in optical binding of two dielectric spheres, *Physical Review Letters*, **96**,

Metzger N K, Marchington R F, Mazilu M, Smith R L, Dholakia K and Wright E M, 2007a, Measurement of the restoring forces acting on two optically bound particles from normal mode correlations, *Physical Review Letters*, **98**, 068102

Metzger N K, Marchington R F, Mazilu M, Smith R L, Dholakia K and Wright E M, 2007b, Measurement of the restoring forces acting on two optically bound particles from normal mode correlations, *Physical Review Letters*, **98**,

Metzger N K, Wright E M, Sibbett W and Dholakia K, 2006c, Visualization of optical binding of microparticles using a femtosecond fiber optical trap, *Optics Express*, **14**, 3677

Milne G, Dholakia K, McGloin D, Volke-Sepulveda K and Zemanek P, 2007a, Transverse particle dynamics in a bessel beam, *Optics Express*, **15**, 13972

Milne G, Rhodes D, MacDonald M and Dholakia K, 2007b, Fractionation of polydisperse colloid with acousto-optically generated potential energy landscapes, *Optics Letters*, **32**, 1144

Mio C, Gong T, Terray A and Marr D W M, 2000, Design of a scanning laser optical trap for multiparticle manipulation, *Review of Scientific Instruments*, **71**, 2196

Mohanty S K, Mohanty K S and Gupta P K, 2005, Dynamics of interaction of rbc with optical tweezers, *Optics Express*, **13**, 4745

Molloy J E, Burns J E, Kendrickjones J, Tregear R T and White D C S, 1995, Movement and force produced by a single myosin head, *Nature*, **378**, 209

Molloy J E and Padgett M J, 2002, Lights, action: Optical tweezers, *Contemporary Physics*, **43**, 241

Neale S L, Macdonald M P, Dholakia K and Krauss T F, 2005, All-optical control of microfluidic components using form birefringence, *Nature Materials*, **4**, 530

Nemet B A, Shabtai Y and Cronin-Golomb M, 2002, Imaging microscopic viscosity with confocal scanning optical tweezers, *Optics Letters*, **27**, 264

Neuman K C and Block S M, 2004, Optical trapping, *Review of Scientific Instruments*, **75**, 2787

Neuman K C, Chadd E H, Liou G F, Bergman K and Block S M, 1999, Characterization of photodamage to escherichia coli in optical traps, *Biophysical Journal*, **77**, 2856

Ng J, Lin Z F, Chan C T and Sheng P, 2005, Photonic clusters formed by dielectric microspheres: Numerical simulations, *Physical Review B*, **72**, 085130

O'Hara K M, Gehm M E, Granada S R, Bali S and Thomas J E, 2000, Stable, strongly attractive, two-state mixture of lithium fermions in an optical trap, *Physical Review Letters*, **85**, 2092

O'Neil A T, MacVicar I, Allen L and Padgett M J, 2002, Intrinsic and extrinsic nature of the orbital angular momentum of a light beam, *Physical Review Letters*, **88**, 053601

O'Neil A T and Padgett M J, 2000, Three-dimensional optical confinement of micron-sized metal particles and the decoupling of the spin and orbital angular momentum within an optical spanner, *Optics Communications*, **185**, 139

Oemrawsingh S S R, Van Houwelingen J A W, Eliel E. R, Woerdman J P, Verstegen. E. J. K, Kloosterboer and 't Hooft.G. W, 2004, Production and characterization of spiral phase plates for optical wavelengths, *Appl. Opt.*, **43**, 688

Okida M O T, Itoh M, and Yatagai T, , 2007, Direct generation of high power Laguerre–Gaussian output from a diode-pumped nd:Yvo4 1.3-μm bounce laser, *Opt. Express* **15**, 7616

Oroszi L, Galajda P, Kirei H, Bottka S and Ormos P, 2006, Direct measurement of torque in an optical trap and its application to double-strand DNA, *Physical Review Letters*, **97**, 058301

Parkin S J, Knoner G, Nieminen T A, Heckenberg N R and Rubinsztein-Dunlop H, 2007, Picoliter viscometry using optically rotated particles, *Physical Review E*, **76**,

Paterson L, MacDonald M P, Arlt J, Sibbett W, Bryant P E and Dholakia K, 2001, Controlled rotation of optically trapped microscopic particles, *Science*, **292**, 912

Paterson L, Papagiakoumou E, Milne G, Garces-Chavez V, Briscoe T, Sibbett W, Dholakia K and Riches A C, 2007, Passive optical separation within a 'nondiffracting' light beam, *Journal of Biomedical Optics*, **12**, 054017

Paterson L, Papagiakoumou E, Milne G, Garces-Chavez V, Tatarkova S A, Sibbett W, Gunn-Moore F J, Bryant P E, Riches A C and Dholakia K, 2005, Light-induced cell separation in a tailored optical landscape, *Applied Physics Letters*, **87**, 123901

Perch-Nielsen I R, Rodrigo P J and Gluckstad J, 2005, Real-time interactive 3d manipulation of particles viewed in two orthogonal observation planes, *Optics Express*, **13**, 2852

Perkins T T, Quake S R, Smith D E and Chu S, 1994, Relaxation of a single DNA molecule observed by optical microscopy, *Science*, **264**, 822

Pesce G, Sasso A and Fusco S, 2005, Viscosity measurements on micron-size scale using optical tweezers, *Review of Scientific Instruments*, **76**, 115105

Polin M, Grier D G and Quake S R, 2006, Anomalous vibrational dispersion in holographically trapped colloidal arrays, *Physical Review Letters*, **96**,

Polin M, Ladavac K, Lee S H, Roichman Y and Grier D G, 2005, Optimized holographic optical traps, *Optics Express*, **13**, 5831

Pontecorvo G, 1963, The leeuwenhoek lecture: Microbial genetics: Retrospect and prospect, *Proceedings of the Royal Society of London. Series B, Biological Sciences (1934-1990)*, **158**, 1

Prentice P, Cuschierp A, Dholakia K, Prausnitz M and Campbell P, 2005, Membrane disruption by optically controlled microbubble cavitation, *Nature Physics*, **1**, 107

Prentice P A, MacDonald M P, Frank T G, Cuschieri A, Spalding G C, Sibbett W, Campbell P A and Dholakia K, 2004, Manipulation and filtration of low index particles with holographic Laguerre-Gaussian optical trap arrays, *Optics Express*, **12**, 593

Ramser K, Enger J, Goksor M, Hanstorp D, Logg K and Kall M, 2005, A microfluidic system enabling Raman measurements of the oxygenation cycle in single optically trapped red blood cells, *Lab on a Chip*, **5**, 431

Reece P J, Garces-Chavez V and Dholakia K, 2006, Near-field optical micromanipulation with cavity enhanced evanescent waves, *Applied Physics Letters*, **88**, 221116

Reihani. S. N. S. and Oddershede L B, 2007, Optimizing immersion media refractive index improves optical trapping by compensating spherical aberrations, *Optics Letters*, **32**, 1998

Rhodes D P, Lancaster G P T, Livesey J, McGloin D, Arlt J and Dholakia K, 2002, Guiding a cold atomic beam along a co-propagating and oblique hollow light guide, *Optics Communications*, **214**, 247

Ricardez-Vargas I, Rodriguez-Montero P, Ramos-Garcia R and Volke-Sepulveda K, 2006, Modulated optical sieve for sorting of polydisperse microparticles, *Applied Physics Letters*, **88**, 121116

Righini M, Zelenina A S, Girard C and Quidant R, 2007, Parallel and selective trapping in a patterned plasmonic landscape, *Nat Phys*, **3**, 477

Rodrigo P J, Eriksen R L, Daria V R and Gluckstad J, 2002, Interactive light-driven and parallel manipulation of inhomogeneous particles, *Optics Express*, **10**, 1550

Rohrbach A, 2005, Stiffness of optical traps: Quantitative agreement between experiment and electromagnetic theory, *Physical Review Letters*, **95**, 168102

Rohrbach A and Stelzer E H K, 2002, Trapping forces, force constants, and potential depths for dielectric spheres in the presence of spherical aberrations, *Applied Optics*, **41**, 2494

Rohrbach A, Tischer C, Neumayer D, Florin E L and Stelzer E H K, 2004, Trapping and tracking a local probe with a photonic force microscope, *Review of Scientific Instruments*, **75**, 2197

Roichman Y and Grier D G, 2005, Holographic assembly of quasicrystalline photonic heterostructures, *Optics Express*, **13**, 5434

Roichman Y, Grier D G and Zaslavsky G, 2007, Anomalous collective dynamics in optically driven colloidal rings, *Physical Review E*, **75**, 020401

Rubinov A N, Katarkevich V M, Afanas'ev A A and Efendiev T S H, 2003, Interaction of interference laser field with an ensemble of particles in liquid, *Optics Communications*, **224**, 97

Sasaki K, Koshioka M, Misawa H, Kitamura N and Masuhara H, 1991, Pattern-formation and flow-control of fine particles by laser-scanning micromanipulation, *Optics Letters*, **16**, 1463

Sasaki K, Koshioka M, Misawa H, Kitamura N and Masuhara H, 1992, Optical trapping of a metal-particle and a water droplet by a scanning laser-beam, *Applied Physics Letters*, **60**, 807

Sato S, Ishigure M and Inaba H, 1991, Optical trapping and rotational manipulation of microscopic particles and biological cells using higher-order mode nd-yag laser-beams, *Electronics Letters*, **27**, 1831

Schiffer M, Rauner M, Kuppens S, Zinner M, Sengstock K and Ertmer W, 1998, Guiding, focusing, and cooling of atoms in a strong dipole potential, *Applied Physics B-Lasers and Optics*, **67**, 705

Schmid S, Thalhammer G, Winkler K, Lang F and Denschlag J H, 2006, Long distance transport of ultracold atoms using a 1d optical lattice, *New Journal of Physics*, **8**, 159

Schmitz C H J, Spatz J P and Curtis J E, 2005, High-precision steering of multiple holographic optical traps, *Optics Express*, **13**, 8678

Seeger S, Monajembashi S, Hutter K J, Futterman G, Wolfrum J and Greulich K O, 1991, Application of laser optical tweezers in immunology and molecular-genetics, *Cytometry*, **12**, 497

Seol Y, Carpenter A E and Perkins T T, 2006, Gold nanoparticles: Enhanced optical trapping and sensitivity coupled with significant heating, *Optics Letters*, **31**, 2429

Shaevitz J W, Abbondanzieri E A, Landick R and Block S M, 2003, Backtracking by single RNA polymerase molecules observed at near-base-pair resolution, *Nature*, **426**, 684

Shao B, Zlatanovic S, Ozkan M, Birkbeck A L and Esener S C, 2006, Manipulation of microspheres and biological cells with multiple agile vcsel traps, *Sensors and Actuators B-Chemical*, **113**, 866

Siegman A E, 1998, How to (maybe) measure laser beam quality, *OSA TOPS*, **17**, 184

Simpson N B, Allen L and Padgett M J, 1996, Optical tweezers and optical spanners with Laguerre-Gaussian modes, *Journal of Modern Optics*, **43**, 2485

Simpson N B, Dholakia K, Allen L and Padgett M J, 1997, Mechanical equivalence of spin and orbital angular momentum of light: An optical spanner, *Optics Letters*, **22**, 52

Simpson N B, McGloin D, Dholakia K, Allen L and Padgett M J, 1998, Optical tweezers with increased axial trapping efficiency, *Journal of Modern Optics*, **45**, 1943

Sinclair G, Jordan P, Leach J, Padgett M J and Cooper J, 2004a, Defining the trapping limits of holographical optical tweezers, *Journal of Modern Optics*, **51**, 409

Sinclair G, Leach J, Jordan P, Gibson G, Yao E, Laczik Z J, Padgett M J and Courtial J, 2004b, Interactive application in holographic optical tweezers of a multi-plane gerchberg-saxton algorithm for three-dimensional light shaping, *Optics Express*, **12**, 1665

Singer W, Frick M, Bernet S and Ritsch-Marte M, 2003, Self-organized array of regularly spaced microbeads in a fiber-optical trap, *Journal of the Optical Society of America B-Optical Physics*, **20**, 1568

Siviloglou G A and Christodoulides D N, 2007, Accelerating finite energy airy beams, *Optics Letters*, **32**, 979

Smith S B, Cui Y J and Bustamante C 2003 *Biophotonics, pt b*, pp 134

Squires T M and Quake S R, 2005, Microfluidics: Fluid physics at the nanoliter scale, *Reviews of Modern Physics*, **77**, 977

Stevenson D J, Lake T K, Agate B, Gárcés-Chávez V, Dholakia K and Gunn-Moore F, 2006, Optically guided neuronal growth at near infrared wavelengths, *Opt. Express* **14**, 9786

Svoboda K and Block S M, 1994a, Biological applications of optical forces, *Annual Review of Biophysics and Biomolecular Structure*, **23**, 247

Svoboda K and Block S M, 1994b, Optical trapping of metallic rayleigh particles, *Optics Letters*, **19**, 930

Tanaka T and Yamamoto S, 2000, Comparison of aberration between axicon and lens, *Optics Communications*, **184**, 113

Tatarkova S A, Carruthers A E and Dholakia K, 2002, One-dimensional optically bound arrays of microscopic particles, *Physical Review Letters*, **89**, 283901

Tatarkova S A, Sibbett W and Dholakia K, 2003, Brownian particle in an optical potential of the washboard type, *Physical Review Letters*, **91**, 038101

Terray A, Oakey J and Marr D W M, 2002, Microfluidic control using colloidal devices, *Science*, **296**, 1841

Thaning A, Jaroszewicz Z and Friberg A T, 2003, Diffractive axicons in oblique illumination: Analysis and experiments and comparison with elliptical axicons, *Applied Optics*, **42**, 9

Theofanidou E, Wilson L, Hossack W J and Arlt J, 2004, Spherical aberration correction for optical tweezers, *Optics Communications*, **236**, 145

Townes Anderson E, St Jules R S, Sherry D M, Lichtenberger J and Hassanain M, 1997, Micromanipulation of retinal cells by optical tweezers, *Investigative Ophthalmology & Visual Science*, **38**, 130

Tricoles G, 1987, Computer generated holograms: An historical review, , *Appl. Opt.*, **26**, 4351

Tsampoula X, Garces-Chavez V, Comrie M, Stevenson D J, Agate B, Brown C T A, Gunn-Moore F and Dholakia K, 2007, Femtosecond cellular transfection using a nondiffracting light beam, *Applied Physics Letters*, **91**, 053902

Vasara A, Turunen J and Friberg A T, 1989, Realization of general nondiffracting beams with computer- generated holograms, *Journal of the Optical Society of America a-Optics Image Science and Vision*, **6**, 1748

Vermeulen K C, van Mameren J, Wuite G J L and Schmidt C F, 2005, Dependence of optical trap stiffness on focusing depth in the presence and absence of spherical aberrations, *Biophysical Journal*, **88**, 663A

Visscher K, Brakenhoff G J and Krol J J, 1993, Micromanipulation by multiple optical traps created by a single fast scanning trap integrated with the bilateral confocal scanning laser microscope, *Cytometry*, **14**, 105

Visscher K, Gross S P and Block S M, 1996, Construction of multiple-beam optical traps with nanometer-resolution position sensing, *Ieee Journal of Selected Topics in Quantum Electronics*, **2**, 1066

Visscher K, Schnitzer M J and Block S M, 1999, Single kinesin molecules studied with a molecular force clamp, *Nature*, **400**, 184

Volke-Sepulveda K, Chavez-Cerda S, Garces-Chavez V and Dholakia K, 2004, Three-dimensional optical forces and transfer of orbital angular momentum from multiringed light beams to spherical microparticles, *Journal of the Optical Society of America B-Optical Physics*, **21**, 1749

Volke-Sepulveda K, Garces-Chavez V, Chavez-Cerda S, Arlt J and Dholakia K, 2002, Orbital angular momentum of a high-order bessel light beam, *Journal of Optics B-Quantum and Semiclassical Optics*, **4**, S82

Volpe G, Kozyreff G and Petrov D, 2007a, Backscattering position detection for photonic force microscopy, *Journal of Applied Physics*, **102**, 084701

Volpe G, Volpe G and Petrov D, 2007b, Brownian motion in a nonhomogeneous force field and photonic force microscope, *Physical Review E (Statistical, Nonlinear, and Soft Matter Physics)*, **76**, 061118

Vossen D L J, van der Horst A, Dogterom M and van Blaaderen A, 2004, Optical tweezers and confocal microscopy for simultaneous three-dimensional manipulation and imaging in concentrated colloidal dispersions, *Review of Scientific Instruments*, **75**, 2960

Wallin A E, Ojala H, Korsback A, Haeggstrom E and Tuma R 2007 *Optical trapping and optical micromanipulation iv*, ed K Dholakia and G C Spalding pp Y6441

Wang M M, Tu E, Raymond D E, Yang J M, Zhang H C, Hagen N, Dees B, Mercer E M, Forster A H, Kariv I, Marchand P J and Butler W F, 2005, Microfluidic sorting of mammalian cells by optical force switching, *Nature Biotechnology*, **23**, 83

Watson J D and Crick F H C, 1953, A structure for deoxyribose nucleic acid, *Nature*, **171**, 737

Whyte G and Courtial J, 2005, Experimental demonstration of holographic three-dimensional light shaping using a gerchberg-saxton algorithm, *New Journal of Physics*, **7**,

Wright E M, Arlt J and Dholakia K, 2000, Toroidal optical dipole traps for atomic bose-einstein condensates using Laguerre-Gaussian beams, *Physical Review A*, **63**, 013608

Wuite G J L, Smith S B, Young M, Keller D and Bustamante C, 2000, Single-molecule studies of the effect of template tension on t7 DNA polymerase activity, *Nature*, **404**, 103

Wulff K D, Cole D G, Clark R L, DiLeonardo R, Leach J, Cooper J, Gibson G and Padgett M J, 2006, Aberration correction in holographic optical tweezers, *Optics Express*, **14**, 4169

Xie C G, Dinno M A and Li Y Q, 2002, Near-infrared Raman spectroscopy of single optically trapped biological cells, *Optics Letters*, **27**, 249

Zernike F, 1955, How i discovered phase contrast, *Science*, **121**, 345

Figure Caption

Figure 1: Force diagrams for Mie transparent sphere. The forces involved in the three dimensional tweezing of a single transparent dielectric microsphere (Mie regime) as illustrated with ray optics. **(a)** shows the microsphere positioned away from the centre of the focus beam, **(b)** shows the microsphere trapped at the centre of the focus beam

Figure 2: Beam steering lens system
The diagram above illustrates a beam steering lens system that is used in an optical trapping system.

Figure 3: Stiffness of an optical tweezers.
A basic diagram that illustrates a particle being perturbed (i.e. Brownian motion) where the restoring forces are proportional to the displacements (Δx & Δz) of the particle from the stable trapping position.

Figure 4: Dual beam optical tweezers setup
(a) Here, a dual beam optical trapping setup is built with a single fiber laser (wavelength 1070nm) and inverted fluorescence biological microscope system. The linearly polarized collimated beam from the 1070nm fiber laser is directed onto a half waveplate ($\lambda/2$) before being split up into two independent beams by the first polarization beam splitter cube (PBS). The optical power in each of the beam can be controlled by rotating the waveplate. Both beams are recombined at the second polarization beam splitter cube (PBS) and expanded by a beam telescope formed by lenses L1 and L2. The beams expand by f_2/f_1. The expanded beams are redirected by a dielectric mirror (M1) onto the steering mirror (M2). A beam steering lens system, lenses L3 and L4, ensures that the expanded beam is well aligned onto the back aperture of the microscope objective (MO) when the steering mirror (M2) is rotated (see figure.2). NIR dichroic mirror (DM) provides a reflectivity efficiency > 90% at 1070nm. A fluorescence illumination module with a mercury lamp (ML) is directed onto fluorescence filter cube (FLC) that illuminates the sample with the same microscope objective (MO). A bright field illumination from a halogen lamp (HL) and a condenser (CO) illuminates the samples. The diffracted light from the sample is collected by the microscope objective and relayed onto CCD camera (CCD) via the tube lens (TL). **(b)** shows two particles trapped in each of the optical tweezers in a dual beam optical trapping system. (**i)** and (**ii)** two polymer of 1μm in diameter trapped and viewed with brightfield and phase contrast microscope objective respectively. (**iii)** two gold nanoparticles of 200nm in diameter trapped and viewed with a differential interference contrast microscope

Figure 5 Operation of a surface based assay optical force measurement system.

The diagram illustrates an optical force clamp recording displacements of single kinesin molecules while maintaining an average load. (Adapted from (Visscher *et al.*, 1999))

Figure 6 DNA force measurements with optical tweezers
(a) shows a schematic of a DNA molecule that is stretched between beads held in a micropipette and a force-measuring optical trap. The measured extension is the sum of contributions from the single-stranded DNA (ssDNA) and double-stranded DNA (dsDNA) segments. **(b)** Force versus extension for dsDNA and ssDNA molecules (Reprinted by permission from Macmillan Publisher Ltd: Nature, Bustamante, C., Bryant, Z. & Smith, S.B. Ten years of tension: single-molecule DNA mechanics. Nature 421, 423-427 (2003), copyright (2003))(Bustamante *et al.*, 2003).

Figure 7 shows the schematic force versus position curves (dark red) shown for both trap beams. (Reprinted by permission from Macmillan Publisher Ltd: Nature, Abbondanzieri, E.A., Greenleaf, W.J., Shaevitz, J.W., Landick, R., Block, S.M. Direct observation of base-pair stepping by RNA polymerase. Nature 438(7067):460-465 (2005) copyright (2005)(Abbondanzieri *et al.*, 2005).

Figure 8 illustration of an interference intensity pattern (inset) from three interfering waves (red lines). Three temporal and spatial coherence light fields overlap to produce three dimensional optical lattices.

Figure 9 Operation of two axis (x-y) acousto-optic deflectors. A single Gaussian beam enters a two axis acousto-optic deflector that subsequently yields the four diffraction orders arranged in a two (x, y) dimensional coordinate system.

Figure 10 Fourier holography and iterative Gerchberg-Saxton (GS) algorithm.
(Courtesy of Ryan Smith and Gabe Spalding)

Figure 11 Phase behavior of colloidal molecular crystals on optical lattices
Contour plots of the lateral density distribution p and the averaged local particle density $ploc(x, y)$ for different light potentials V_0. The horizontal axes are x and y, respectively. All units are in μm. (Reprinted with permission from American Physical Society, M Brunner and C Bechinger Phase Behavior of Colloidal Molecular Crystals on Triangular Light Lattices Physical review letters. 88 24830 (2005),Copyright (2005))(Brunner and Bechinger, 2002)

Figure 12 : Wang et al. active cell sorter
Microfluidic sorting of mammalian cells by optical force switching. Nature Biotechnology 23, 83-87 (2005) (Reprinted by permission from Macmillan Publisher

Ltd: Nature Biotechnology ,Wang, M.M. et al. Microfluidic sorting of mammalian cells by optical force switching. Nature Biotechnology 23, 83-87 (2005).copyright (2005))(Wang *et al.*, 2005)

Figure.13 AOD sorting
Shows the plotted trajectories of the four different types of silica spheres (D) 2.3 μm,(C) 3.0 μm, (B) 5.17 μm, and (A) 6.84 μm sorted through the time sharing optical landscape (see insert). (Reprinted with permission from Optical Society of America, G. Milne, D. Rhodes, M. MacDonald, and K. Dholakia, "Fractionation of polydisperse colloid with acousto-optically generated potential energy landscapes," Optics Letters, vol. 32, pp. 1144-1146, (2007) copyright 2007)(Milne *et al.*, 2007b)

Figure 14 Schematic implementation of holographic optical traps.
A laser beam is reflected by two mirrors M1, M2 and M3 is expanded and directed onto a liquid crystal spatial light modulation (SLM), which imprints a computer generated hologram (CGH) onto its wavefronts. The 200 × 200 pixel region of a CGH shown encodes a pattern, $I(r)$ of 119 optical tweezers that are arranged in a quasiperiodic arrangements. The phase hologram is relayed using relay optics and onto the input pupil of an objective lens that focuses it into holographic optical traps. Each optical tweezers traps a colloidal sphere of 1.5 micrometer in diameter. (Reprinted with permission from Optical Society of America, D. G. Grier and Y. Roichman, Holographic optical trapping, Applied Optics 45, 880-887 (2006) copyright 2006).(Grier and Roichman, 2006)

Figure 15 Setup of multiple optical traps generated with AODs and the corresponding confocal images of optically assembled three dimensional colloidal crystals.
(a) shows the setup used for creating arrays of tweezers in two separate planes. A mirror M3 after the acoustic optics deflected (AOD) reflects the beam into a 1:1 telescope formed by two lenses ($L5$ and $L6$, both with focal length of 120 mm). A polarizing beam splitting cube $C3$ is placed in front of the Pockels cell to remove any horizontal component of the polarization introduced by the AODs. A mirror M4, the lenses L7 and L8 (with focal lengths of 65 and 140 mm) expand the beam to overfill the back aperture of the objective. A polarizing beam splitter cube C4 splits the laser beam into two separate paths. In each of the paths the beam passes through a 1:1 telescope formed by a pair of lenses ($L9a,b$ and $L10a,b$ all f =90 mm). The lenses $L9a, b$ are positioned in a plane conjugate to the back focal plane of the upright objective. After recombination of the two beams using a polarizing beam splitter cube $C5$, the combined beam is coupled into the microscope with the mirrors M5, M6 and lenses L3 and L4. A movement of lens L3 results in a collective displacement of the two traps. The upright objective was used for trapping, while the inverted objective was used for imaging. The part of the setup drawn in light gray was not used when two trapping planes were created. **(b)** shows the images of the three dimensional optically assembled fluorescence structures. The scale bars are 1 μm. (Reprinted with permission from AIP, D. L. J. Vossen, A. van der Horst, M. Dogterom, and A. van Blaaderen, "Optical tweezers and confocal microscopy for

simultaneous three-dimensional manipulation and imaging in concentrated colloidal dispersions," Rev. Sci. Instrum. 75, 2960-2970 (2004)).(Vossen *et al.*, 2004)

Figure.16 Schematic diagram of a time-shared holographic optical trapping apparatus.

Trap arrays are formed using a high NA objective in a commercial optical microscope in conjunction with two acousto-optic deflectors and a spatial light modulator (SLM) to produce a time-shared (3D) array of optical traps. The plane of the SLM, a, is imaged into the microscope objective entrance aperture (OEA) a*, and the corresponding planes b and c are imaged into the focal region of the microscope. The same microscope that is used to produce the cell traps is also used for viewing (via the blue beam). The inset in the lower left shows an example of a 2D 5x5 array of P. Aeruginosa formed using this apparatus and subsequently embedded in hydrogel. The distances are: AODs—L1=165 mm; L1—L2= 650 mm; L2—SLM =332 mm; SLM—L3=421 mm; L3—L4=1400 mm; and L4—OEA =493 mm, where the focal lengths are L1=150mm, L2=500mm, L3=1000mm, L4=400mm. (Reprinted with permission from Biophysical Journal, Akselrod, G.M. et al. Laser-guided assembly of heterotypic three-dimensional living cell microarrays. Biophysical Journal 91, 3465-3473 (2006). copyright 2006).(Akselrod *et al.*, 2006)

Figure 17: Various orders of the Laguerre Gaussian beams (inset shows a computer generated hologram for LG_0^1)

In the paraxial approximation, optical vortices can be expressed as laser beam modes, known as Laguerre-Gaussian modes, LG_p^l. The laser modes are characterised by two integer indices namely *l*, azimuthal indices, and *p* is the radial indices. Inset is the computer generated hologram for LG_0^1

Figure 18: Helical wavefront of a LG_0^1 beam. Scattering from such a wavefront can lead to particle rotation.

Figure 19: Spin and orbital angular momentum transfer with circularly polarized LG_0^1 beam

Successive frames of the video image showing the stop–start behavior of a 2-μm-diameter Teflon particle held with an optical spanner (Reprinted with permission from Optical Society of America, N. B. Simpson, K. Dholakia, L. Allen and M. J. Padgett, Mechanical equivalence of spin and orbital angular momentum of light: An optical spanner Optics Letters **22**, No. 1, 52-54 (1997)) (Simpson *et al.*, 1997)

Figure 20: Numerical simulation of off axis optical vortex beam and experimental images of the fusion of droplets with off-axis optical vortex beams
Numerical calculation of the far-field diffraction intensity pattern of an optical vortex beam, LG_{01}, of beam waist, w, with its azimuthal phase change displaced away from the central axis at different transverse locations (y) on the beam waist and orthogonally across the propagation direction; **(a) y**= 0, **(b)** y= w/4, **(c)** y= w/2, **(d)** y= w, and **(e)** to **(g)** shows sequence of images showing vortex-trap-induced fusion of two aqueous droplets in acetophenone (with 0.0025% w/w SPAN 80). The scale bar represents 10 μm (Reprint with permission from RSC Lorenz, R.M. et al. Vortex-trap-induced fusion of femtoliter-volume aqueous droplets. Analytical Chemistry 79, 224-228 (2007). Copyright (2007) American Chemical Society)(Lorenz *et al.*, 2007)

Figure 21 Microfluidic flow generated with an array of optical vortices
Time-lapse composite of 16 images in half-second intervals of colloidal spheres in the holographic pump.(Reprinted with permission from Optical Society of America, K. Ladavac and D. Grier, "Microoptomechanical pumps assembled and driven by holographic optical vortex arrays," Opt. Express **12**, 1144-1149 (2004)).(Ladavac and Grier, 2004)

Figure 22: Optically driven colloidal ring.
(a) Projected intensity pattern for an optical vortex with. **(b)** Video microscope image of three colloidal silica spheres trapped on the optical vortex. **(c)** Measured intensity variations around the optical vortex's circumference.(reprinted with permission from American physical society, , Y. Roichman, G. M. Zaslavsky and D. G. Grier, Anomalous collective dynamics in optically driven colloidal rings *Physical Review E* **75**, 020401(R) (2007) copyright 2007) (Roichman *et al.*, 2007)

Figure 23: Illustration of an axicon generated Bessel beam and its three dimensional intensity profile.
(a) illustrates the generation of a zero order Bessel beam with a non-diffractive distance of z_{max} from a Gaussian beam of beam waist (w) through the use of an axicon lens element (angle γ). **(b)** shows the three dimensional intensity profile of a Bessel beam. (Adapted and reprint with Permission from author(Cizmar, 2006))

Figure 24: Optical trapping setup with a zeroth order Bessel beam
Experimental arrangement for Bessel tweezing: Lenses f1=50 mm and f2=250 mm expand the beam to illuminate the axicon, which generates the Bessel beam. Lenses f3=250 mm and f4=25 mm reduce this Bessel beam to one with a central maximum of ≈9.4 μm diameter. Lens f4 is adjusted to manipulate the particles. The inset shows a picture and cross-sectional profile of the Bessel light beam which propagates in the vertical direction. (Reprinted with permission from Elsevier J. Arlt, V. Garces-Chavez,

W. Sibbett and K. Dholakia, Optical micro-manipulation using a Bessel light beam Optics Communications 197, 239-245 (2001))(Arlt *et al.*, 2001b)

Figure 25: Observation of the reconstruction of a zeroth order Bessel beam in trapping

(a) Inverted Bessel beam optical tweezers experimental set-up (Reprint by permission from Macmillan Publisher Ltd: Nature Garces-Chavez, V., McGloin, D., Melville, H., Sibbett, W. & Dholakia, K. Simultaneous micromanipulation in multiple planes using a self-reconstructing light beam. Nature **419**, 145-147 (2002) copyright (2005))(Garces-Chavez *et al.*, 2002a). (Bottom) The central core of the Bessel beam facilitates long range guiding of microparticles. Two-photon fluorescence signal from two fluorescent microspheres of diameter 5 μm are optically confined and propelled with femtosecond Bessel beam (pulse duration = 100 fs, central wavelength = 750 mW, diameter of central core= 4 μm). The beam reforming approximately 90 μm in front of the trapped sphere. (Reprinted with permission from IOP, K Dholakia, H Little, C T A Brown, B Agate, D McGloin, L Paterson and W Sibbett, "Imaging in optical micromanipulation using two-photon excitation", New J. Phys. **6** 136 2004 copyright (2004))(Dholakia *et al.*, 2004)

Figure 26 Optical conveyer belt

(Top) Illustration of counter-propagating geometry with two Bessel beams should result in a very long chain of standing wave traps. By varying the phase of one of the beam, the standing wave can be converted into an extended linear array of optical traps for delivery of micro-objects (blue sphere) over large distances so called "Optical Conveyor Belt". (Bottom) Simultaneous optical confinement and delivery of polystyrene particles of radius 100 nm over a distance of 60 μm using the mechanism of optical conveyor belt. (Reprint with Permission from author (Cizmar, 2006))

Figure 27: Brownian motion of particles confined within the concentric rings of a Bessel beam.

Typical transversal trajectory of radius=1.15 micrometer silica sphere in a Bessel beam.(reprint from permission from optical society of American, Milne, G., Dholakia, K., McGloin, D., Volke-Sepulveda, K. & Zemanek, P. Transverse particle dynamics in a Bessel beam. Optics Express 15, 13972-13987 (2007 copyright 2007). (Milne *et al.*, 2007a)

Figure 28: Use of Bessel beam for the sorting and isolation of CD2 T-lymphocytes from a sample of mononuclear cells.

(Reprinted with permission from American Institute of Physics, Paterson, L. et al. Light-induced cell separation in a tailored optical landscape. Applied Physics Letters 87, 123901-123903 (2005),Copyright (2005)) (Paterson *et al.*, 2005)

Figure 1: Force diagrams for Mie transparent sphere.

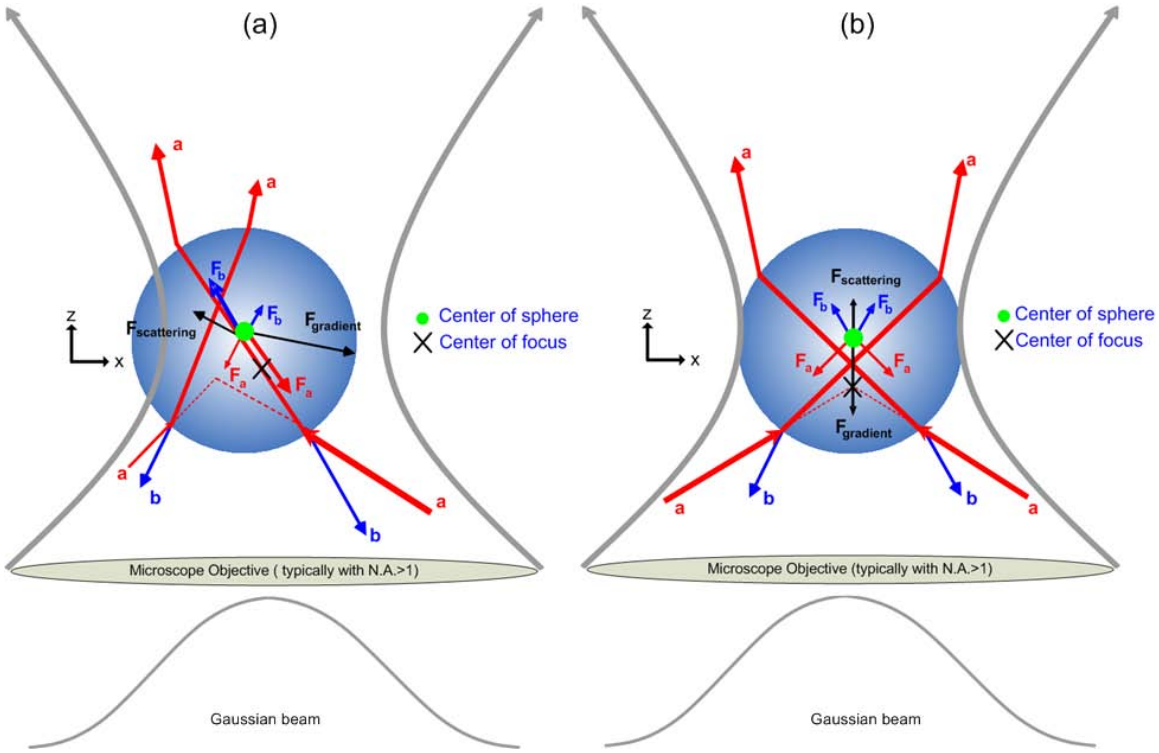

Figure 2: Beam steering lens system

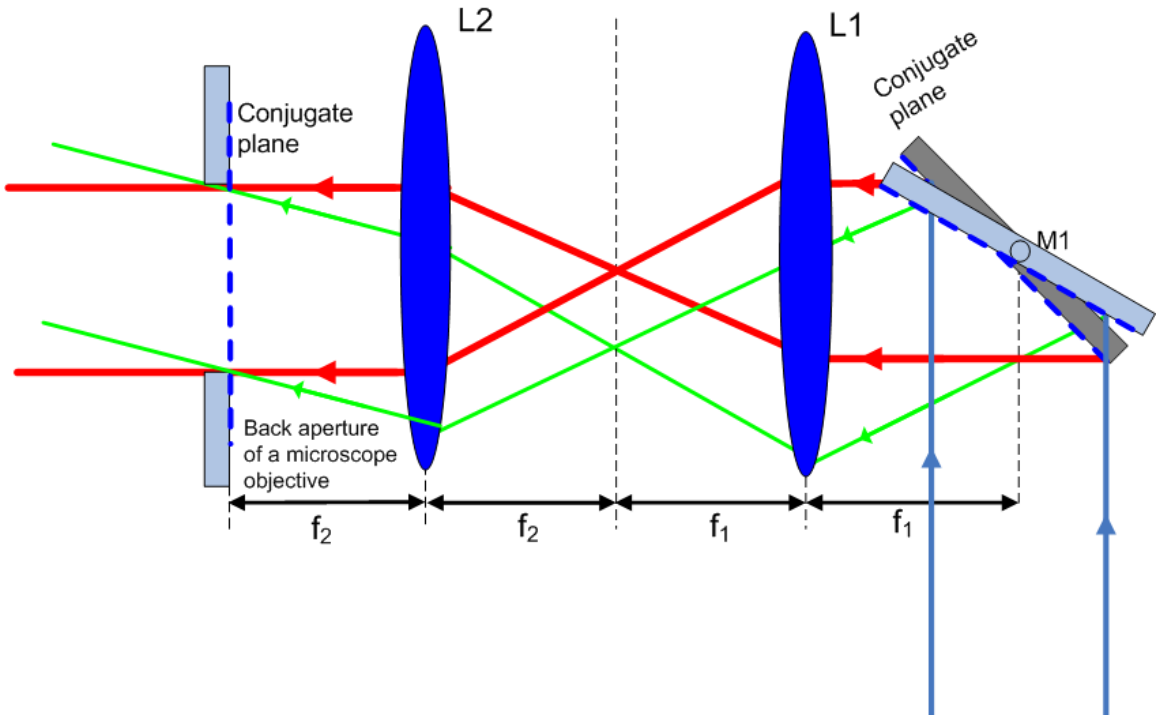

Figure 3: Stiffness of an optical tweezers.

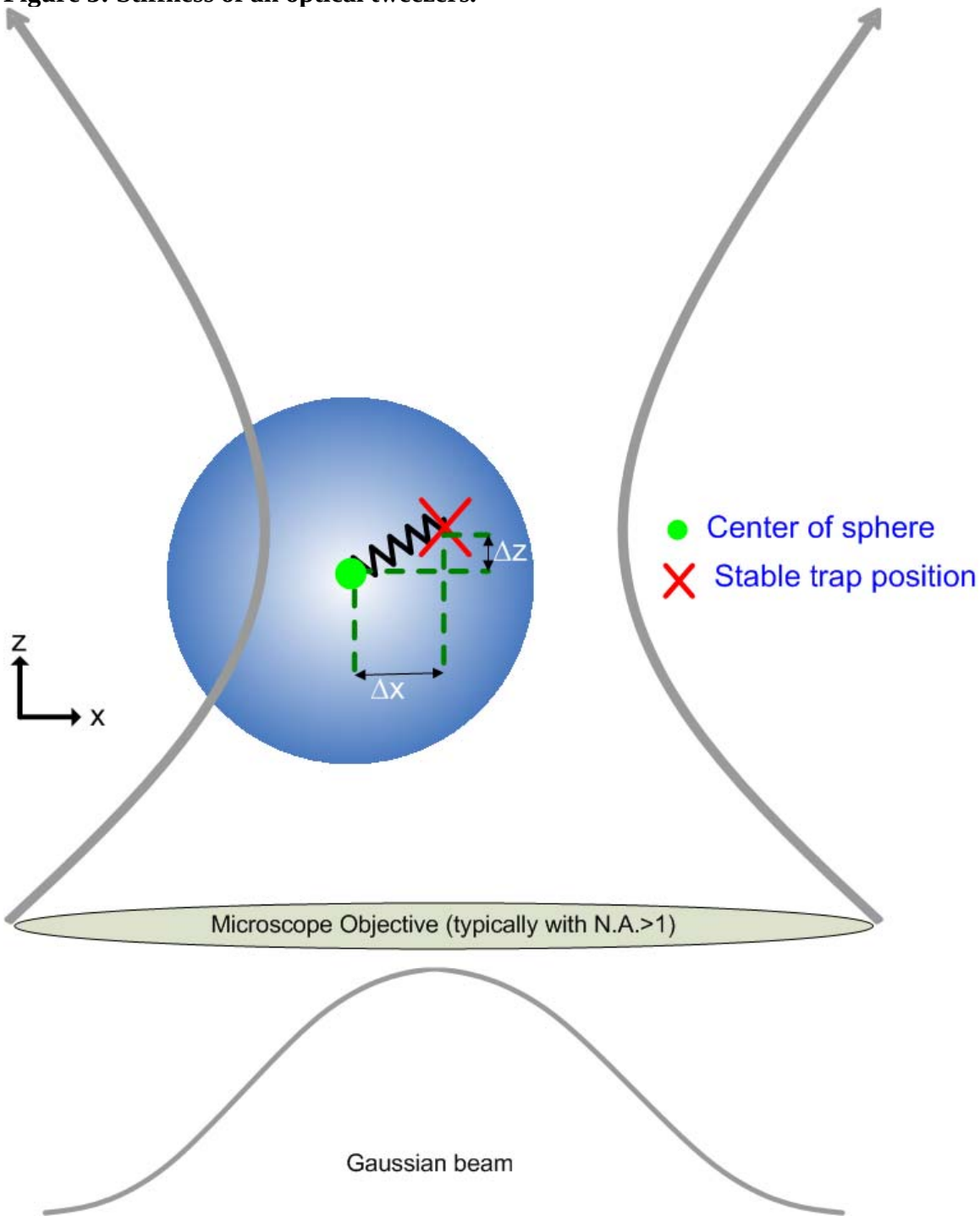

Figure 4: Dual beam optical tweezers setup

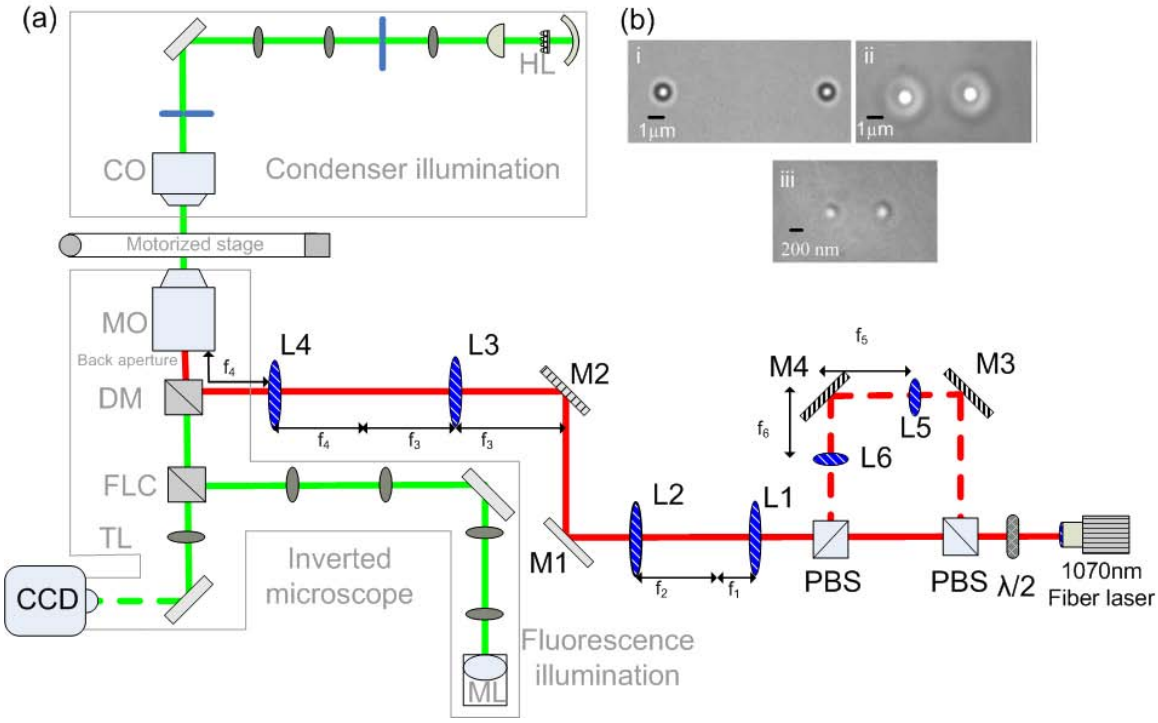

Figure 5 Operation of a surface based assay optical force measurement system.

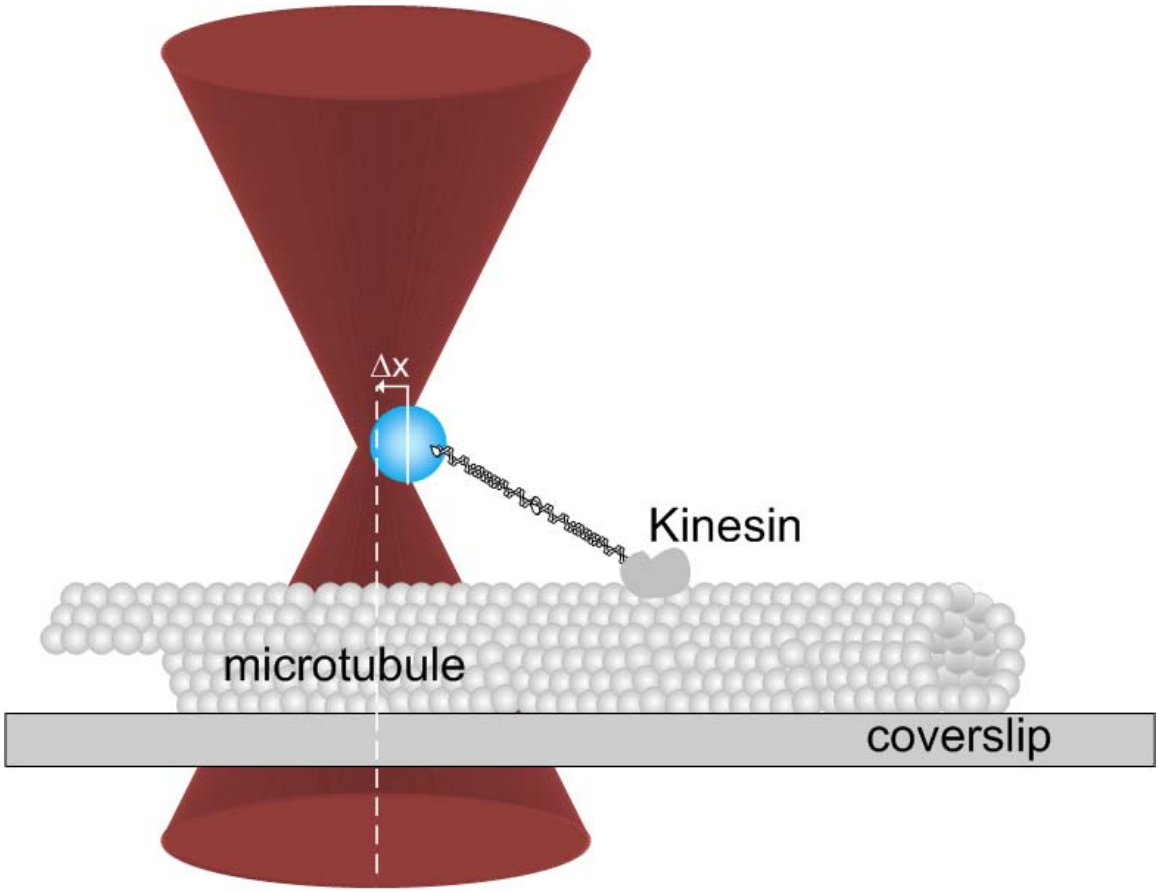

Figure 6 DNA force measurements with optical tweezers

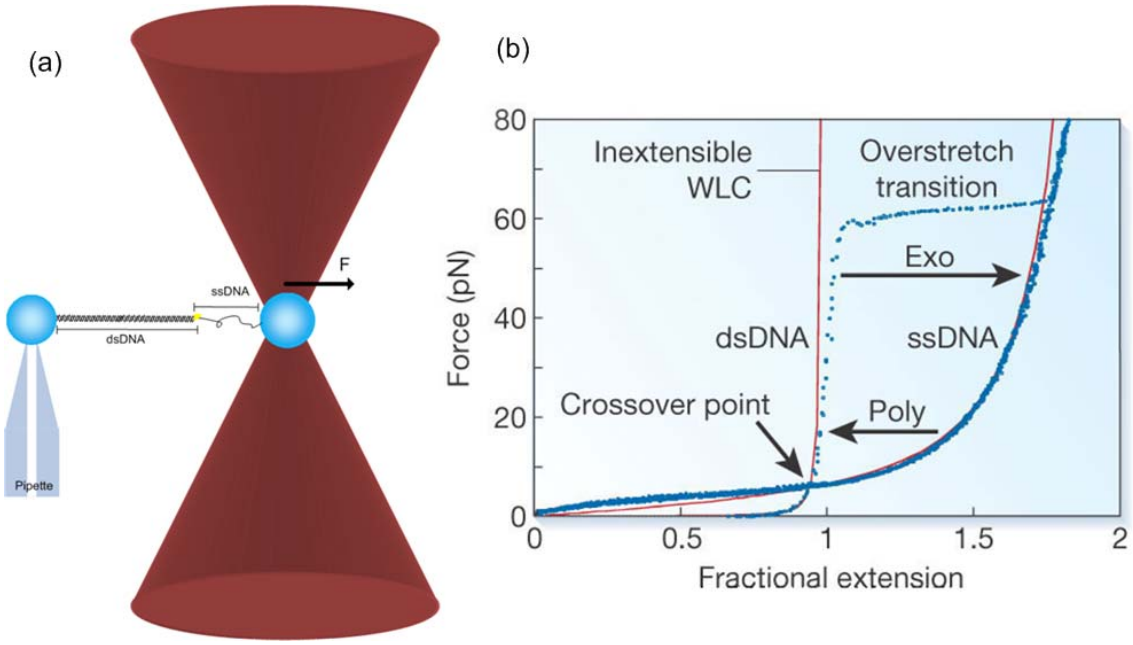

Figure 7 shows the schematic force versus position curves (dark red) shown for both trap beams (not drawn to scale).

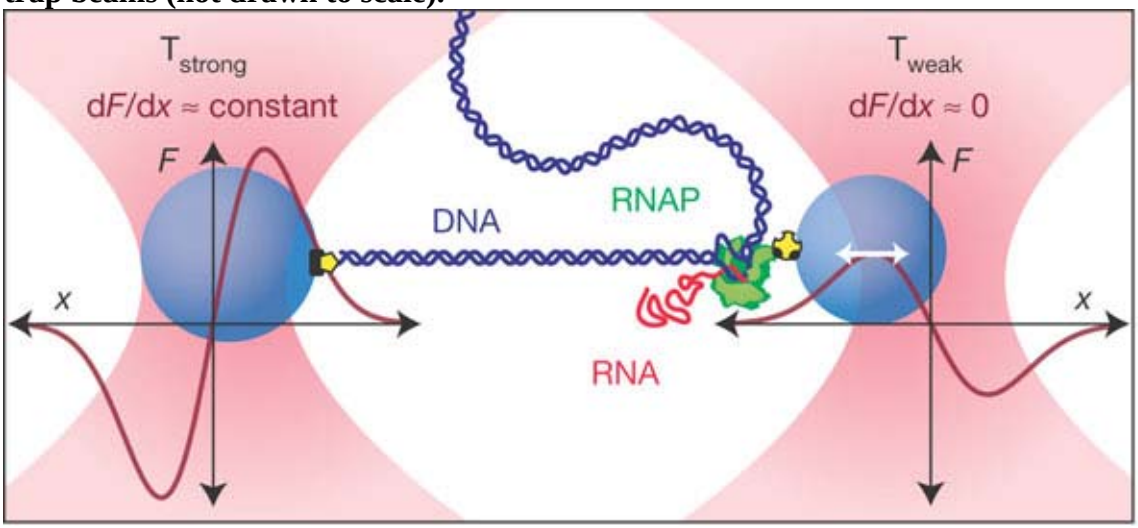

Figure 8 illustration of an interference intensity pattern (inset) from three interfering waves (red lines).

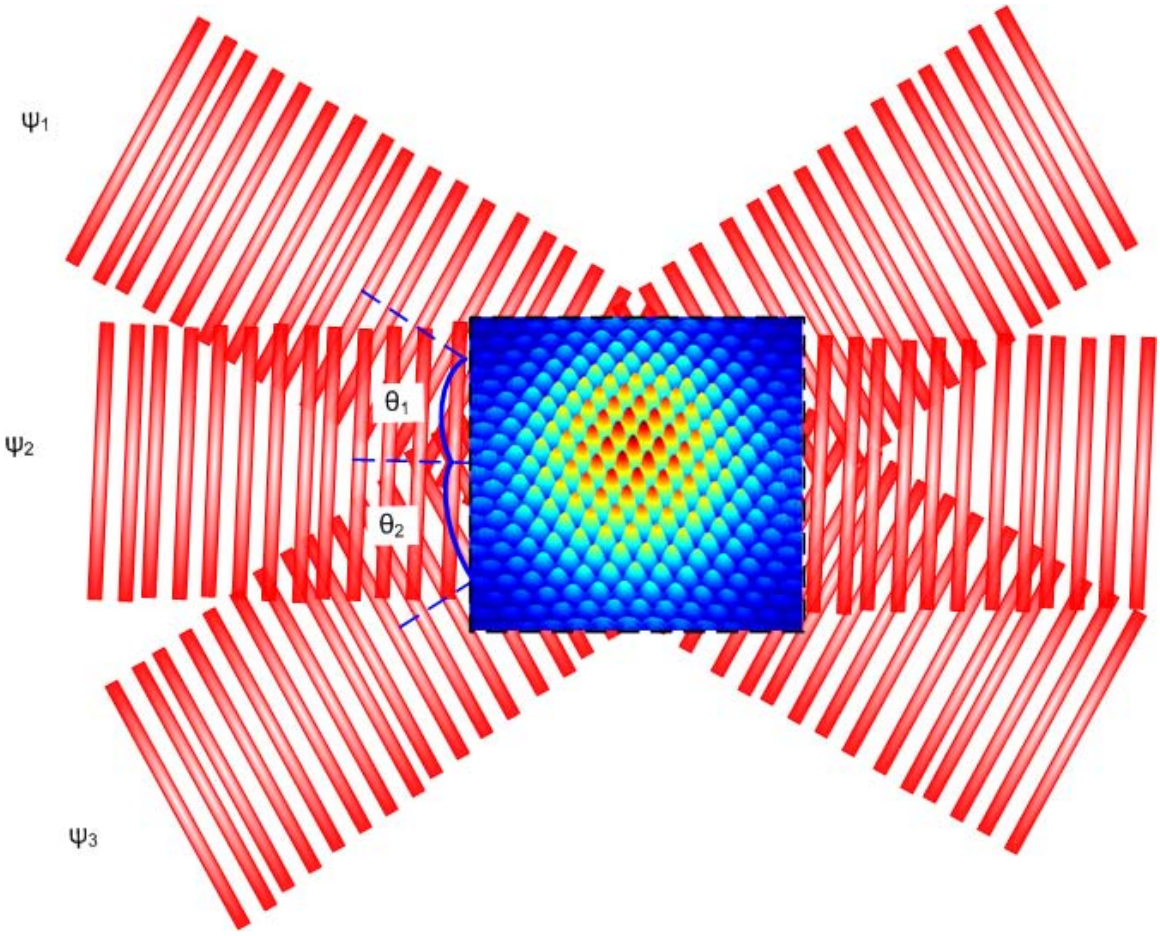

Figure 9 Operation of a pair of acousto-optic deflector.

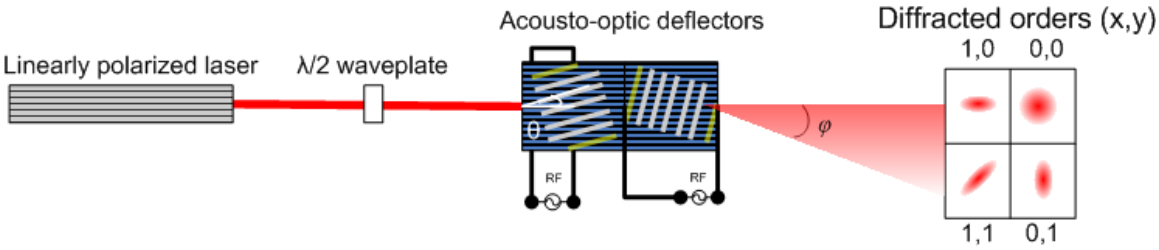

Figure 10 Fourier holography and iterative Gerchberg-Saxton (GS) algorithm.

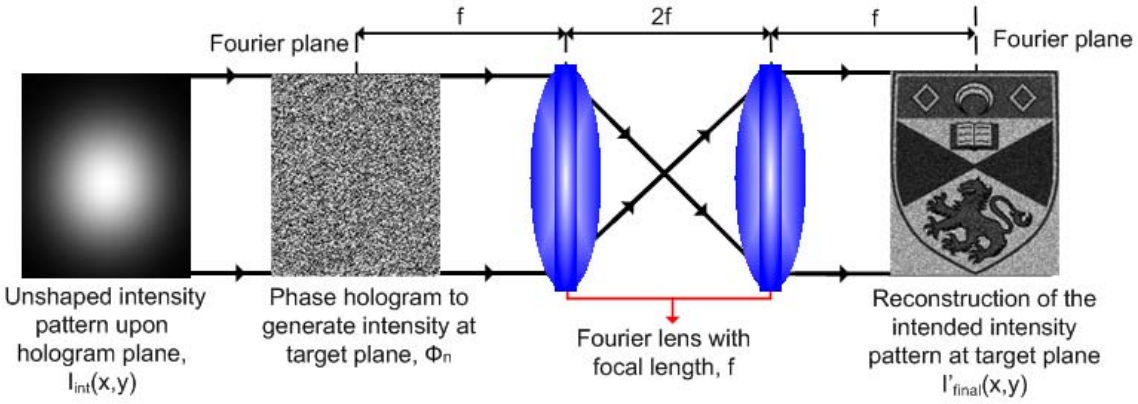

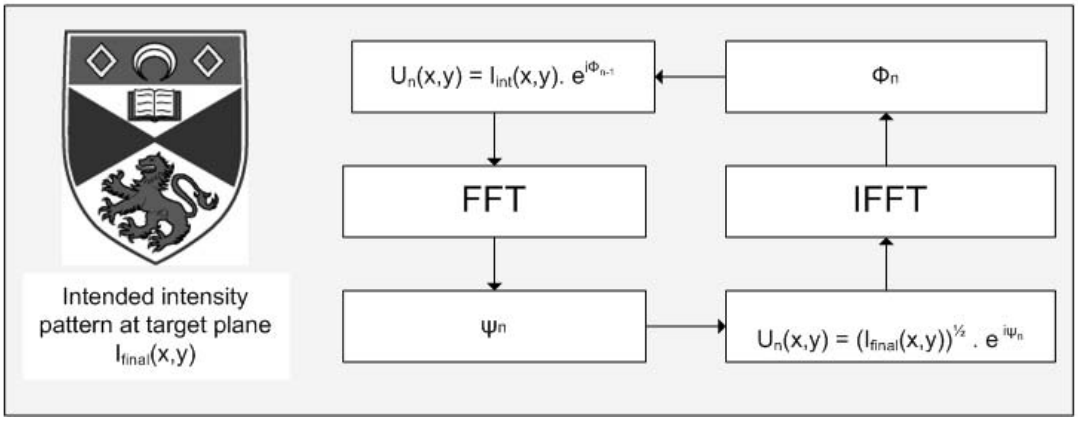

Figure 11 Phase behavior of colloidal molecular crystals on optical lattices

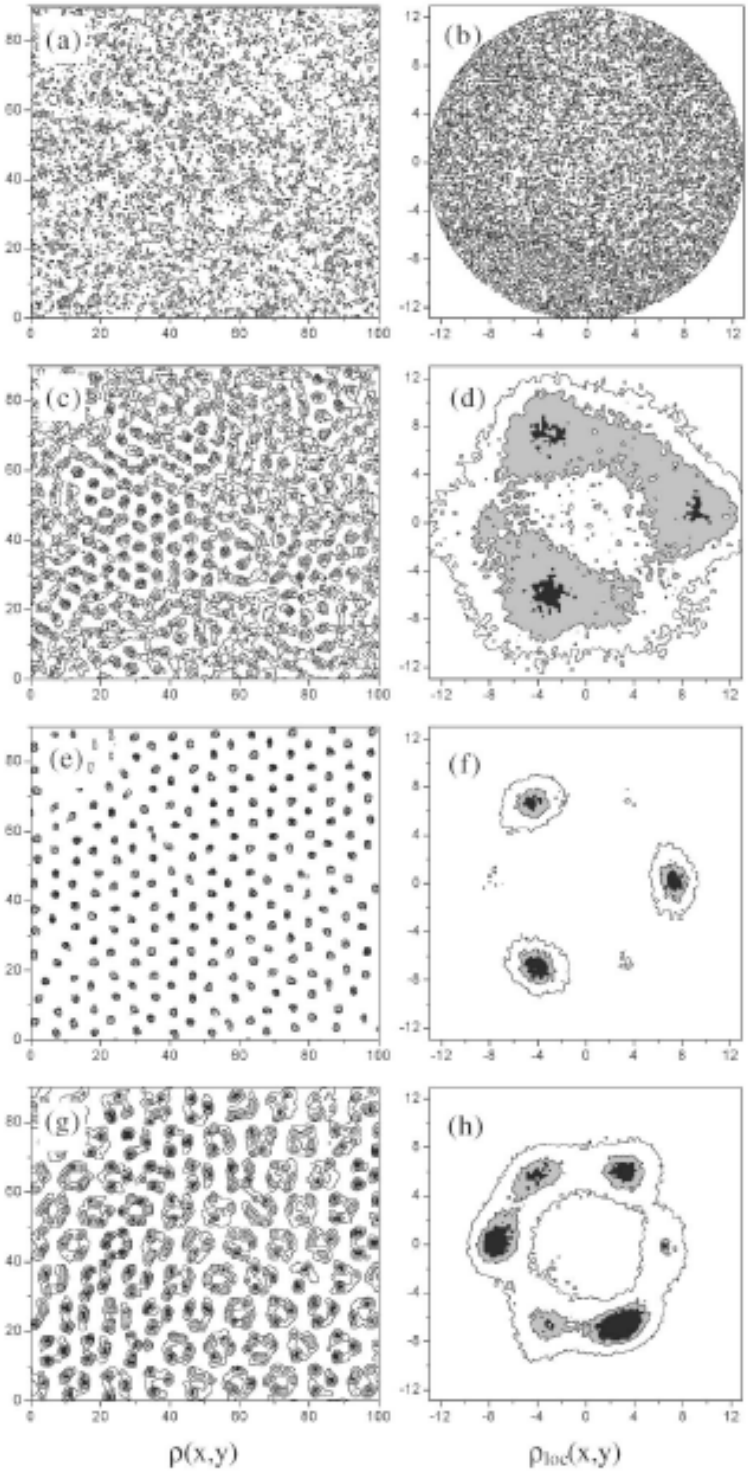

Figure 12 : Wang et al. active cell sorter

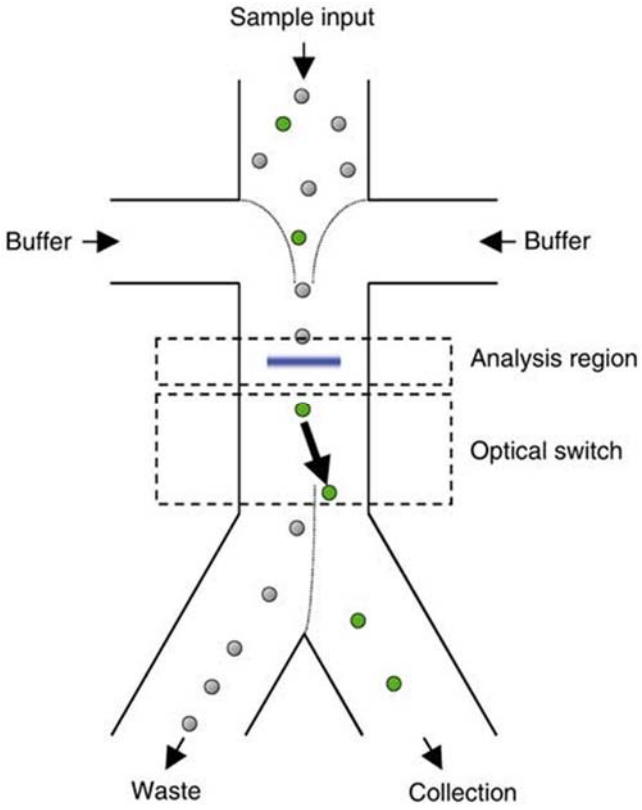

Figure.13 AOD sorting

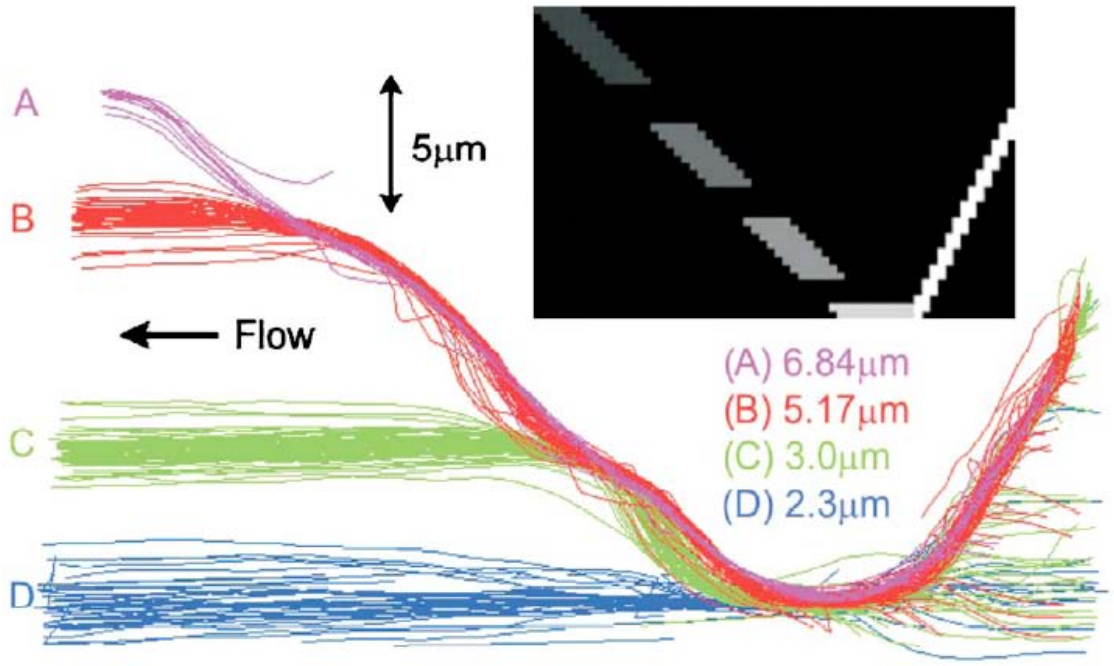

Figure 14. Schematic implementation of holographic optical traps.

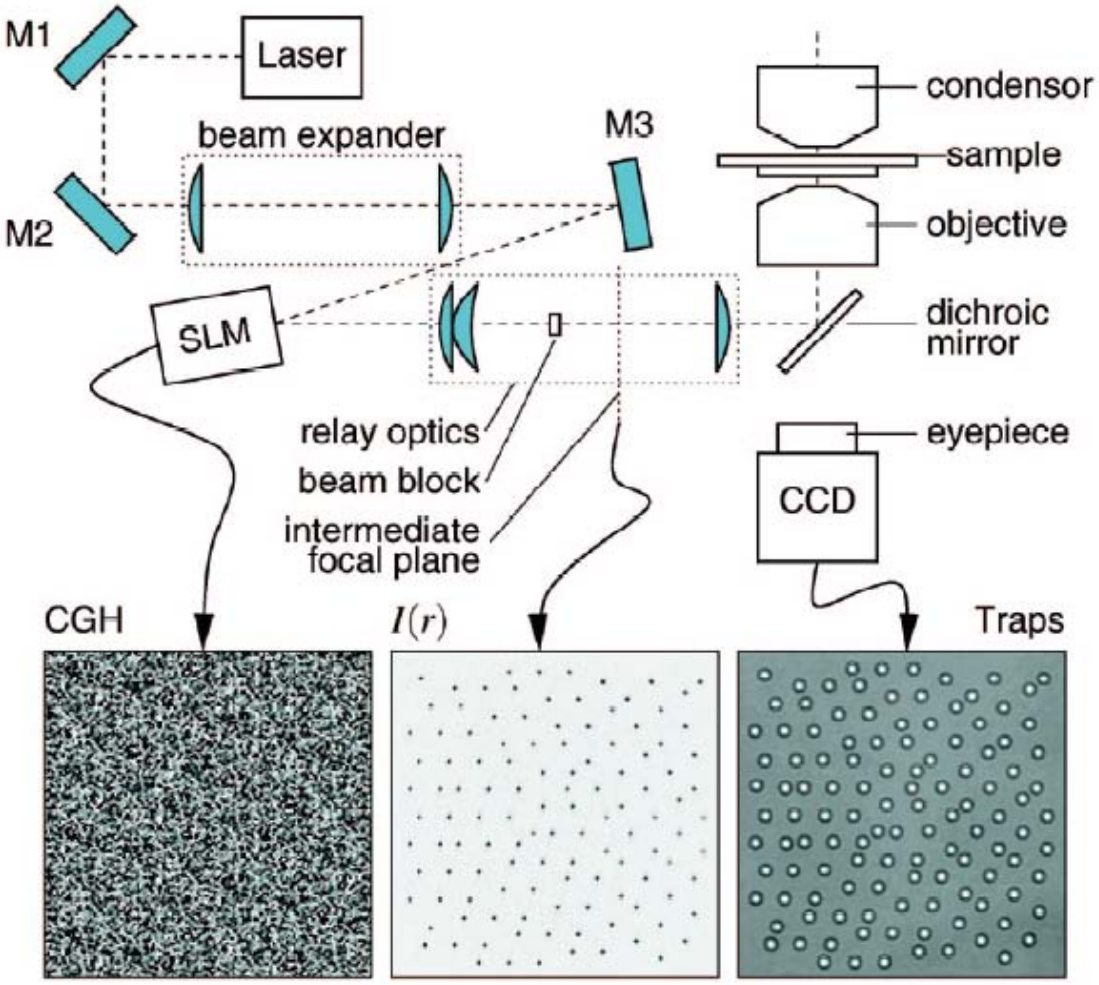

Figure 15 Setup of multiple optical traps generated with AODs and the corresponding confocal images of optically assembled three dimensional colloidal crystals.

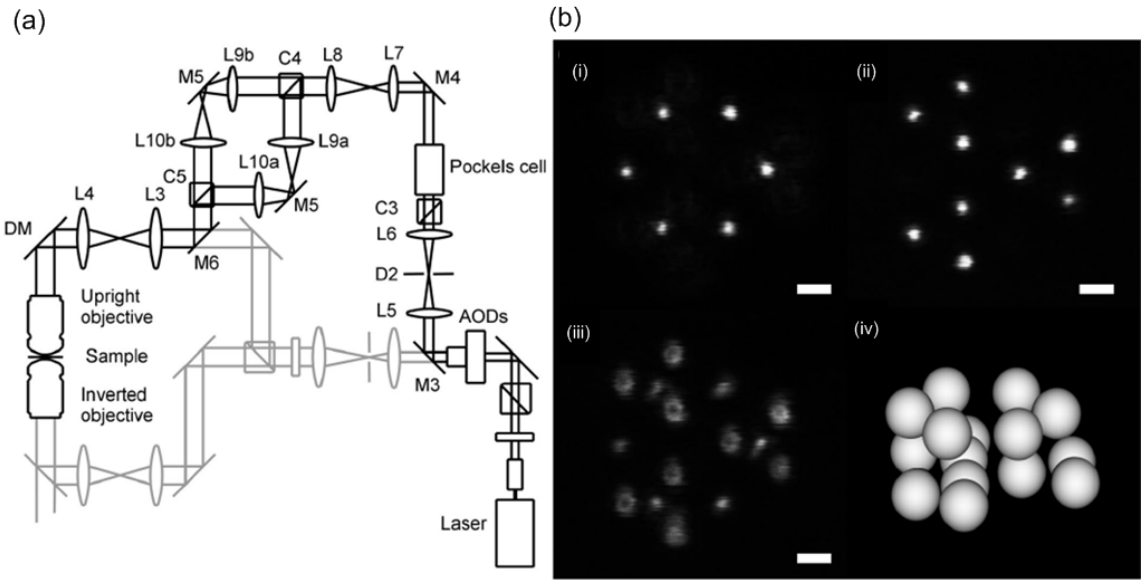

Figure.16 Schematic diagram of a time-shared holographic optical trapping apparatus.

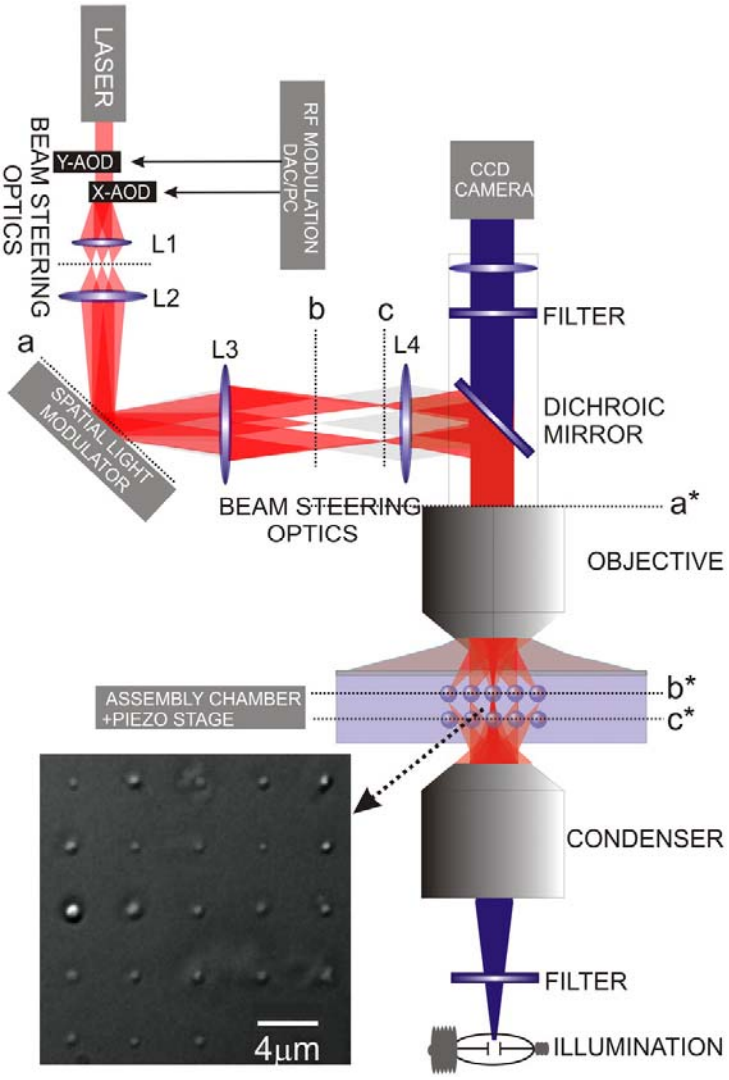

Figure 17: Various orders of the Laguerre Gaussian beams (inset shows a computer generated hologram for LG_0^1)

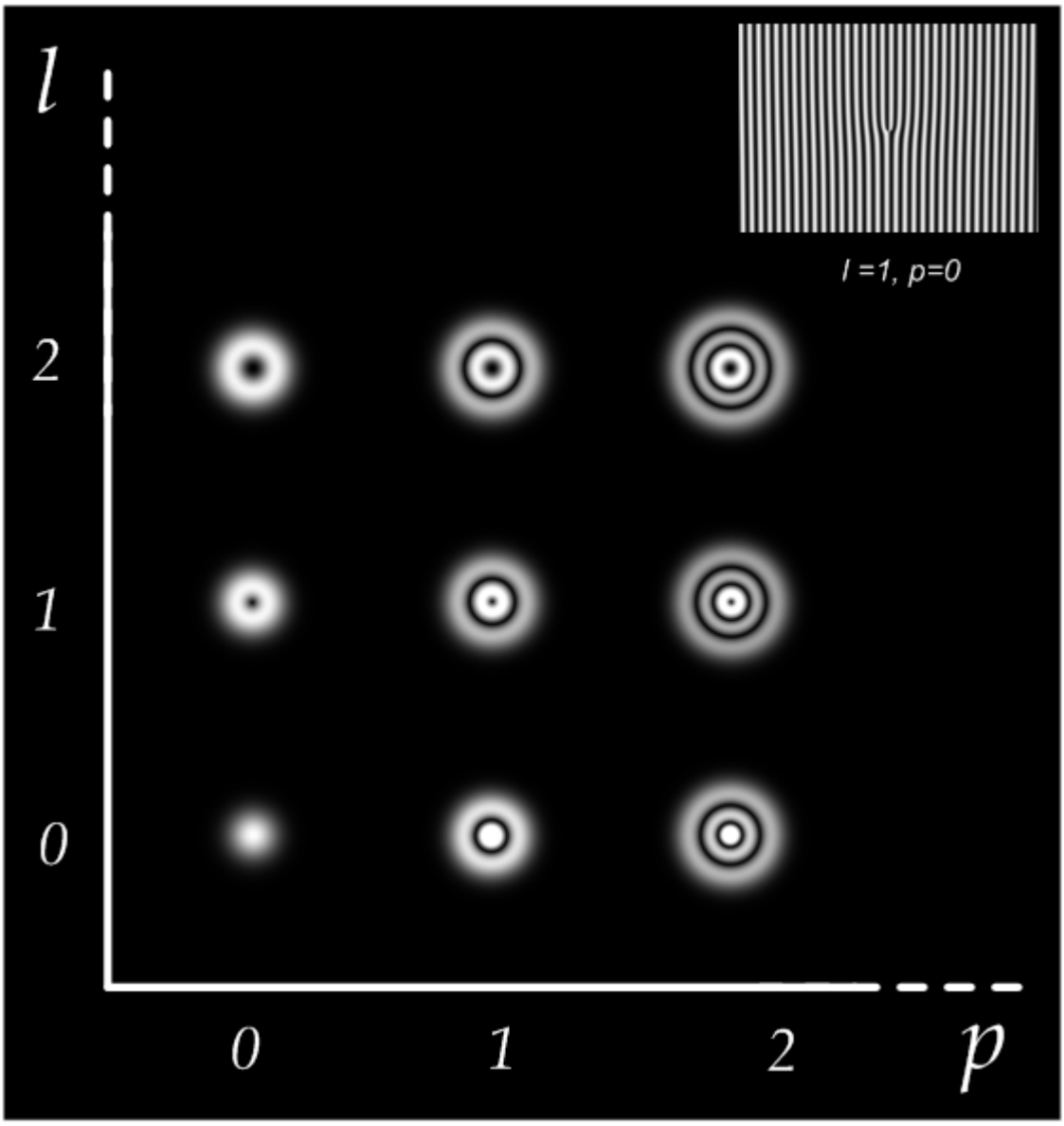

Figure 18: Helical wavefront of a LG_0^1 beam.

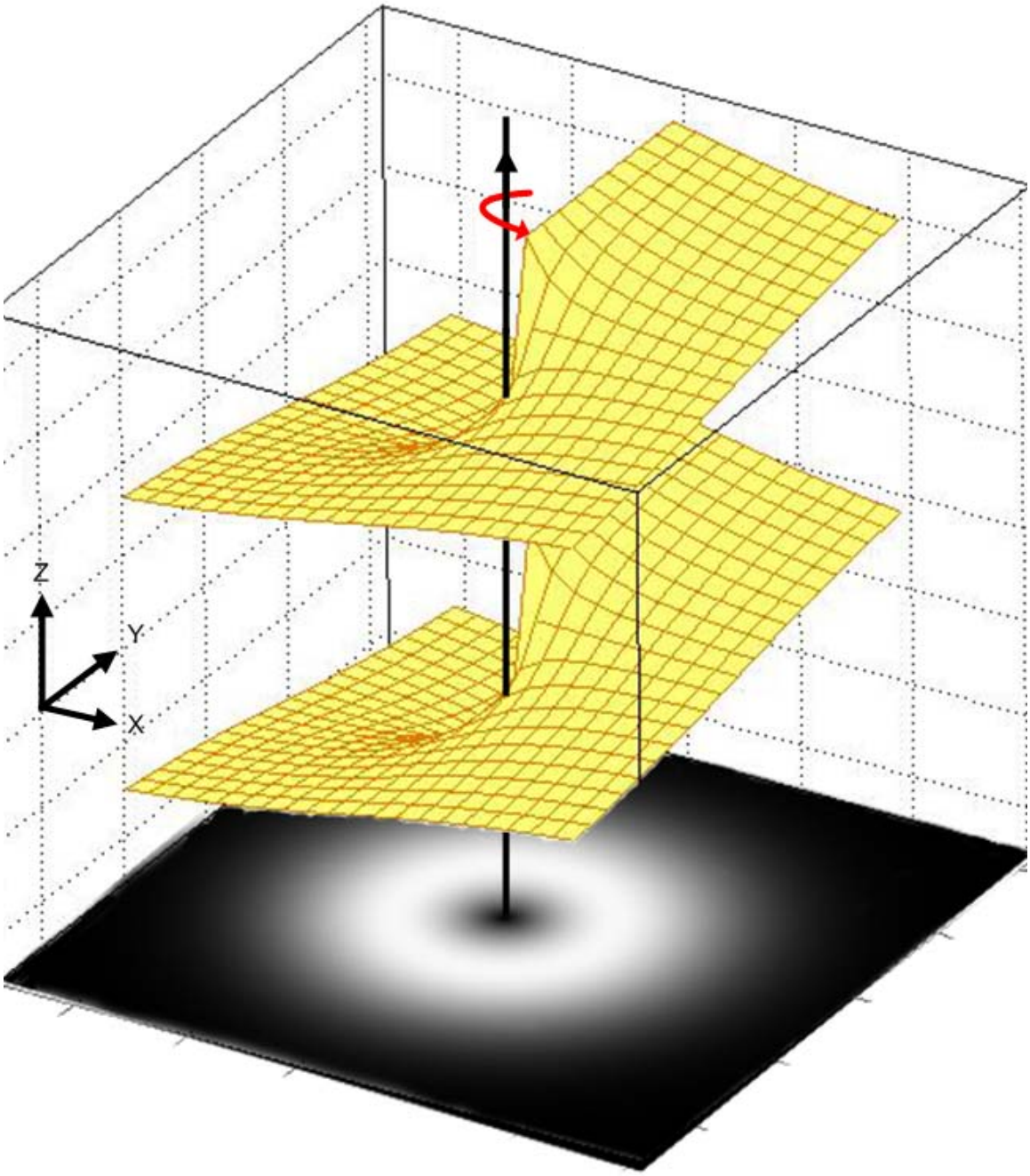

Figure 19: Spin and orbital angular momentum transfer with circularly polarized LG_0^1 beam

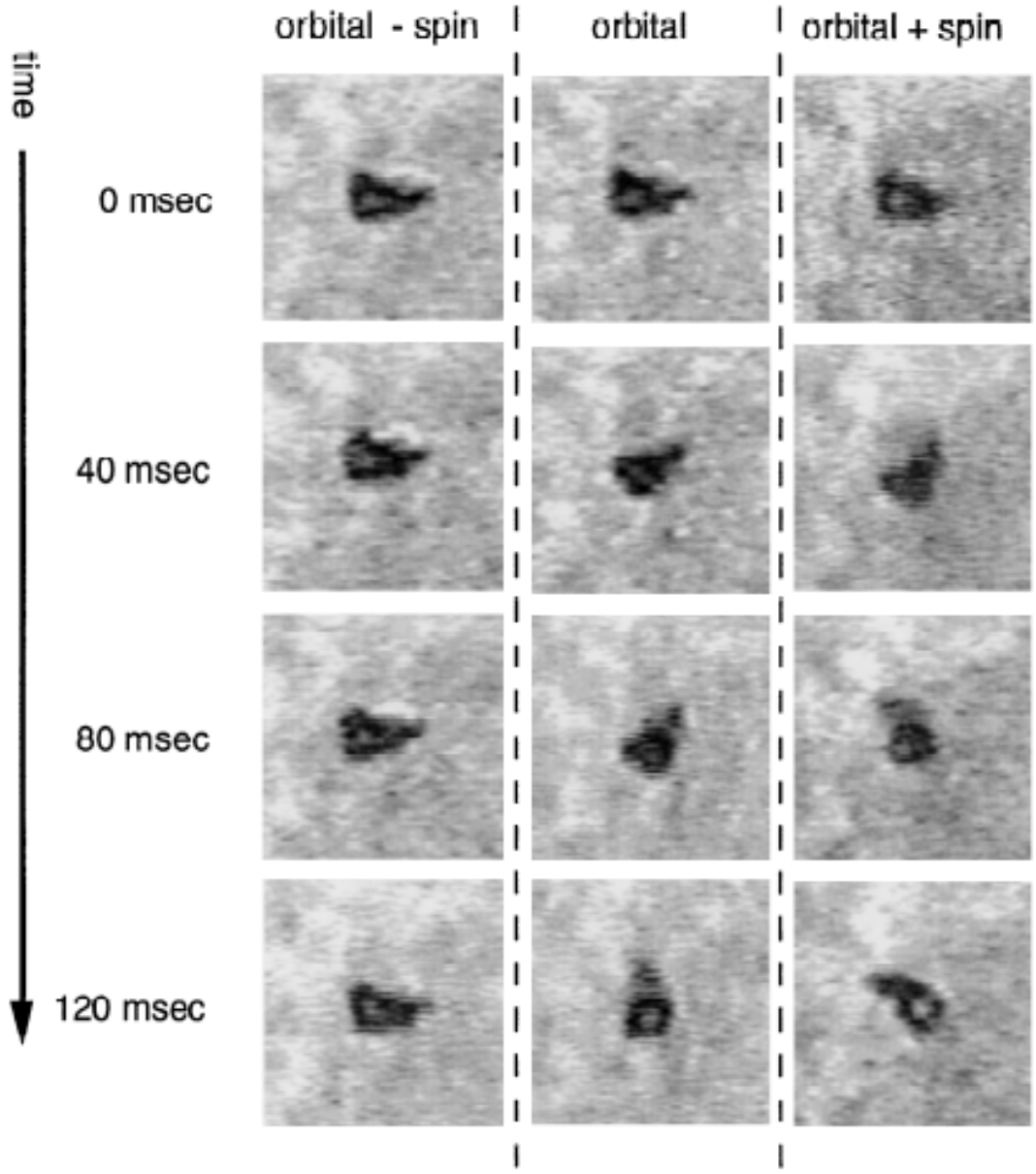

Figure 20: Numerical simulation of off axis optical vortex beam and experimental images of the fusion of droplets with off-axis optical vortex beams

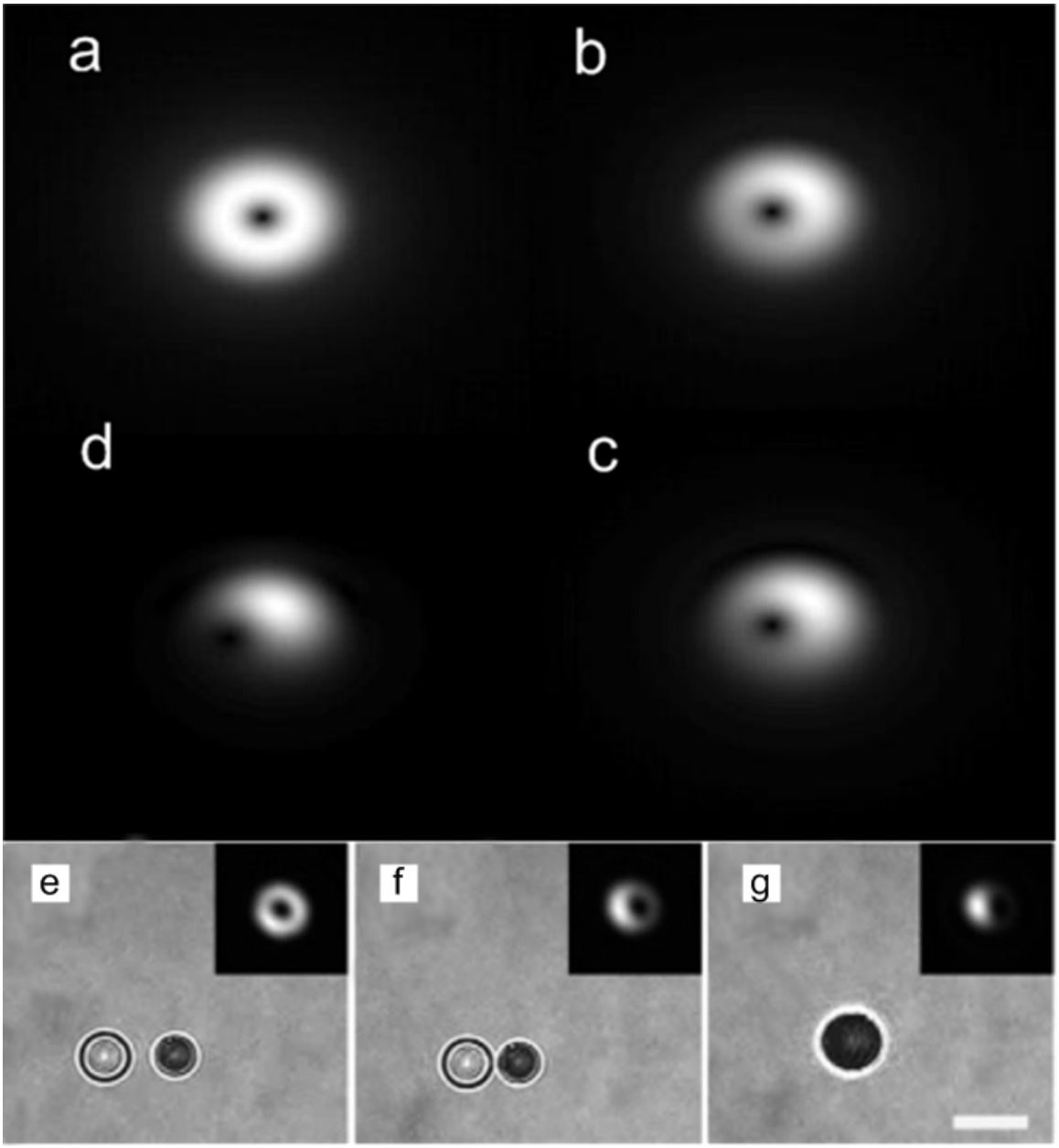

Figure 21 Microfluidic flow generated with an array of optical vortices

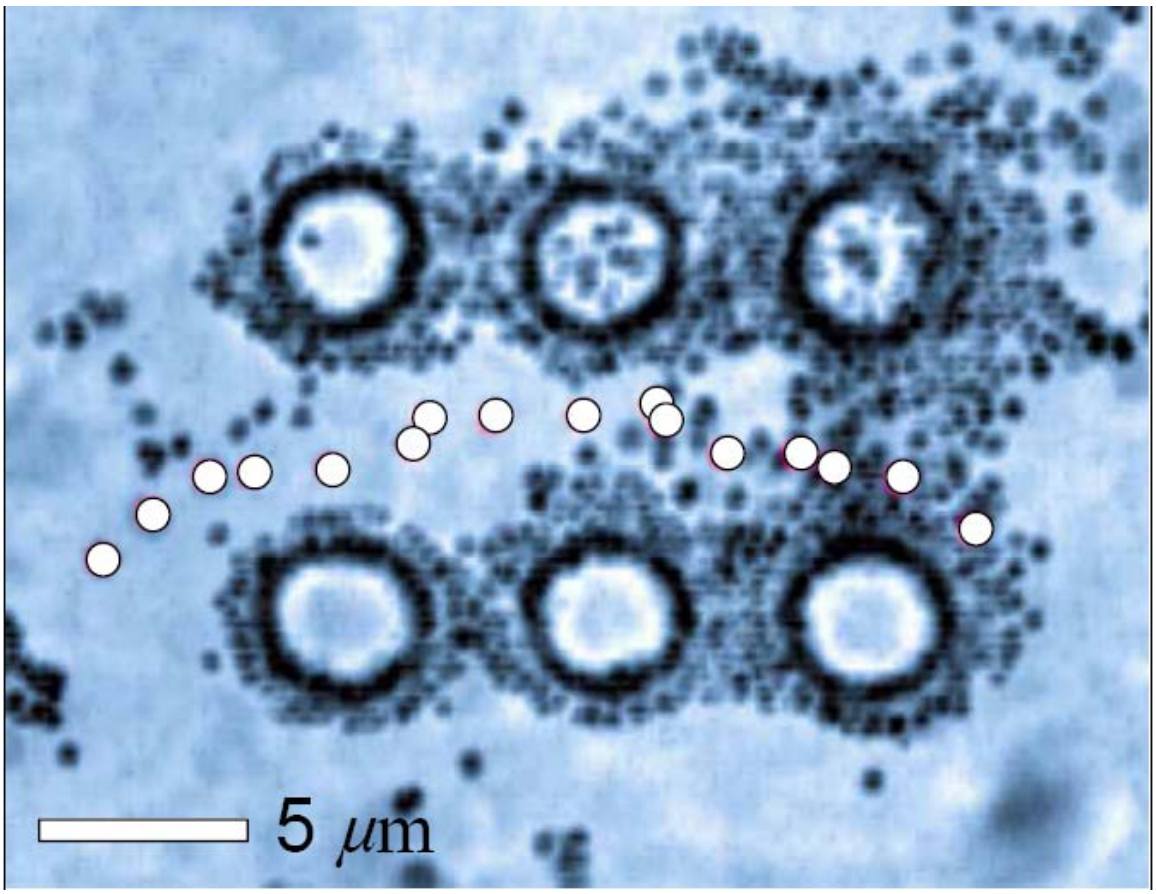

Figure 22: Optically driven colloidal ring.

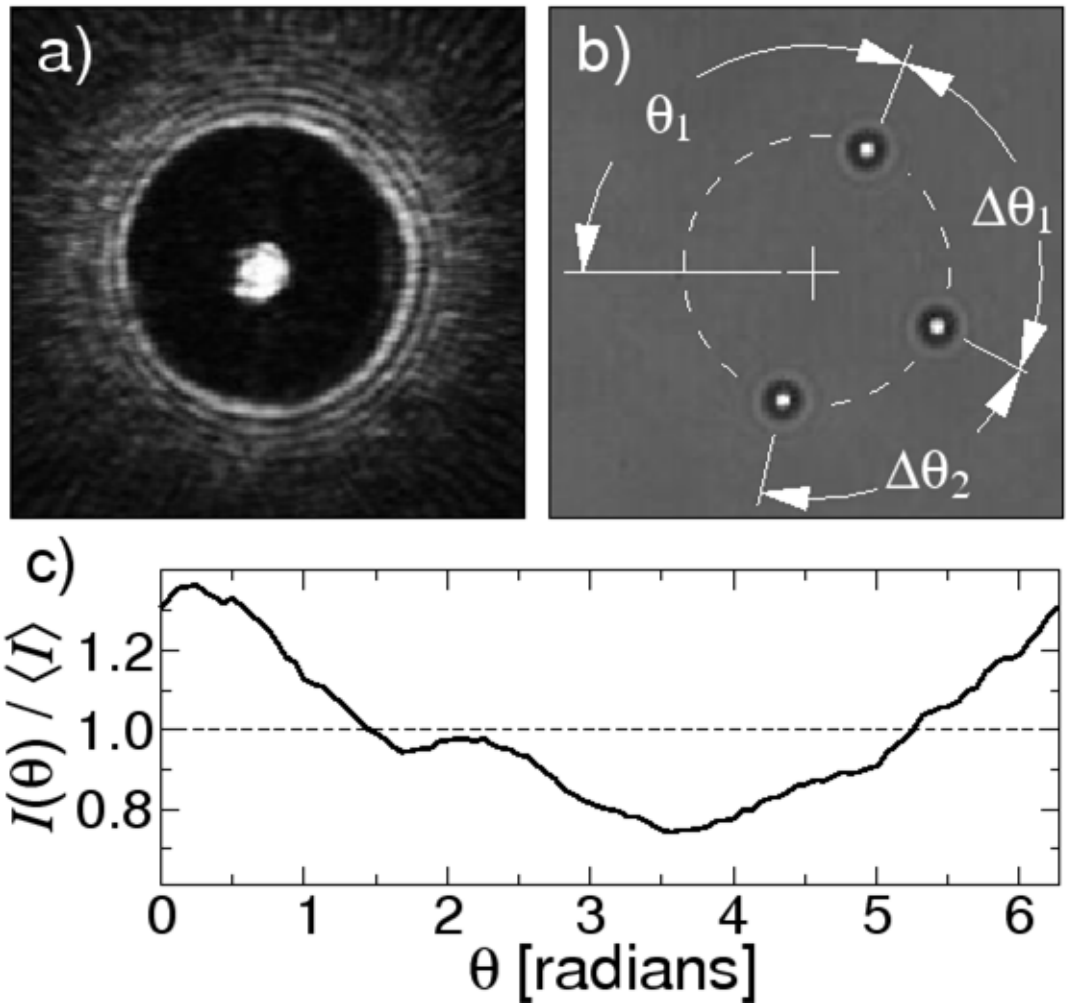

Figure 23: Illustration of an axicon generated Bessel beam and its three dimensional intensity profile.

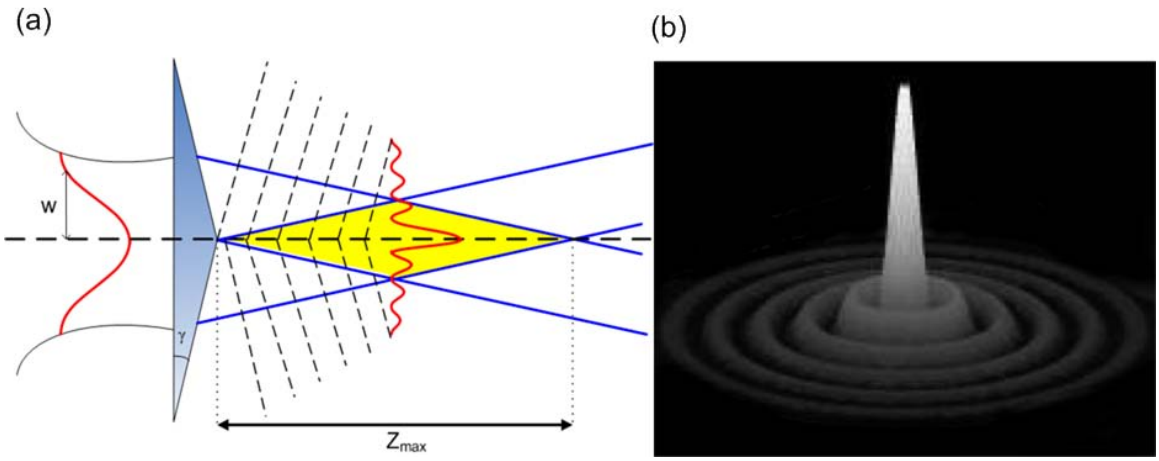

Figure 24: Optical trapping setup with a zeroth order Bessel beam

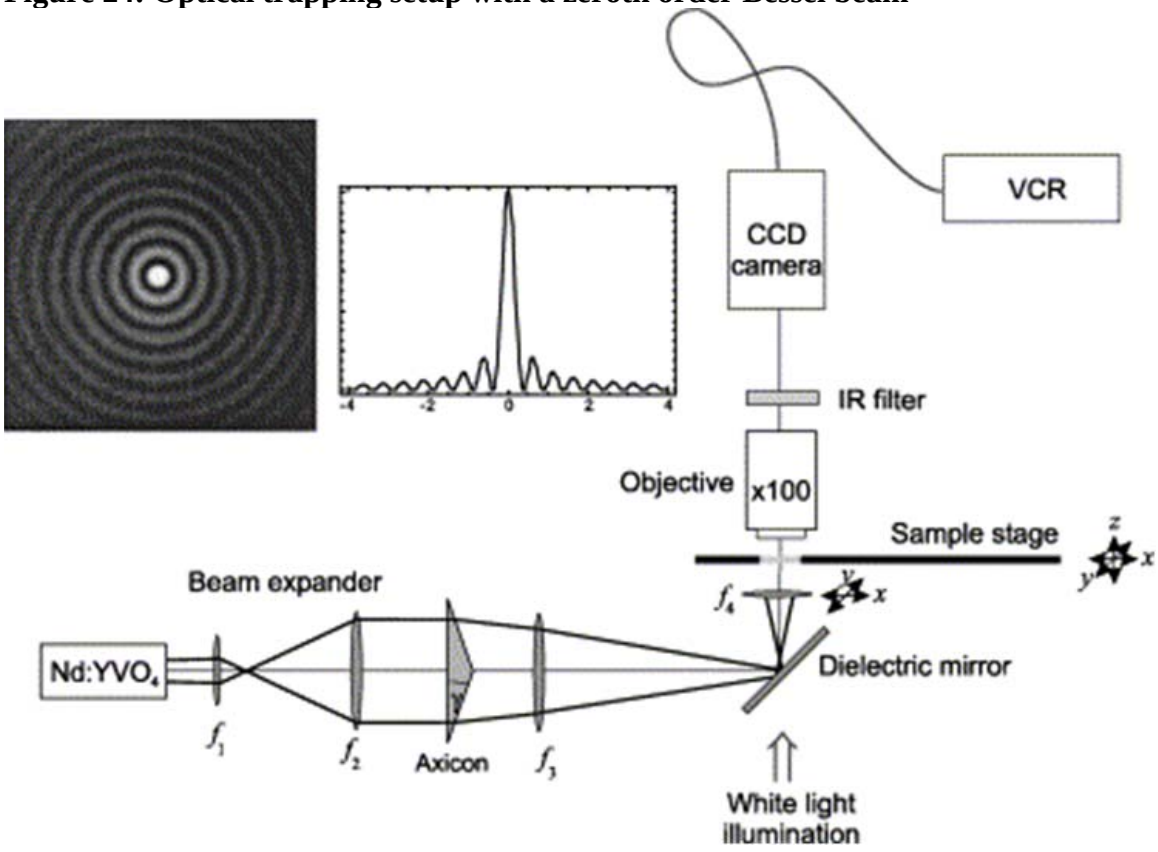

Figure 25: Observation of the reconstruction of a zeroth order Bessel beam in trapping

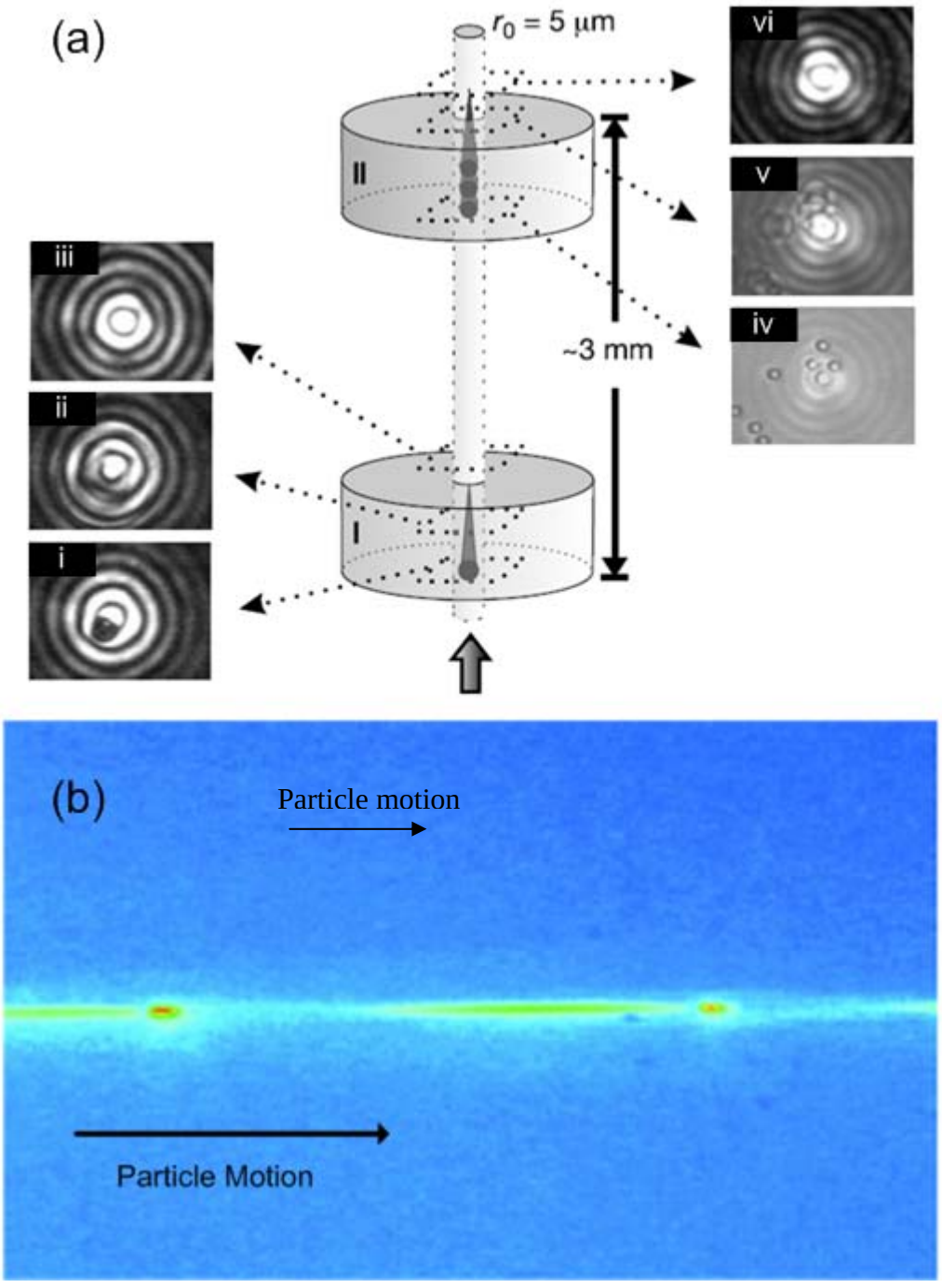

Figure 26 Optical conveyer belt

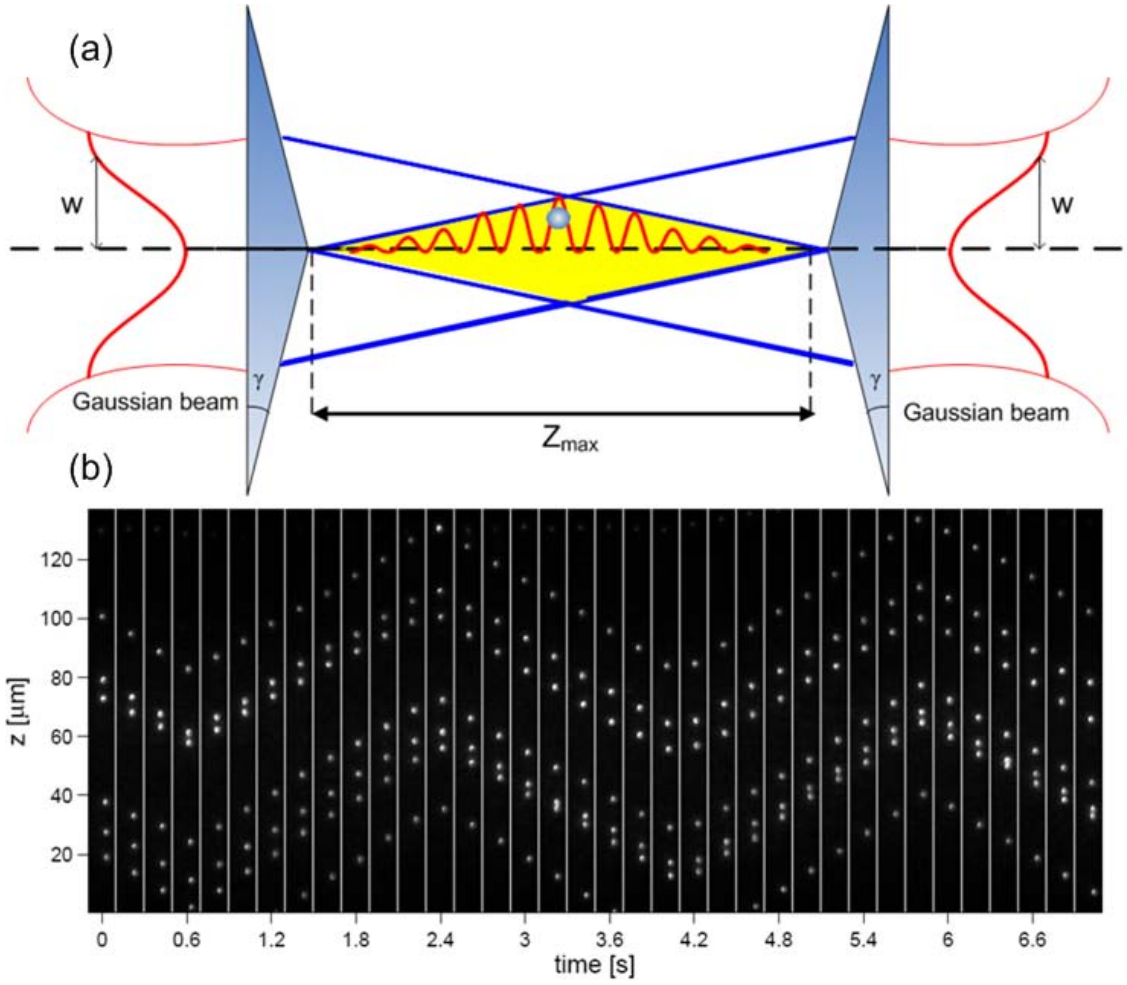

Figure 27: Brownian motion of particles confined within the concentric rings of a Bessel beam.

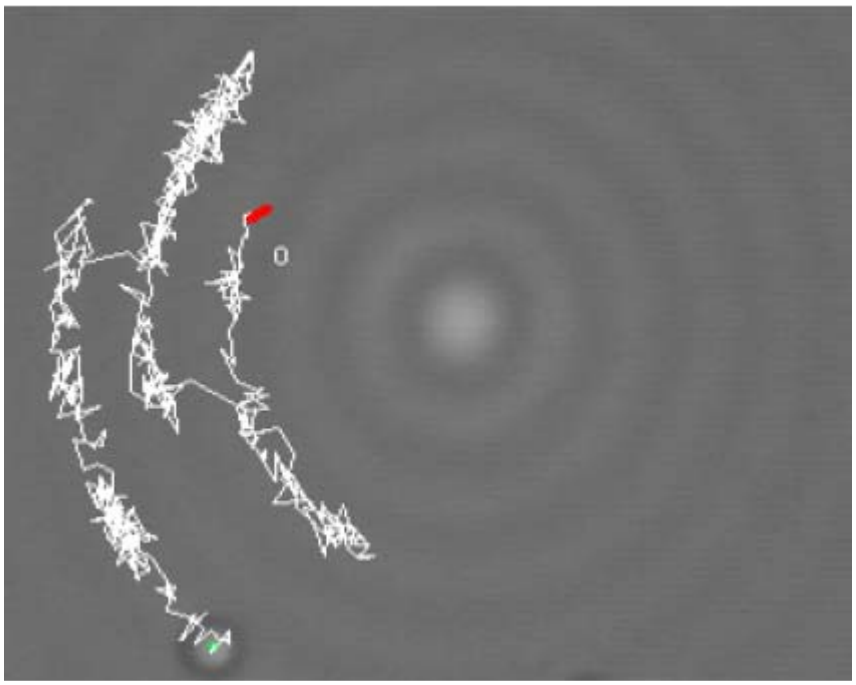

Figure 28: Use of Bessel beam for the sorting and isolation of CD2 T-lymphocytes from a sample of mononuclear cells.